THE ROLE OF CORTICAL DISINHIBITION IN A PROGRESSIVE MOUSE MODEL OF PARKINSON'S DISEASE

by

Rebecca L. Hood

A DISSERTATION

Presented to the Department of Behavioral Neuroscience
Oregon Health & Science University School of Medicine
in partial fulfillment of
the requirements for the degree of

Doctor of Philosophy

School of Medicine
Oregon Health & Science University

CERTIFICATE OF APPROVAL

This is to certify that the PhD dissertation of
Rebecca L. Hood
has been approved

Charles Meshul, PhD, Mentor/Advisor

Deb Finn, PhD, Committee Chair

Verginia Cuzon Carlson PhD, Member

Jodi McBride, PhD, Member

Joseph Quinn, MD, Member

Table of Contents

List of Figures

List of Abbreviations

6-OHDA:	6-hydroxydopamine
AAV:	Adeno-associated virus
BDA:	Biotinylated dextran amine
CO:	Cytochrome oxidase
CPu:	Caudate putamen
Cre:	Cre-recombinase
DAB:	Diaminobenzadine
DAT:	Dopamine transporter
DBS:	Deep brain stimulation
EM:	Electron microscopy
GABA:	Gamma-aminobutyric acid
GPe:	External segment of the globus pallidus
GPi:	Internal segment of the globus pallidus
IT:	Intertelencephalic tract
MPTP:	1-methyl-4-phenyl-1,2,3,6-tetrahydropyridine
MSN:	Medium spiny neuron
OD:	Optical density
PD:	Parkinson’s disease
PT:	Pyramidal tract
RNAi:	RNA interference
rTMS:	Repetitive transcranial magnetic stimulation
SN:	Substantia nigra
SNpc:	Substantia nigra pars compacta
SNpr:	Substantia nigra pars reticulata
STN:	Subthalamic nucleus
TH:	Tyrosine hydroxylase
UPDRS:	Unified Parkinson’s disease rating scale

Vgat:	Vesicular GABA transporter (gene)
VGAT:	Vesicular GABA transporter (protein)
VGLUT:	Vesicular glutamate transporter
wt:	Wild type

Acknowledgements

First, I want to thank my family who has always been unfailingly supportive. My parents have never stopped encouraging me to pursue whatever I wanted at the time, whether it was being a cowgirl artist (short-lived) or getting my doctorate in neuroscience (actualized). From sympathetically listening while I complained about every obstacle, test, and annoyance I faced in graduate school to celebrating my milestones and achievements, I cannot thank you enough for everything you've done for me. I'm so lucky to have you as my parents. I always want to make you proud, and I hope I have. And thank you to D.D., Patty, Jamie, Dave, Amy, and Pete for doing your best to not let their eyes glaze over when I talked about things like viral titers and electron microscopy, and for your support, encouragement, and love. Thank you so much.

Thank you to the students of the behavioral neuroscience department, without whom I'm positive I wouldn't have made it through. The backpacking trips, hikes, barbecues, surprise parties, conference co-housing, lunches, brunches, and celebratory or sympathetic beers at Suki's have been among the highlights of my time at OHSU. I will forever be grateful that I ended up at OHSU at the same time as all of you, and I will continue to be inspired by your drive, intelligence, and ideas. Thanks for being my friends and science role models. Also, thanks for loaning me your dogs when I was having a particularly rough week and just needed some dog time.

Thank you to the behavioral neuroscience department administrators and coordinators: Kris, Jeanne, Christine, Jake, Suzanne, Garet, and Andrey. You've all been incredibly patient in reminding me about deadlines, notifying me about outstanding paperwork, and alerting me about leftover food in the office. Thanks especially to Jeanne,

who was always ready to talk about our animals when I needed a break from research or studying.

My time at OHSU would have been immeasurably harder without everyone else in the Meshul lab. While many, many wonderful people have come and gone in the time that I've been in school, I would be remiss if I didn't specifically thank Cindy Moore, who keeps the lab functioning. Thank you for developing all of our optimized protocols so I could brag about how quickly we could do immunohistochemistry, thank you for never, ever being impatient when I asked you (for the umpteenth time) whether I should omit the hydrogen peroxide step or not, and thanks for siding with me about DAB labeling.

Thank you to my advisory committee: Deb, Gin, and Jodi. You've provided me with so much guidance and advice (even when I wasn't happy to hear it), and I know it made my dissertation so much stronger. You've pushed me to be a better scientist but have always been encouraging and sympathetic. Thank you for your thoughtful feedback, comments, and for being available when I needed an emergency get together or late afternoon Friday meeting. Deb, I want to thank you specifically for always being encouraging and so easy to talk with about this whole process, and for knowing exactly which forms I needed and when. And thank you to Joe, a recent addition to my committee, for being generous with your time and being willing to share your expertise. I can't tell you how much I appreciate it.

And last but certainly not least, I owe a huge amount of thanks to my mentor, Charlie Meshul. I'm not sure how I got lucky enough to end up in your lab when I moved to Portland, but it certainly had a huge influence on me. I can't thank you enough for

everything you've done for me, really. From making tea every morning, your willingness to drop everything to discuss results or troubleshoot a problem, your patience with my tendency to wait until the last minute to get things done, and your understanding, compassion, and enthusiasm, you have reminded me that science is fun. I couldn't have asked for a better mentor, and I'm positive that I wouldn't have produced this (or any) dissertation if it wasn't for you. Thank you.

Abstract

Parkinson's disease (PD) is a neurodegenerative disorder characterized by declining motor function. While the etiology is not understood, a hallmark of PD is a loss of dopaminergic cells in the substantia nigra pars compacta (SNpc), which provide the dopamine tone for the basal ganglia. The decline in dopamine levels in the striatum, the projection target of the SNpc, leads to a dysregulation of signaling between the nuclei of the basal ganglia, leading to decreased output from the motor thalamus and consequent motor dysfunction. Current therapies provide symptomatic relief, but to date, no treatment has been proven capable of altering PD progression, necessitating the need for a different treatment strategy. In PD, the motor cortex receives the diminished output signal from the motor thalamus and sends dampened excitatory projections to several parts of the basal ganglia, including the striatum, subthalamic nucleus (STN), and SNpc. As such, the motor cortex is an attractive therapeutic target for potentially ameliorating the dysregulation of the basal ganglia that occurs in PD. In these studies, I describe the use of posited cortical disinhibition to attenuate lesioning observed in a progressive mouse model of PD utilizing the neurotoxin 1-methyl-4-phenyl-1,2,3,6-tetrahydropyridine (MPTP). The progressive MPTP model elicited a 57% loss of TH-expressing SNpc cells in control animals and 78% loss of TH-expressing terminals in the striatum. Posited cortical disinhibition was achieved by using a Cre-lox system in which *Vgat*$^{flox/flox}$ mice underwent a unilateral adeno-associated viral injection into the motor cortex to express Cre recombinase. Expression of Cre in inhibitory GABAergic interneurons significantly reduces the amount of GABA released, dampening the main

source of inhibitory signaling within the motor cortex. In chapter 2, I investigated the potential of cortical disinhibition to protect the SNpc cells and their axon terminals against MPTP lesioning. Tyrosine hydroxylase (TH) is the rate-limiting enzyme involved in the synthesis of dopamine and is used as a marker for dopaminergic cell and terminal loss. MPTP lesioning was prevented by posited cortical disinhibition, and, despite the unilateral injection, this protection was bilateral. Chapter 3 assessed the potential of posited cortical disinhibition to induce recovery after MPTP lesioning to mimic a clinical study design. Posited cortical disinhibition caused a recovery in gait deficits resulting from MPTP lesioning while stimulating an increase in midbrain TH expression. Further investigation into the mechanism underlying this recovery suggested that activation of the hyperdirect pathway, leading from the motor cortex to the STN, could be responsible for the observed effects of posited cortical disinhibition. Taken together, these studies describe a potential for cortical disinhibition to be a viable novel treatment for PD.

Chapter 1: Introduction

Parkinson's disease (PD) is a progressive neurodegenerative disorder affecting the basal ganglia, the system of nuclei that coordinate and enable motor control. PD is the second-most common neurodegenerative disorder after Alzheimer's disease, affecting an estimated 0.3% of the population (Kowal, Dall, Chakrabarti, Storm, & Jain, 2013). As it is observed more frequently with increased age, PD prevalence increases to 1-2% for people over 65 and 4-5% for people over 85 (Huse et al., 2005; Kowal et al., 2013). Current estimates of economic burden suggest that the cost is approximately $22,800 per patient, resulting in an expenditure of over $14.4 billion in 2010 (Kowal et al., 2013). With an aging population, Kowal et al. (2013) estimated that the current number of 630,000 people in the United States diagnosed with PD will double by 2040, significantly increasing the burden on the economy, health care systems, and caregivers (Kowal et al., 2013). As PD progresses, patients become less independent and are at greater risk for falls, requiring more medical attention and care (Auyeung et al., 2012). Epidemiological studies indicate that patients with PD, especially the 25-40% who develop dementia, are at in increased risk of mortality compared to age-matched controls (de Lau & Breteler, 2006).

PD was first described in medical literature by James Parkinson in 1817 (Parkinson, 2002), but earlier descriptions exist in ancient Indian and Chinese texts, first appearing around 1000 BC (Manyam, 1990). Jean-Martin Charcot later expanded Parkinson's initial description, identifying bradykinesia, or slowed movements, as a distinguishing characteristic of the disease (Goetz, 1986). Neurologists continued to

describe PD symptomology and refine the description of the disease, resulting in a staging system to classify the progression of PD that is still used today (Hoehn & Yahr, 1967). While PD symptomology has been well described, the underlying etiology has been more difficult to ascertain. Nearly 100 years after Parkinson's initial publication, Brissaud proposed that PD symptoms are attributable to substantia nigra (SN) damage (Goetz, 2011). Subsequent research in the 20th century implicated striatal dysfunction in PD and considered a more circuit-based view of basal ganglia alterations (Goetz, 2011).

With little knowledge about PD pathogenesis, early therapies were of limited benefit, at best. Parkinson recommended bloodletting from the neck to reduce blood away from the brain and spinal cord (Goetz, 2011). The first ubiquitous pharmacological PD treatment involved the use of belladonna alkaloids, later discovered to be beneficial through modulation of the cholinergic/dopaminergic balance of the striatum (Goetz, 2011). Charcot understood the potential of anticholinergic compounds to attenuate PD-associated tremors and frequently prescribed them to his patients, but also believed that "vibratory therapy," in which patients were shaken or wore a vibrating helmet, was beneficial (Goetz, 2011). With the later understanding of dopamine localization in the brain and the discovery that dopamine is depleted in the striatum of PD patients, dopamine replacement became the main pharmacological treatment for PD (Ehringer & Hornykiewicz, 1960).

Currently, the etiology of PD is still unknown. Certain risk factors, including a history of traumatic brain injury, having a profession involving exposure to pesticides or herbicides, and living in a rural area all confer an increased risk of developing PD, but there are no common substances or mechanisms that have been identified that might

explain the etiology (Olanow & Tatton, 1999). Additionally, there are genetic risk factors that have been identified and forms of familial PD exist, but these are mostly associated with early-onset PD (Olanow & Tatton, 1999) and current animal models of PD utilizing

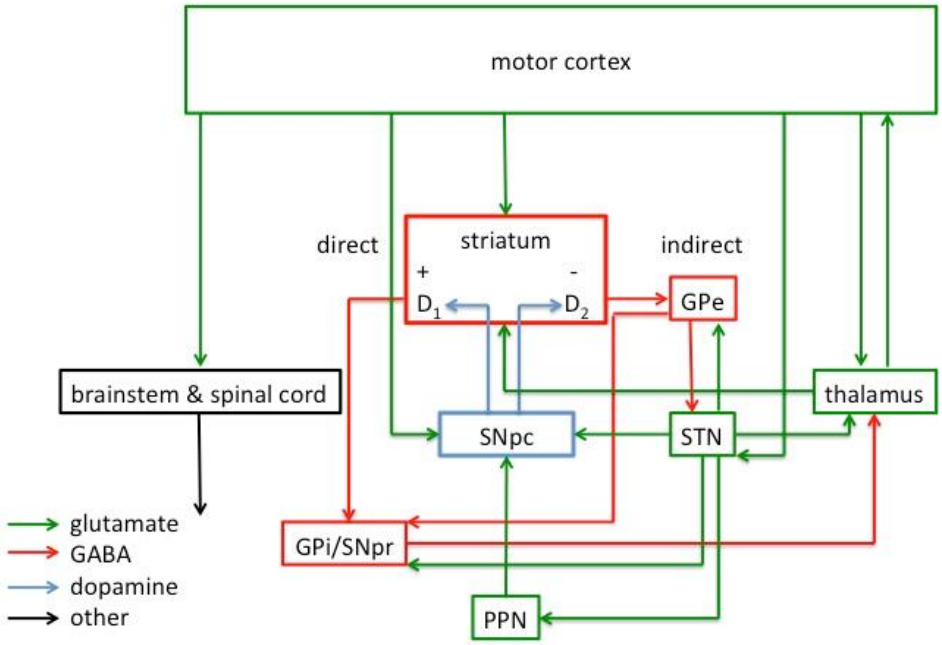

Figure 1. Basal ganglia circuitry diagram
Arrows indicate connections between regions of the basal ganglia, motor cortex, and brainstem. Colors indicate the major neurotransmitter present in the projection: green is glutamate (excitatory) and red is GABA (inhibitory). The direct pathway begins with dopaminergic input from the substantia nigra pars compacta (SNpc) synapsing on dopamine D_1 receptor-expressing medium spiny neurons (MSNs) in the striatum. The direct pathway MSNs send a GABAergic projection to the internal segment of the globus pallidus (GPi) and substantia nigra pars reticulata (SNpr), both of which send a GABAergic projection to the motor thalamus. The indirect pathway begins with dopaminergic projections synapsing on D_2-expressing MSNs which then project to the external segment of the globus pallidus (GPe). The GPe forms GABAergic synapses onto the subthalamic nucleus (STN), which sends a glutamatergic projection primarily to the SNpr, but has also been shown to innervate the SNpc. The GABAergic neurons in the SNpr then project to the motor thalamus, which sends an excitatory glutamatergic projection to the motor cortex. Other described pathways within the basal ganglia are also depicted in the diagram.

genetic models have encountered difficulty with recapitulating the loss observed in PD patients. Many of the genes linked to an increased risk of PD affect mitochondrial function or morphology, providing an interesting clue to understanding PD etiology, but to date no cause has been identified (Olanow & Tatton, 1999).

Parkinson's disease (PD) is a neurodegenerative disorder affecting the basal ganglia, the system of nuclei that coordinate and enable motor control. The hallmark pathology is observed in the substantia nigra pars compacta (SNpc), where dopaminergic cells are gradually lost. These cells project to the striatum where they release dopamine and form the start of two distinct pathways: the direct and indirect pathways. The loss of dopamine tone in the striatum results in a dysregulation of the excitatory and inhibitory signaling that modulate motor control (Obeso et al., 2008). A schematic of these changes is presented for clarity in Figure 1.

Specifically, dopamine levels decrease precipitously in the striatum, which receives both glutamatergic input from the cortex as well as dopaminergic input from the SNpc (Bernheimer, Birkmayer, Hornykiewicz, Jellinger, & Seitelberger, 1973). Within the striatum, dopamine receptors on medium spiny neurons (MSNs) are the initial site of differentiation of the direct and indirect pathways. Excitatory dopamine D_1-like receptors located on MSNs are the origin of the direct pathway, whose neurons project directly to both divisions of the substantia nigra, the pars reticulata (SNpr) and the SNpc, and the internal segment of the globus pallidus (GPi) (DeLong, 1990). From there, the direct pathway continues via GABAergic projections to the motor thalamus, which in turn sends glutamatergic projections to the motor cortex. The indirect pathway originates with inhibitory dopamine D_2-like receptors located on a separate subset of striatal MSNs

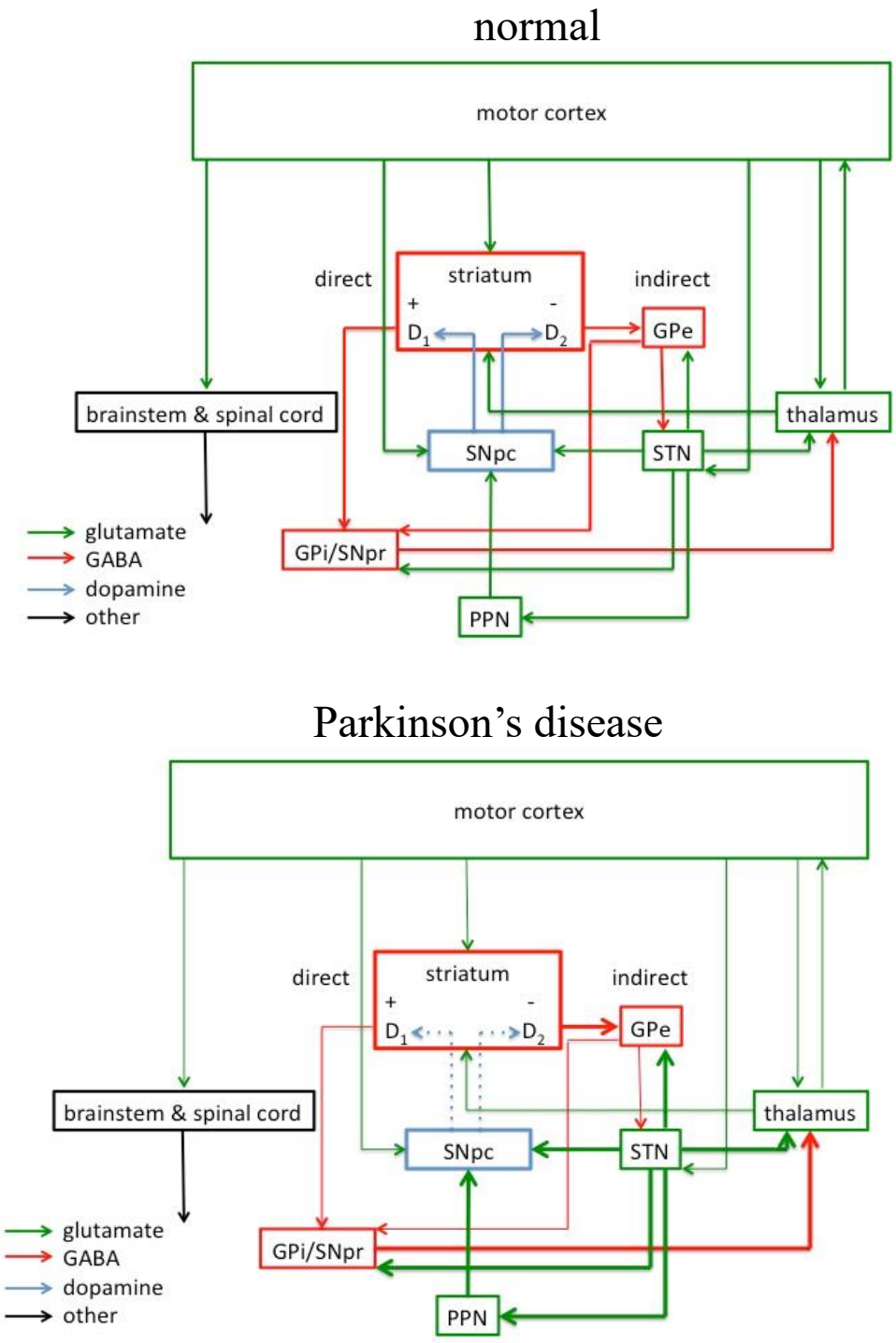

Figure 2. Alterations in basal ganglia circuitry as a consequence of dopamine loss in PD

The loss of dopaminergic input from the SNpc alters output signaling from the striatum, resulting in an alteration of activity of the basal ganglia pathways. Thinner lines represent a decrease in the activity of the specific pathway while heavier lines indicate an increase in activity, relative to signaling in an intact brain.

which project to the external segment of the globus pallidus (GPe). The GPe then sends GABAergic efferents to the glutamatergic subthalamic nucleus (STN) with the excitatory contacts from this nucleus synapsing onto the SNpc, SNpr and the GPi. At this point, the indirect pathway converges with the direct pathway and continues to the motor thalamus and motor cortex. The motor cortex projects to the brainstem and spinal cord, but also sends efferents back to the thalamus, STN, SNpc, and striatum. The excitatory signal of the glutamate input from the cortex into the striatum is coupled with variable effects of dopamine (depending on the receptor being stimulated), resulting in a complex system of motor movement regulation. This circuitry is an oversimplification of the actual neuroanatomy of the basal ganglia; most regions receiving afferents send reciprocal projections back to the origin of the projections and new signaling pathways are still being elucidated, making a comprehensive description of signaling within the basal ganglia complicated.

Because the basal ganglia nuclei are heavily interconnected, a decrease in one input results in a dysregulation of the entire system. The loss of dopaminergic tone results in an increase in the activity of the indirect pathway and a concurrent depression of direct pathway activity, leading to a decrease in glutamatergic output from the thalamus to the motor cortex. More specifically, the loss of dopamine into the striatum disinhibits D_2-receptor MSNs, resulting in increased GABAergic output to the GPe. The GPe is more inhibited and therefore sends fewer inhibitory signals to the STN, GPi, and SNpr, which in turn results in an increase in GABAergic signaling to the thalamus via the indirect pathway. For the direct pathway, a decrease in dopamine results in a dampening of signaling from D_1-expressing MSNs, which leads to decreased GABAergic innervation

of the GPi and SNr and subsequent increase in inhibitory signaling to the thalamus. These changes are illustrated in figure 2. Again, this circuit diagram represents a framework for understanding some of the underlying changes that occur in the basal ganglia in PD, but it fails to capture all changes that occur, including changes in firing rate of certain nuclei, reorganization of efferent synapses, or compensatory mechanisms such as sprouting that have been observed (Nambu, 2008).

Clinically, PD presents with myriad symptoms. Often referred to as a "boutique disease" in reference to the individualistic nature of the symptoms, there are some general commonalities that occur between patients. These include tremor, bradykinesia (slowness of movement), rigidity, difficulty initiating voluntary movements, alterations in gait, and eventually cognitive impairments (Jankovic, 2008). Because of the varied nature of the presentation of PD, it is often difficult to make a definitive diagnosis until the disease has progressed to a later stage. Current estimates suggest that PD patients don't exhibit any motor symptoms until a 50-60% loss of dopaminergic cells in the SNpc has occurred, making early diagnosis and treatment challenging (Kordower et al., 2013). Additionally, PD is currently considered to be idiopathic, meaning that treatments are focused on symptomatic relief and not the underlying pathology, which is not yet understood.

The predominant pharmacotherapy for PD is levodopa, a dopamine precursor that can cross the blood brain barrier and is converted to dopamine in the brain and acts as a replacement for endogenous dopamine. A recent delayed-start clinical trial showed no indication that levodopa administration altered the progression of the disease in patients with early stage PD, signifying that while levodopa can provide symptomatic relief, the underlying degeneration continues to occur unabated and the efficacy of levodopa

diminishes (Verschuur et al., 2019). Surgical therapies exist and are typically implemented when levodopa alone is no longer effective or is required in such high doses that side effects, typically dyskinesia, are no longer tolerable. Deep brain stimulation (DBS) is the most common surgical treatment for PD and consists of electrodes implanted in the STN or GPi, depending on the symptomology and needs of the patient (Johnson, Miocinovic, McIntyre, & Vitek, 2008). The outcome is generally positive: Kumar et al. (2010) described a 40% decrease in levodopa dosage after STN electrode implantation, as well as a 58% improvement in the Unified Parkinson's Disease Rating Scale (UPDRS) score when patients were off medication. However, like pharmacotherapy, DBS is effective at attenuating symptoms but does not slow down the progression of degeneration (Hilker et al., 2005). As such, more effective treatments that can alter disease progression or even elicit recovery in the basal ganglia are needed.

One difficulty with treating PD arises from the pathogenesis of the disease: the brain is capable of adapting to the loss of dopamine until 50-60% of the cells are lost, at which point dopaminergic denervation becomes too overwhelming for compensatory measures (Kordower et al., 2013). As such, when over half of the dopaminergic cells are already lost before diagnosis and onset of treatment are initiated, it is difficult to elicit any recovery with such a significant lesion. Many preclinical studies employ a neuroprotective study design, that is, the treatment is administered before any cell loss occurs. In theory, effective therapies that arise from this study design could be utilized in cases of early diagnosis, or could be evaluated in the context of blocking any further cell loss from occurring. However, no therapy arising from animal studies has been successfully translated to a disease-altering treatment in PD patients to date. Basic

researchers have begun to utilize alternative study designs to more closely model the clinical course of the disease. Neurointervention studies, in which a treatment is administered during progression of the disease model, or neurorestoration studies, where lesioning is complete before any treatment is initiated, are more translationally relevant but have yet to produce a treatment that is effective at slowing degeneration in PD patients. Implementation of these study designs are greatly limited by the model being used.

It is inherently difficult to model a disease in which the underlying cause is not known, so a multitude of PD models exist that recapitulate certain aspects of PD. Recent elucidation of gene mutations associated with PD have allowed for the development of genetic models. α-Synuclein was the first gene implicated in familial PD and is the most ubiquitous protein found in Lewy bodies, inclusion bodies that form in neurons in later stages of PD (Polymeropoulos et al., 1997). However, transgenic α-synuclein models have not been able to elicit a significant SNpc cell loss, although transgenic mice do exhibit some motor dysfunction and loss of striatal dopamine (Blandini & Armentero, 2012). Gain-of-function mutations in the gene encoding leucine-rich repeat serine/threonine kinase 2 (LRRK2) are the most prevalent mutations in familial PD, but transgenic models have had limited success in modeling SNpc cell loss (Xu, Shenoy, & Li, 2011). Overexpression of mutant LRRK2 can elicit behavioral deficits, but no significant cell loss has been observed in LRRK2 models (Li et al., 2009). Other genetic models associated with autosomal PD have been employed, but all show modest SNpc cell loss, at best (Blandini & Armentero, 2012). The lack of significant SNpc cell loss, a fundamental characteristic of PD, limits the translational relevance of genetic models.

The earliest animal models of PD employed neurotoxins to lesion brain regions and elicit a loss mimicking that in PD. Most toxin models utilize molecules that have a high affinity for the dopamine transporter (DAT), allowing the toxin to selectively target dopaminergic cells. Toxins can be administered locally to the basal ganglia, typically the striatum or medial forebrain bundle (MFB) through which efferent fibers from the SNpc to the striatum pass. 6-hydroxydopamine (6-OHDA) was the first toxin used to develop an animal model of PD and is commonly used today (Schober, 2004). Typically, 6-OHDA is infused unilaterally in rodents so that the contralateral hemisphere can be used as an internal control and to allow for behavioral assessments of rotations following either direct or indirect activation of dopamine receptors (Blandini, Armentero, & Martignoni, 2008). But while PD can present with asymmetry, especially in early stages, a large lesion in a single hemisphere is not a representative model of PD. Additionally, nearly all 6-OHDA models consist of a single focal injection of 6-OHDA which elicits cell loss within a few days (Blandini & Armentero, 2012). This loss is extremely fast compared to the rate of cell loss in PD patients, which occurs over decades, and fails to elicit neuroadaptations that are known to occur during preclinical and early-stage PD (Kordower et al., 2013).

Other toxins can be administered systemically. This class consists of pesticides such as paraquat and rotenone that are toxic to dopaminergic cells, but exhibit only moderate toxicity that makes achieving a lesion equivalent to that observed in symptomatic PD patients exceedingly difficult (Blandini & Armentero, 2012). 1-methyl-4-phenyl-1,2,3,6-tetrahydropyridine (MPTP) can also be administered systemically, is selectively taken up by dopaminergic cells, and displays greater neuronal toxicity than

paraquat and rotenone (Betarbet, Sherer, & Greenamyre, 2002). MPTP must be converted to its active metabolite, 1-methyl-4-phenylpyridinium (MPP^+) by monoamine oxidase B (MAO-B) to be bioactive. Rat brains only convert MPTP to MPP^+ in a few sites, all outside of the basal ganglia, resulting in limited toxicity of MPTP in rat models (Nakamura & Vincent, 1986). However, MPTP is highly toxic to both mice and monkeys, and MPTP lesions elicit motor dysfunction in monkeys that closely parallels symptoms observed in PD patients (Porras, Li, & Bezard, 2012). Both 6-OHDA and MPP^+ inhibit complex I of the mitochondrial electron transport chain, resulting in a generation of reactive oxygen species and cell death (Schober, 2004). A diagram of 6-OHDA- and MPTP-induced toxicity is shown in figure 3.

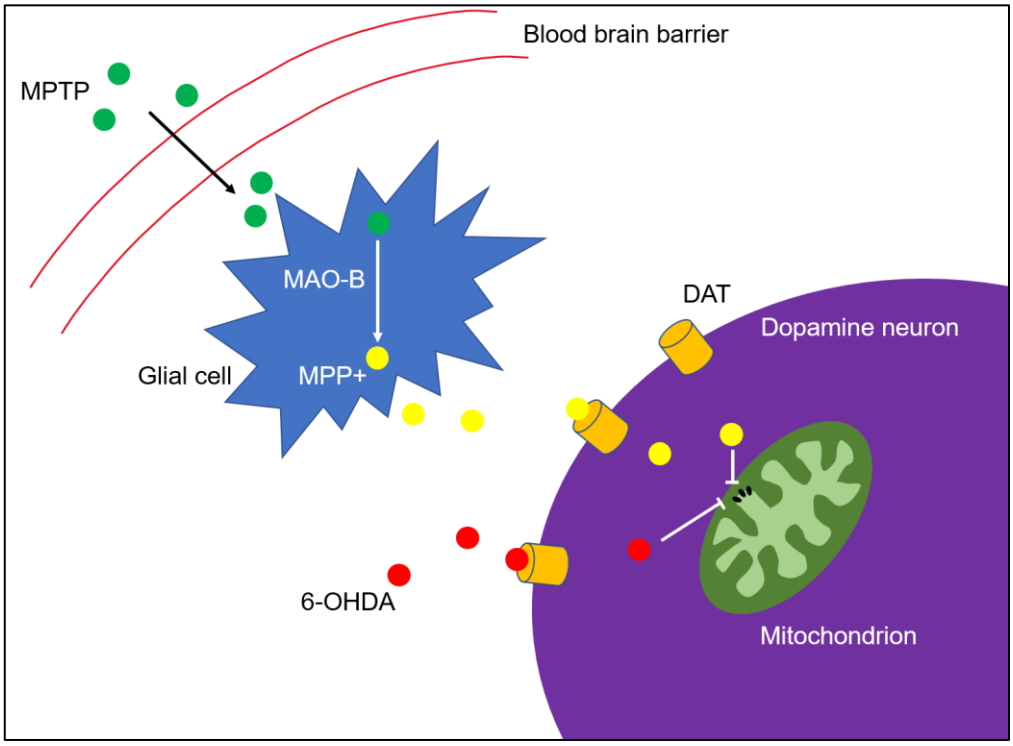

Figure 3. Schematic of neurotoxins leading to dopaminergic cell death
Systemically administered MPTP can cross the blood brain barrier, where it is converted to the toxic MPP^+ molecule by MAO-B in glial cells. 6-OHDA and MPP^+ are both selectively taken up by the dopamine transporter (DAT), where they inhibit complex I of mitochondria, leading to cell death.

MPTP is typically administered in acute (4 administrations of 20 mg/kg dose delivered 2 hours apart) or subacute (daily injections of 20-30 mg/kg for 5 days) doses over the course of hours or a few days (Gibrat et al., 2009; Meredith & Rademacher, 2011). This results in a similar limitation to 6-OHDA models: while the lesions are bilateral, lesioning occurring over a few days does not capture potential neuroadaptations that occur during a slowly progressing degeneration. Additionally, animals can show spontaneous recovery after MPTP administration has ceased, potentially confounding long-term therapeutic studies (Petroske, Meredith, Callen, Totterdell, & Lau, 2001). MPTP is a potent toxin specific to dopaminergic cells, but current models still lack translational relevance.

To address these shortcomings, Goldberg et al. (2011) developed a progressive MPTP mouse model of PD. MPTP is administered to C57BL/6J mice 5 days/week for 4 weeks, with the dose getting progressively higher each week. The initial characterization of this model used doses of 4 mg/kg for week 1, 8 mg/kg for week 2, 16 mg/kg for week 3, and 32 mg/kg for week 4. Loss was evaluated by measuring immunolabeling of tyrosine hydroxylase (TH), the rate-limiting enzyme in the synthesis of dopamine. This progressive model elicited a progressive loss of TH-expressing neurons in the SNpc, ultimately resulting in a 62% cell loss, equivalent to early-stage PD (Goldberg et al., 2011). Additionally, immunoreactivity of TH-expressing terminals in the striatum was reduced by 74% compared to vehicle animals, and striatal dopamine was depleted by 70% at the end of 4 weeks of MPTP administration (Goldberg et al., 2011). A qualitative description of this TH loss over the course of 4 weeks of progressive MPTP administration is provided in figure 4. Behaviorally, this model elicits reproducible gait

dysfunction, making observed behavioral changes translationally relevant (Goldberg, Hampton, McCue, Kale, & Meshul, 2011). The progressive nature of the model also allows for neuroprotection, neurointervention, and neurorestoration study designs, where

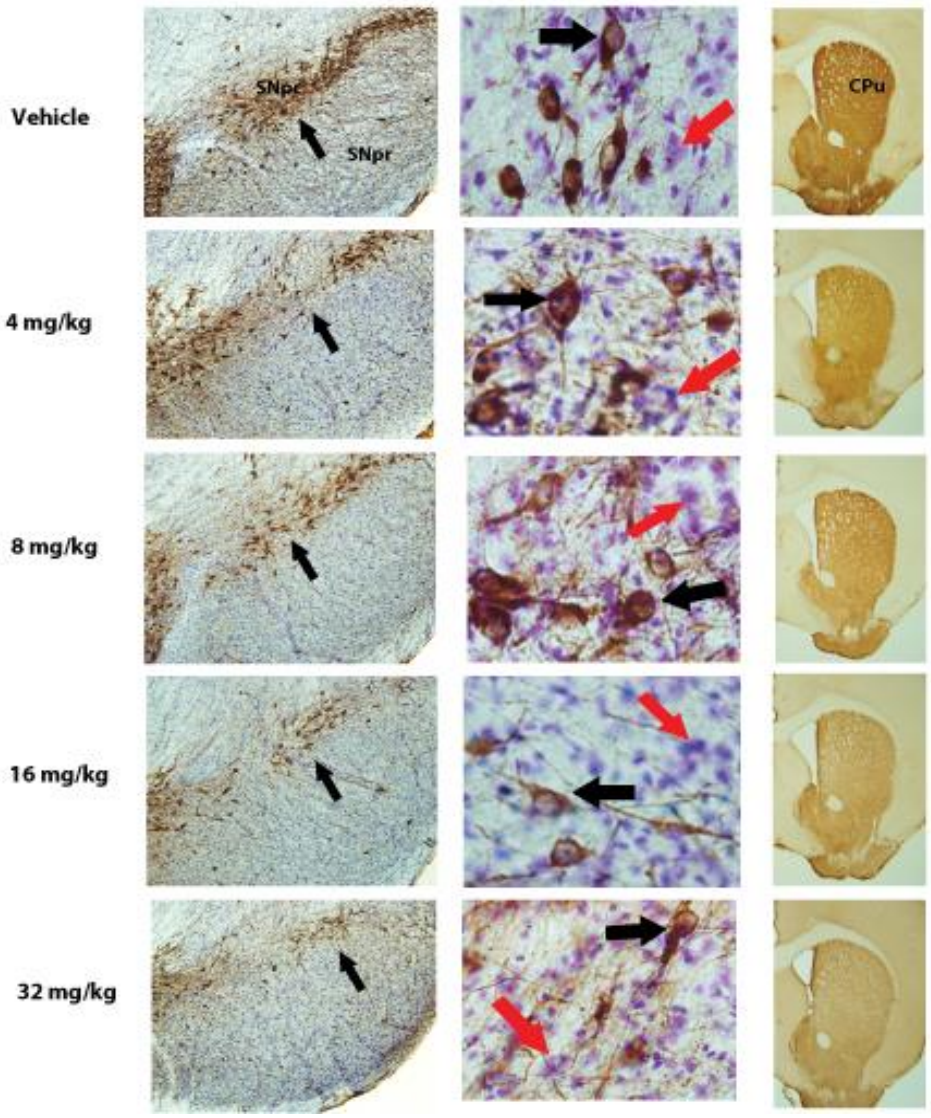

Figure 4. Progressive TH loss after MPTP lesioning
TH labeling in the SNpc (left column), cell bodies of the SNpc (middle column), and the striatum (right column). The intensity of the brown color correlates to the amount of TH protein and decreases as MPTP dosages increase. Black arrows indicate TH-positive cells, red arrows indicate TH-negative cell bodies. The listed dosages indicate the dose of MPTP administered that week (mg/kg/day, 5 days/wk), samples were taken after the full week of indicated MPTP administration. Figure reprinted from Goldberg, et al., 2011, with permission from authors.

therapy can be initiated before, during, or after MPTP administration, respectively. We have also found that progressive administration of MPTP at lower doses than those used in acute and subacute models spares dopaminergic neurons in the ventral tegmental area (VTA), a limbic brain region medial to the SNpc that is also relatively spared in PD (Pflibsen et al., 2015).

The progressive MPTP model has been used to evaluate various pharmacological and nonpharmacological treatments, including an FDA-approved anti-inflammatory/immunomodulatory drug, a compound that stimulates the brain-derived neurotrophic factor (BDNF) receptor TrkB, exercise, and social enrichment (Churchill et al. 2019; Sconce et al. 2015; Hood et al. 2016; Goldberg et al. 2012). However, this model has not been used to investigate the therapeutic potential of targeting specific brain regions implicated in PD dysfunction. While DBS of the GPi and STN is an effective treatment in terms of symptomatic relief for several years, other brain regions may also be viable therapeutic targets potentially capable of altering disease progression.

Output from the motor thalamus is routed through the motor cortex before signals travel to the brainstem and spinal cord, making the motor cortex an attractive candidate to target to rectify dysfunctional signaling from the basal ganglia. Additionally, the motor cortex strongly innervates the striatum and STN, both regions known to be dysregulated in PD. Corticostriatal projections have previously been demonstrated to be underactive in both PD models and patients (Stephens et al., 2005; Strafella, Ko, Grant, Fraraccio, & Monchi, 2005). The canonical decrease in thalamocortical activity resulting from dopamine denervation contributes to a positive feedback loop in which the cortical innervation of the basal ganglia is depressed, resulting in even less output from the

thalamus. Therefore, it is possible that targeting the motor cortex could help to attenuate the dysregulation of basal ganglia signaling that occurs in PD.

In fact, alteration of motor cortex activity has already been attempted in both PD models and patients. Optogenetic stimulation of the motor cortex specifically targeting the hyperdirect (corticosubthalamic) pathway in 6-OHDA-lesioned mice attenuated bradykinesia and hypokinesia, presumably due to an increase in glutamatergic activity of cortical efferents (Sanders & Jaeger, 2016). PD patients undergoing repetitive transcranial magnetic stimulation (rTMS) of the motor cortex experienced improved motor performance and a return of cortical excitability back to baseline (Lefaucheur et al., 2004). Lenz & Vlachos (2016) have theorized that rTMS acts by decreasing GABAergic neurotransmission in the region of interest, indicating that rTMS may attenuate PD motor deficits by a removal of the local GABAergic brake provided by interneurons, resulting in cortical disinhibition.

These studies indicate that an increase in the activity of the motor cortex is effective at ameliorating motor dysfunction in PD, but none have directly studied downstream alterations in the basal ganglia that may underlie the observed behavioral recovery. While the use of an animal model in the optogenetic study facilitates further investigation of neurobiological changes in the brain, the bouts of stimulation were limited to just 5 minutes. Ideally, a mouse model examining the long-term effects of an alteration of cortical activity would involve sustained alteration. Cre-lox system technology is an established, straightforward way to manipulate gene expression in a focal brain region.

The Cre-lox system is a method of gene manipulation by which genes flanked by loxP sequences can be targeted for recombination by Cre recombinase (Sauer, 1998). The orientation of the loxP sequences determines the resultant effect: genes can be excised, inverted, or translocated. Excision, utilized here, is irreversible. This technique allows for a high degree of selectivity as Cre expression can be restricted to cell or tissue types through the use of specialized breeding or tissue-specific promoters. Alternatively, injection of an adeno-associated virus or lentivirus to induce Cre expression allows for both temporal and regional specificity, a significant advantage over global gene knockout models previously used. The Cre-lox system presents a method by which a specific gene in a specific brain region can be targeted at a desired point in time, making it an incredibly powerful tool for scientific research.

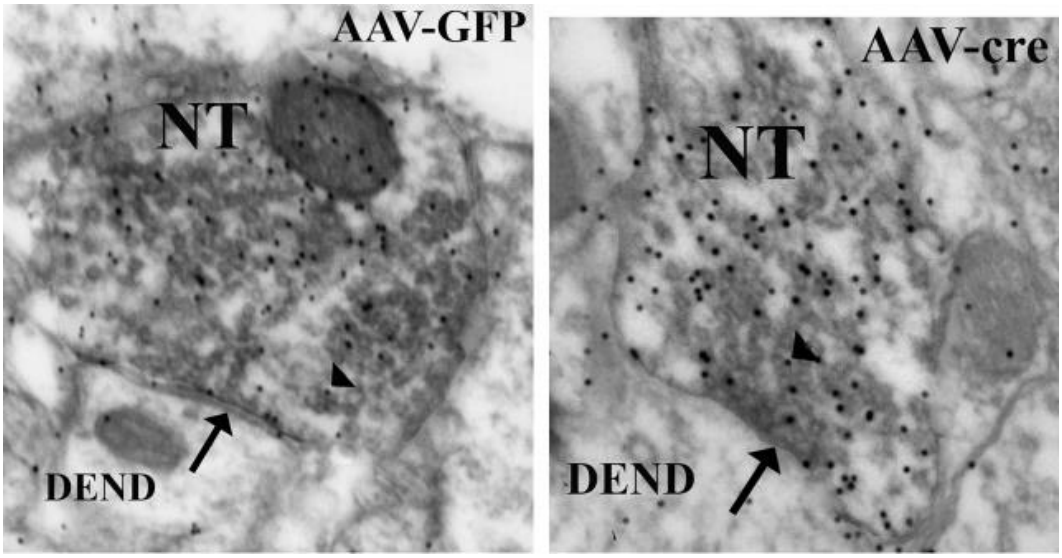

Figure 5. Accumulation of immunogold-labeled GABA in nerve terminals after Cre-mediated *Vgat* knockdown
The density of GABA immunogold particles (indicated by the arrowhead) was significantly increased in AAV-Cre-GFP-injected mice compared to AAV-GFP-injected controls, suggesting that the Cre-mediated knockdown of *Vgat* decreases the release of GABA from nerve terminals. "NT" indicates nerve terminal, "DEND" indicates dendrite, arrows indicate the synapse where the nerve terminal is making contact onto the dendrite.

The availability of a *Vgat*$^{flox/flox}$ mouse line provides the possibility to modify GABAergic signaling by excision of the floxed *Vgat* gene, which encodes for the vesicular GABA transporter (VGAT) (Tong, Ye, Jones, Elmquist, & Lowell, 2008). Unlike the vesicular glutamate transporters (VGLUT), there is only one isoform of VGAT, meaning that the knockout of VGAT would dampen GABAergic signaling without any potential compensation from co-expressed isoforms. As cortical GABAergic interneurons attenuate the activity of cortical projection neurons, they are convenient targets by which to modulate the output of cortical neurons. Cortical GABAergic interneurons are highly variable in terms of morphology, connectivity, development, and arborization, but as all suppress cortical activation and require VGAT for neurotransmission, they are considered as a single group for the purposes of this study.

The Cre-mediated knockdown of *Vgat* in the *Vgat*$^{flox/flox}$ mouse has been verified by Tong, et al. (2008) in the hypothalamus, but this system could be utilized to prevent GABAergic signaling in any brain region targeted by an adeno-associated virus expressing both Cre as well as enhanced green fluorescent protein (AAV-Cre-GFP) injection. Unpublished EM data from our lab to verify GABA accumulation in nerve terminals after *Vgat* knockdown in the entopeduncular nucleus (EPN)/GPi (Figure 5) showed an accumulation of the neurotransmitter in the nerve terminal, as GABA is no longer able to be packaged into synapses and released. This is indicated by a significant increase in GABA immunogold labeling density in the nerve terminal (79 ± 16 particles/μm^2 in control AAV-GFP-injected *Vgat*$^{flox/flox}$ animals vs 133 ± 11 particles/μm^2 in AAV-Cre-GFP-injected *Vgat*$^{flox/flox}$ animals, $p<0.05$). The significant increase in GABA immunogold particle density is a strong indicator that, in our hands, the Cre-

mediated knockdown of *Vgat* results in a decrease in GABA release from targeted nerve terminals.

Based on previous validation and pilot data from our lab, posited cortical disinhibition can be achieved by a focal AAV-Cre-GFP injection into the motor cortex of a $Vgat^{flox/flox}$ mouse, significantly decreasing local GABAergic inhibition of cortical neurons and increasing glutamatergic output. The Cre-lox system results in a permanent excision of the floxed gene, so this technique yields a long-term posited cortical disinhibition, making it possible to study long-term effects of posited cortical disinhibition in a PD model.

The following chapters evaluate posited cortical disinhibition as a potential therapy in the progressive MPTP mouse model of PD in both neuroprotective (Chapter 2) and neurorestorative (Chapter 3) study designs. Both the behavioral and neurobiological effects of posited cortical disinhibition in a PD model are described, and measures of changes in the activity of basal ganglia nuclei are used to provide a potential mechanism for the observed changes. The global hypothesis for these studies is that posited cortical disinhibition will effectively ameliorate MPTP-induced deficits in both motor behavior and basal ganglia anatomy.

Specific Aims

Chapter 2: Neuroprotective potential of posited cortical disinhibition in a progressive MPTP model of PD

Specific Aim 1: To evaluate the potential of posited cortical disinhibition to prevent behavioral deficits caused by MPTP administration

Hypothesis: Posited cortical disinhibition will protect against gait dysfunction caused by MPTP lesioning.

Specific Aim 2: To assess the ability of posited cortical disinhibition to protect against TH loss and subsequent alterations of glutamatergic signaling within the basal ganglia caused by MPTP lesioning

Hypothesis: Posited cortical disinhibition will prevent MPTP-induced lesioning of TH-expressing nerve terminals in the striatum through activation of the corticostriatal pathway

Chapter 3: Neurorestorative potential of posited cortical disinhibition in a progressive MPTP model of PD

Specific Aim 1: To determine if posited cortical disinhibition can ameliorate behavioral deficits after progressive MPTP lesioning

Hypothesis: Posited cortical disinhibition will decrease motor impairments in gait caused by MPTP lesioning

Specific Aim 2: To evaluate the potential of posited cortical disinhibition to attenuate dopaminergic and glutamatergic changes in the basal ganglia after MPTP lesioning

Hypothesis: Posited cortical disinhibition will increase cortical glutamatergic output and increase TH expression in the basal ganglia

Chapter 2: Neuroprotective potential of posited cortical disinhibition in a progressive MPTP model of PD

2.1 Introduction

Parkinson's disease (PD) is a neurodegenerative disorder that results in gradually worsening bradykinesia, rigidity, resting tremor, gait impairment, and cognitive deficits. Primarily characterized by a loss of dopaminergic cells in the substantia nigra pars compacta (SNpc), PD results in a loss of dopamine tone in the basal ganglia, thereby dysregulating the excitatory and inhibitory signaling that modulate motor control (Obeso et al., 2008). The striatum, which receives a dampened dopaminergic input from the SNpc, also undergoes a decrease in glutamatergic innervation as a result of the alteration in basal ganglia signaling (Stephens et al., 2005). The interconnected nature of this circuitry suggests that targeting a specific area could have downstream effects within the basal ganglia. Attempts to increase dopamine levels pharmacologically or correct the imbalance in basal ganglia signaling via targeted deep brain stimulation (DBS) of specific basal ganglia nuclei have been shown to provide symptomatic relief but fail to slow the progression of the disease (Hilker et al., 2005; Rizzone et al., 2014). As such, alternative therapeutic targets must be considered.

One consequence of the disruption of the basal ganglia circuitry is a modification in cortical activity (Lefaucheur, 2005; Ridding, Rothwell, Inzelberg, & Rothwell, 1995; Sabatini et al., 2000). Numerous imaging studies have shown altered activity of the motor cortex in PD patients, both at rest and during movement (Lotze et al., 1999; Sabatini et

al., 2000; Wu et al., 2009). Sen et al. (2010) showed in a longitudinal fMRI study of PD patients that recruitment of areas within the motor cortical circuit becomes stronger over time, suggesting that cortical signaling becomes less efficient and increased recruitment could be a compensatory mechanism. Repetitive transcranial magnetic stimulation (rTMS) has been shown to provide some symptomatic relief to PD patients, although these benefits exist only for the duration of the stimulation (Lefaucheur et al., 2004). More recently, motor cortex stimulation by subdural electrodes implanted unilaterally over the motor cortex has been shown to also bilaterally decrease motor deficits in PD patients and represents a safer surgical option than DBS (Canavero et al., 2002). To that end, this chapter considers the alteration of the motor cortex as a potential neuroprotective strategy and proof of principle that motor cortex disinhibition can alter PD disease state.

Though current therapies improve motor symptoms, there has been no evidence of disease alteration. Therefore, this study focused on the potential of motor cortex disinhibition to be neuroprotective and delay further disease progression. Current literature suggests three potential pathways by which motor cortex disinhibition could be protective. First, disinhibition of the motor cortex could activate the direct pathway via corticostriatal projections, leading to compensation for the loss of dopaminergic tone and abatement of motor symptoms. Second, disinhibition of the motor cortex could activate the hyperdirect pathway, a therapeutic target that lies between the motor cortex and subthalamic nucleus (STN) (Nambu, Tokuno, & Takada, 2002). Third, disinhibition of the motor cortex could directly activate the corticonigral pathway, resulting in a direct increase in glutamatergic input to the substantia nigra (Naito & Kita, 1994). Though

corticonigral projections are not commonly studied, *in vitro* studies suggested that dopaminergic midbrain cultures require innervation through voltage-gated sodium channels to survive, with the blockade of these channels leading to eventual cell death (T. Aumann & Horne, 2012a; Salthun-Lassalle, Hirsch, Wolfart, Ruberg, & Michel, 2004). Therefore, it is possible that increasing the excitatory input to the substantia nigra by activating the corticonigral pathway, could protect cells against potential damage that occurs in both patients with PD and PD animal models.

While many rodent models of PD involve an acute dose of neurotoxin—often unilaterally to spare the contralateral side as a control—these models do not reflect the progressive nature of PD. Gradual loss has been hypothesized to result in compensatory remodeling in the brains of PD patients until these compensatory mechanisms fail, leading to noticeable motor symptoms (Kordower et al., 2013). Acute models do not allow for these neuroadaptations and therefore may not accurately reflect changes that occur in the basal ganglia, even though certain commonalities between lesions in humans and animals in these models may exist. Typically, lesion models of PD result in a loss of dopaminergic cell bodies in the SNpc and their projections to the striatum, as assessed by measuring levels of tyrosine hydroxylase (TH), the rate-limiting enzyme involved in dopamine synthesis. In an attempt to mimic the gradual development of PD, we utilize a progressive neurotoxin model that yields similar lesions to those observed in PD patients. Specifically, four weeks of progressively higher doses of systemic administration of 1-methyl-4-phenyl-1,2,3,6-tetrahydropyridine (MPTP) generates SNpc cell loss and sustained decrease in TH expression in striatal nerve terminals (Goldberg et al., 2011). These lesions are bilateral and correlate with the amount of loss (approximately 50%) in

PD patients exhibiting early PD symptoms (Kordower et al., 2013). It is our belief that this toxin model is more translationally relevant than acute models, thereby increasing the likelihood that therapies that are effective in animal models can successfully be translated to PD patients. The progressive model also allows for the investigation of disease modification, a goal of future PD therapies. In the current study, the progressive model was utilized to examine the neuroprotective potential of altering inhibitory signaling in the motor cortex, specifically by preventing signaling by the inhibitory neurotransmitter γ-aminobutyric acid (GABA).

Berretta et al. (1997) previously showed that a pharmacological blockade of inhibitory $GABA_A$ receptors in the motor cortex results in increased expression of the immediate-early gene cFos in both cortex and striatum, suggesting that attenuation of GABA signaling in the cortex results in a disinhibition of the corticostriatal pathway. This disinhibition could also result in the potential activation of the hyperdirect (i.e., corticosubthalamic) and corticonigral pathways. This manipulation, however, is transient and not suitable to examine sustained changes to the motor cortex. Therefore, I employed a flox-Cre system targeting the gene *Vgat*, which encodes for the vesicular GABA transporter (VGAT) protein. Deletion of *Vgat* prevents the packaging of GABA into vesicles by GABAergic interneurons, decreasing the amount of inhibitory signaling in the region of gene deletion. Tong, et al. (2008) initially generated and characterized $Vgat^{flox/flox}$ mice and showed that, with Cre present, inhibitory postsynaptic potentials (IPSPs) were completely abolished both *in vitro* and *in vivo*. I hypothesized that the deletion of *Vgat* in the motor cortex, resulting in attenuation of GABA activity, will be neuroprotective in our progressive model of PD, preventing SNpc cell loss and

preserving TH-positive nerve terminals in the striatum, thereby preventing MPTP-induced gait deficits. Additionally, I hypothesize that the deletion of *Vgat* will activate the corticostriatal, hyperdirect, or corticonigral pathways, resulting in changes in striatal glutamate signaling.

2.2 Methods

2.2.1 Animals

Male C57BL/6J (wild-type) mice (Jackson Labs, Bar Harbor, ME) or *Vgat*$^{flox/flox}$ (floxed) mice on a mixed C57BL/6J/FVB/129 background backcrossed once onto a C57BL/6J background (kindly provided by Dr. Patrick Fuller, Harvard University) were group housed and maintained on a 12-h light/dark cycle (on/off: 0600/1800) with ad libitum access to water and chow. Wild-type mice were used as controls to ensure that the *Vgat*$^{flox/flox}$ mice were not differentially sensitive to MPTP. All experiments were carried out in accordance with federal guidelines of the Public Health Service Policy on the Humane Care and Use of Laboratory Animals and approval by the Portland VA IACUC.

2.2.2 Study design

Surgeries were performed and mice were allowed to recover for 8 weeks to allow for the Cre expression and *Vgat* excision. Baseline testing was performed before lesioning to

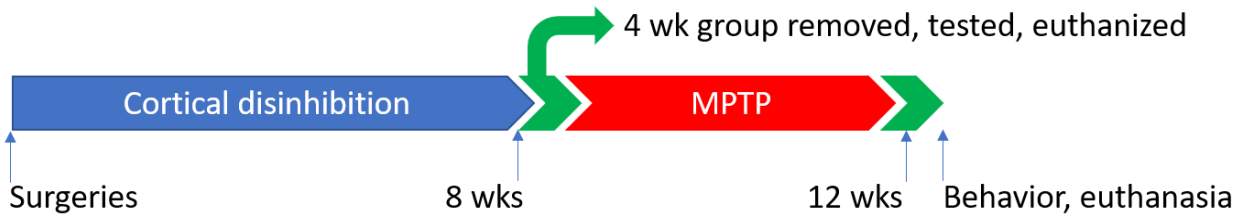

Figure 6. Schematic of neuroprotection study timeline
Surgeries to disinhibit the cortex were performed at the beginning of the experiment and 8 weeks allowed for the virus to express and knockdown *Vgat*. After 8 weeks, MPTP was administered for 4 weeks before final behavioral assessments and euthanasia. "Testing" refers to behavioral testing (DigiGait and grip strength).

assess potential behavioral effects of posited cortical disinhibition alone. MPTP was administered as described for 4 weeks, after which time behavioral testing was performed before mice were euthanized.

2.2.3 Intracranial surgeries

Injections:

When mice were at least 8 weeks old, they were anesthetized with isoflurane and placed in a mouse stereotaxic frame (Kopf Instruments, Tujunga, CA). A midline incision was made, and a unilateral burr hole was drilled over the motor cortex (AP=+2.0mm, ML=-1.5mm, DV=-1.0mm from bregma). A glass pipette containing AAV-Cre-GFP or AAV-GFP (130 nl, 1 x 10^{13} vector genome copies/ml, serotype rh10, provided by Dr. Patrick Fuller, Harvard University) was lowered to the previously stated coordinates and the contents were infused slowly over 5 min. After the injection, the pipette was left in place for 5 min to allow for diffusion from the injection site. Mice were allowed to recover for 8 weeks before progressive MPTP lesioning began. These surgeries were performed by Dr. Patrick Fuller, Harvard University.

Guide cannulae implantations:

A separate cohort of C57BL/6J mice were anesthetized with isoflurane and a 3 mm microdialysis guide cannula (Synaptech, Marquette, WI) was stereotaxically implanted into the ipsilateral dorsolateral striatum (AP=+0.7mm, ML=+2.2mm, DV=-2.6mm from

bregma). Three small stainless steel screws were placed into the skull and dental cement was used to secure the cannula.

Biotinylated dextran amine (BDA) injections:

Mice were anesthetized and stereotaxically injected in the motor cortex using the same coordinates as the viral injections with BDA (10,000 MW; Life Technologies, Grand Island, NY) as previously described by Reiner et al. (2000). 500 µL of a 10% (w/v in 0.1M phosphate buffer) BDA solution were infused slowly over 5 min. The pipette was left in place for an additional 5 min to allow for diffusion of BDA solution away from the injection site. For the current study, mice were perfused 6 days after the surgeries to allow for BDA transport.

2.2.4 MPTP administration

Mice were injected intraperitoneally 5 days/week with progressively higher doses of MPTP for 4 total weeks. Mice were given 8 mg/kg during week 1, 16 mg/kg during week 2, 24 mg/kg during week 3, and 32 mg/kg during week 4. Normal saline was used as a vehicle.

2.2.5 Tissue fixation and sectioning

One week after the last dose of MPTP, mice were deeply anesthetized with ketamine/xylazine (1%/0.1%) cocktail and perfused transcardially with electron microscopy fixative containing 1% glutaraldehyde, 0.5% paraformaldehyde, and 0.1% picric acid in 0.1M phosphate buffer, pH 7.3. The midbrain was fixed overnight in 2% paraformaldehyde in 0.1M phosphate buffer, pH7.3. Tissue was then cut into 40-60 µm-

thick sections using a vibratome (Ted Pella Inc., Redding, CA). Slices throughout the rostro-caudal extent of the striatum and SN were collected for subsequent processing.

2.2.6 Immunohistochemistry (IHC)

Six slices that extended through the region of interest (for the striatum, slices were collected from AP=+0.26 to AP=+1.54mm from bregma, for the SN, slices were collected from AP=-2.92 to AP=-3.64) were selected for immunohistochemical processing. All incubations were carried out in the PELCO BioWave® Pro microwave (Ted Pella Inc., Redding, CA) with the temperature limit set to not exceed 35^{o}C. Rinsing steps occurred under normal atmospheric pressure unless otherwise stated. Antibody incubations occurred under continuous vacuum. Tissue was rinsed twice in phosphate buffered saline (PBS) for 1 min/rinse at 150 watts (W) after each incubation step unless otherwise stated. Antigen retrieval was performed in 10 mM sodium citrate, pH 6.0, for 5 min at 550 W with the vacuum off. The tissue was then incubated in 3% hydrogen peroxide at 150 W for 1 min with the vacuum on. The next incubation occurred in 0.5% Triton X-100 for 5 min, 550 W under vacuum. Tissue was then exposed to the primary TH (1:500; Immunostar, Hudson, WI) or GFP (1:500, Fitzgerald, Acton, MA) antibody for 12 min at 200 W 4 times with the following cycle: 2 min on, 2 min off, 2 min on, 5 min off. The tissue was incubated with biotinylated goat anti-rabbit secondary antibody (Vector Laboratories, Burlingame, CA) for 15 min at 200 W for two cycles consisting of 4 min on, 3 min off, 4 min on, 5 min off. After secondary incubation, tissue was washed once in PBS and a second time in working imidazole buffer (5% 0.2M imidazole buffer, pH 9.0 and 16% 0.1M sodium acetate, pH 7.2). Tissue was exposed to ABC (avidin-biotin complex) (Vector Laboratories, Burlingame, CA) for 11 min at 150 W under

vacuum for 1 cycle consisting of 4 min on, 3 min off, 4 min on. The tissue was then incubated in diaminobenzadine [DAB (Sigma Aldrich, St. Louis, MO); 0.5 ug/ml in 1.5% hydrogen peroxide] for 10 min under continuous vacuum at 200W. Finally, the tissue was rinsed once in working imidazole buffer and once in PBS before being mounted, cover-slipped, and imaged on a Zeiss Axioplan light microscope (Carl Zeiss, Inc., West Germany) and a MBF Bioscience Digital Microscope Camera (Williston, VT). Omission of secondary antibody revealed no evidence of labeling. For striatal immunohistochemistry experiments, 5 mice/group were used for wt + veh, wt + MPTP, *Vgat*$^{flox/flox}$+ AAV-GFP + veh, and *Vgat*$^{flox/flox}$+ AAV-GFP + MPTP groups. 7 mice were included in the *Vgat*$^{flox/flox}$+ AAV-Cre-GFP + veh group, and 14 mice were used for the *Vgat*$^{flox/flox}$+ AAV-Cre-GFP + MPTP group.

2.2.7 Cytochrome oxidase (CO)

Tissue slices were processed in the PELCO Biowave®Pro Microwave (Ted Pella Inc., Redding, CA). Antigen retrieval was performed in a 0.1 mM EDTA solution in Tris buffer, pH 9.0 for 5 min at 550 W with the vacuum cycling. Tissue was washed in a working imidazole buffer (5% imidazole buffer (0.2M), pH 9.0 and 16% sodium acetate (0.1M), pH 7.2) four times, one min/rinse at 150 W with the vacuum off. Tissue was then incubated in a 4% sucrose solution in working imidazole buffer for 5 min at 550 W with the vacuum cycling. The tissue was next incubated in a staining solution (0.05% DAB, 0.25% cytochrome c, and 4% sucrose in working imidazole) for 10 min at 200 W with the vacuum on. Tissue was then rinsed three times in working imidazole for 1 min/rinse with the vacuum off, followed by two rinses in PBS for 1 min/rinse with the vacuum off. The tissue slices were finally rinsed in a dilute PBS solution (1:4 PBS:H_2O) for 1 min

with the vacuum off before being mounted on gel-coated slides, cover-slipped, and imaged. For the CO study, 4 mice/group were used for wt + veh and wt + MPTP groups, and 6 mice/group were used for *Vgat*$^{flox/flox}$+ AAV-Cre-GFP + veh and *Vgat*$^{flox/flox}$+ AAV-Cre-GFP + MPTP groups.

2.2.8 Optical density analysis

Images of tissue processed for TH or CO were analyzed using Image-Pro Plus software (version 6.3, Media Cybernetics, Silver Spring, MD). 4-6 slices per animal extending throughout the rostro-caudal extent of the region of interest were analyzed. The region of interest was manually traced using an atlas for guidance and a computer-generated mean optical OD was recorded. Values were averaged to obtain a single OD value for each animal.

2.2.9 Cell surface counts

Counts of TH-immunoreactive cells in the SNpc were performed non-stereologically. This method may underestimate the number of cells, however recent comparisons of cell counting techniques provide evidence that it was an appropriate measure (Baquet, Williams, Brody, & Smeyne, 2009; Benes & Lange, 2001). We have recently reported that both stereological and cell surface counting methods resulted in identical findings (Churchill et al., 2017). Counts for each slice were averaged from 6 slices equally spaced throughout the rostrocaudal extent of the SNpc to obtain an average number of cells/animal for comparisons. For the cell counts, 5 mice/group were used for wt + veh and wt + MPTP groups, and 6 mice/group were used for *Vgat*$^{flox/flox}$+ AAV-Cre-GFP + veh and *Vgat*$^{flox/flox}$+ AAV-Cre-GFP + MPTP groups.

2.2.10 Electron microscopy

Tissue (2 slices/animal) was pre-embed processed for VGLUT1 (1:10,000 rabbit polyclonal, Synaptic Systems, Germany) as described above for TH/IHC. Tissue was then embedded in Epon-Spurs resin overnight at 60^{o}C. Blocks of the region of interest were thin sectioned using an Ultracut ultramicrotome (Leica, Buffalo Grove, IL) to 60 nm thickness using a diamond knife (Diatome, Hatfield, PA) and post-embed labeled with glutamate immunogold labeling. At least 2 thin sections/animal were obtained. Glutamate antibody (rabbit polyclonal, Sigma Chemical Co., St. Louis, MO) was incubated with thin-sectioned tissue overnight after being diluted 1:250 in tris-buffered saline with 0.1% Tween-20 (TBST), pH 7.6 with 1 mM aspartate before incubation with goat anti-rabbit IgG conjugated to 12 nm gold (Amersham, Arlington Heights, IL; diluted 1:25 in TBST, pH 8.2). Photographs of VGLUT-1 labeled terminals (10 terminals/animal) were taken randomly throughout the neuropil section at a final magnification of 40,000X within the area or layer of interest on a JEOL 1400 transmission electron microscope equipped with an AMT digital camera (Danvers, MA). We previously reported that incubation of the antibody with 3mM glutamate resulted in no immuno-gold labeling, showing the specificity of the glutamate labeling (Meshul et al., 1994).

To quantify glutamate labeling, the number of immunogold particles located within a DAB-labeled terminal were counted using Image-Pro Plus software. Particle counts were done automatically but checked and corrected manually as necessary. Additionally, terminal area was measured automatically by the software and the density of gold particles per square micron of nerve terminal area was calculated for each animal.

The density of gold particles/μm^2 of nerve terminal area for the vesicular/cytoplasmic and metabolic pools was determined for each animal and the mean density for each treatment group calculated. Background labeling was determined within glial cell processes and was found to be 10 immuno-gold-labeled particles/μm^2 (Meshul et al., 1994). This was subtracted from the density of presynaptic and dendritic spine immuno-gold-labeled glutamate within the nerve terminals and postsynaptic labeling within spines. The density of gold particles/μm^2 of nerve terminal or spine area was calculated for each animal. All EM experiments included 4 animals/group.

2.2.11 Microdialysis and sample collection

A week after guide cannula implantation, mice were lightly anesthetized with isoflurane and a microdialysis probe (3 mm with 1 mm membrane; Synaptech, Marquette, WI) was inserted through the guide cannula. Artificial cerebrospinal fluid (aCSF; 140 mM NaCl, 3.4 mM KCl, 1.5 mM $CaCl_2$, 1.0 mM $MgCl_2$, 1.4 mM NaH_2PO_4, and 4.85 mM $NaHPO_4$, pH 7.4) with 10 µM dexamethasone to reduce inflammation as established by Nesbitt et al. (2013) was perfused through the probe with a flow rate of 2.0 µl/min. After 30 minutes of acclimation, fractions were collected every 15 minutes for 1 hour. In order to remove glutamate transporter activity as a potential variable of glutamate levels, L-trans-pyrrolidine-2,4-dicarboxylic acid (PDC) was used after baseline levels were established. The PDC challenge (1 mM PDC in aCSF) was administered in the dialysis infusion and fractions were collected for an additional two hours. 0.2M H_3PO_4 was added to all fractions to prevent oxidation and dialysate samples were stored at -20^oC until analysis by high performance liquid chromatography (HPLC). 5 animals were used per group.

2.2.12 High performance liquid chromatography

Glutamate concentrations of dialysate fractions were determined using a modification of a previously reported method (Schuster, 1988). Briefly, dialysates were derivatized with o-phthalaldehyde (OPA) in borate buffer. The mixture was injected onto a reverse-phase C18 column (Zorbax C-18, Agilent, Santa Clara, CA) with a mobile phase consisting of a linear gradient of solvent A (0.018% (v/v) TEA and 0.3% (v/v) THF in 20 mM sodium acetate, pH 7.2) and solvent B (40% (v/v) acetonitrile, 40% (v/v) methanol, and 20% (v/v) 100 mM sodium acetate, pH 7.4). Glutamate derivatives were detected using an excitation wavelength of 240 nM and an emission wavelength of 450 nm.

2.2.13 Gait analysis

Analysis of gait was performed using a DigiGait treadmill (Mouse Specifics, Inc., Quincy, MA). The treadmill consists of a transparent, motor-driven belt with a high-speed digital camera positioned underneath for ventral plane videography. Gait was assessed a single time before MPTP administration and three days following the last dose of MPTP. Gait metrics studied were based on those previously found to be affected by MPTP administration (Goldberg et al., 2011) and consisted of stride length, stride frequency, stride duration, and stride length variability using software from Mouse Specifics, Inc. (Quincy, MA). 7 animals/group were tested for gait analysis.

2.2.14 Statistical analysis

All data are reported as the mean ± SEM unless otherwise noted. Three-way analysis of variance (ANOVA) was used to detect significant differences based on group, treatment, or hemisphere when appropriate using JMP statistical software. If hemisphere was not included in the analysis, a two-way ANOVA was used. If a significant effect was found,

a post hoc Tukey-Kramer HSD test was used to compare groups. Data involving a comparison of two groups was evaluated using a Student's t-test.

2.3 Results

2.3.1 Characterization of posited cortical disinhibition

To confirm placement and expression of the viral vectors, slices at the level of viral injection were processed immunohistochemically for GFP (Fig. 7). As expected, GFP expression was localized unilaterally to the motor cortex. Based on the number of sequential slices of the cortex, it is estimated that the viral injection affected a span of approximately 840 microns throughout the rostrocaudal extent of the motor cortex from AP=+2.42 to AP=+1.58 from bregma. Though only the interneurons in the motor cortex were affected by the viral injection [as the *Vgat* gene is floxed and therefore only cells that release GABA would be directly influenced, as previously described by Tong et al. (2008)], it is presumed that the attenuation of GABA inhibition onto cortical cell bodies projecting elsewhere throughout the brain would have effects that extend beyond the motor cortex. Therefore, an anterograde tracing experiment was conducted with BDA to determine regions receiving projections from this region of the motor cortex (Figure 8). Based on the hypothesized mechanism of potential protection, regions of particular interest were the striatum (Figure 8A), STN (Figure 8B) and SN (Figures. 8C, 8D), where bilateral BDA labeling was observed.

2.3.2 Behavioral changes after posited cortical disinhibition

All mice were evaluated for gait disturbances at the conclusion of the MPTP lesioning period using a DigiGait machine, but no significant differences were found between any of the groups (data not shown). Because the 78% loss in striatal TH expression

corresponds to TH loss at early-stage PD patients who exhibit subtle motor phenotypes (Kordower et al., 2013), this result is not wholly unexpected. In addition, *Vgat*$^{flox/flox}$ mice may not respond to MPTP in the same way as wt mice as they are not on a complete C57BL6/J background. We have not observed consistent gait deficits in our progressive model, although acute models do show motor dysfunction (Sedelis, Schwarting, & Huston, 2001). These results are discussed in more detail in the subsequent section.

2.3.3 Neuroprotection after posited cortical disinhibition

To examine the neuroprotective potential of *Vgat* deletion within the motor cortex, I deleted *Vgat* first before administering MPTP. This ensured that any changes in the basal ganglia took place before neurotoxic insult. We have previously shown that our progressive model reliably generates lesions similar to those observed in PD patients, notably a decrease in dorsolateral striatal TH expression and a loss of TH-expressing

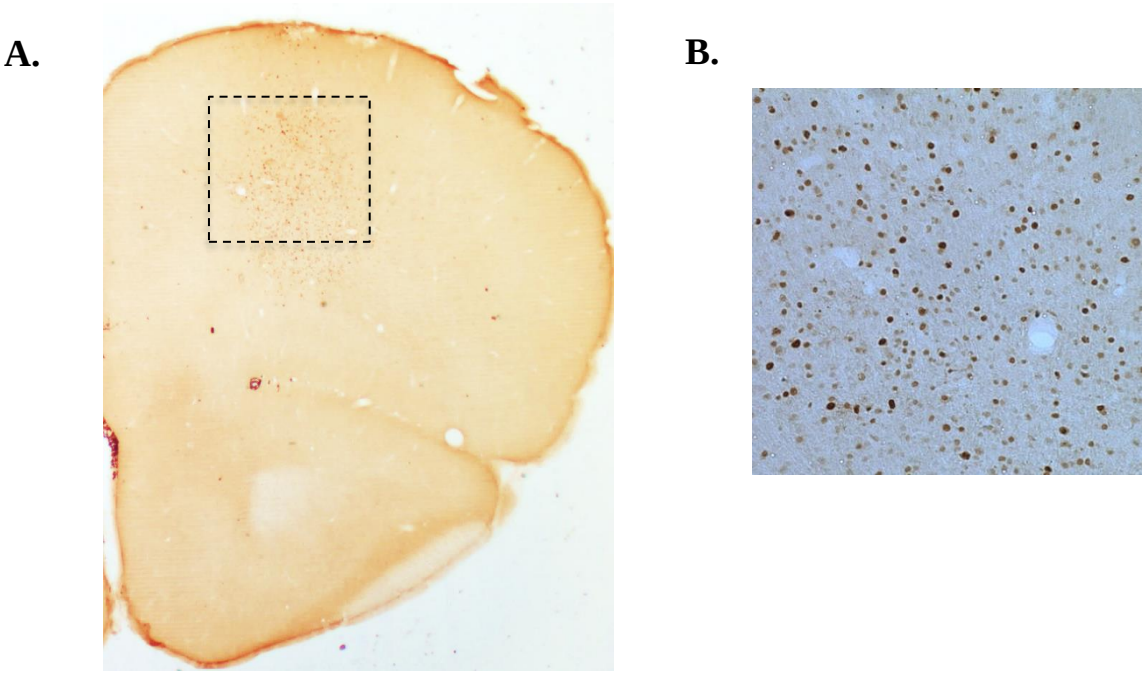

Figure 7. Cortical GFP expression
Photomicrograph showing unilateral GFP expression as visualized immunohistochemically with DAB **(A)** with the outlined area of interest enlarged for detail **(B)**.

cells in the SNpc (Goldberg et al., 2011). In keeping with previous findings, *Vgat*$^{flox/flox}$ animals that received AAV-GFP infusions into the motor cortex showed an 80% loss of TH optical density after MPTP compared to animals receiving vehicle injections, while wt animals showed a 78% decrease in TH expression after lesioning, suggesting that this

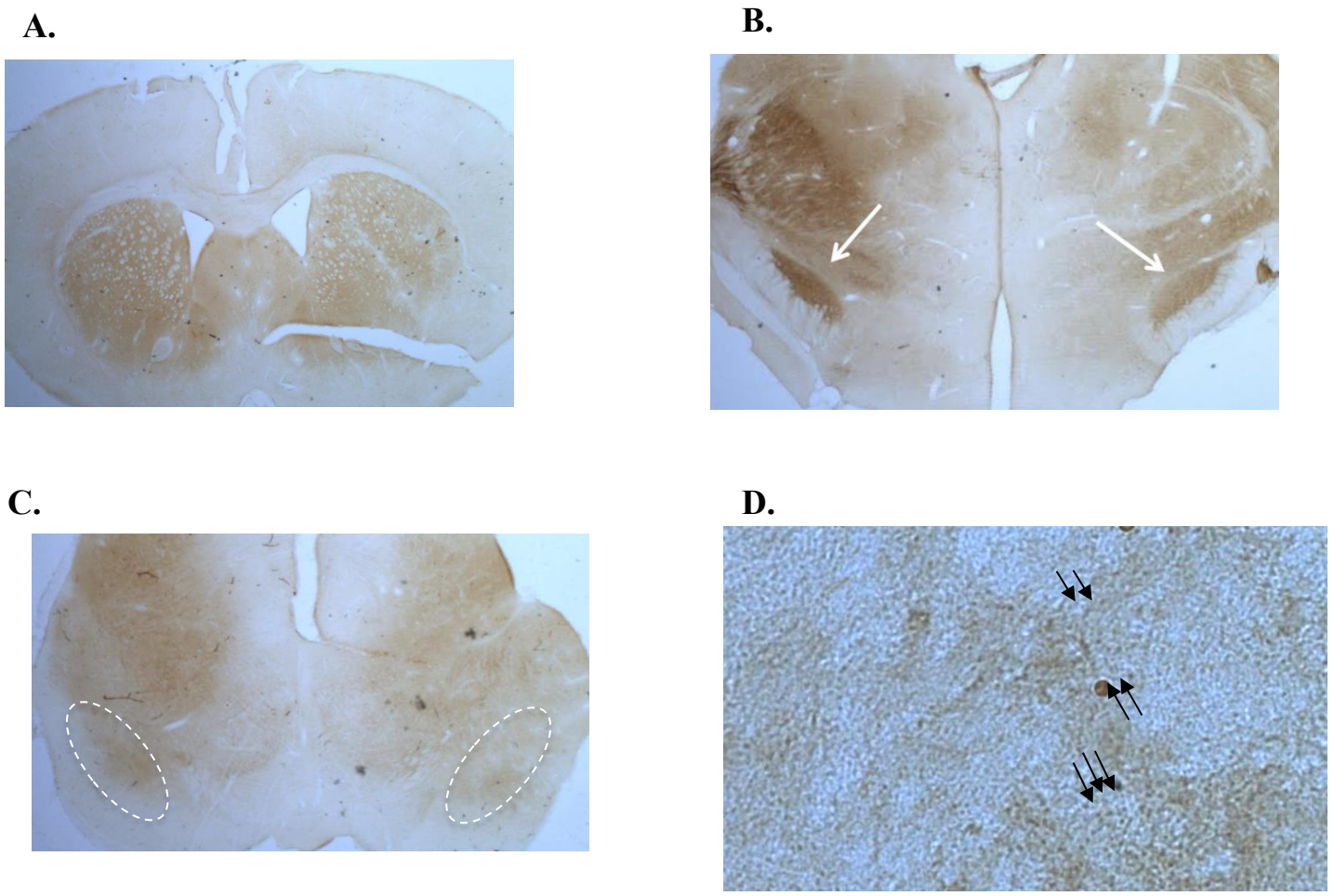

Figure 8. BDA tracing of cortical projections
Photomicrograph showing anterograde BDA transport from the injection site in the motor cortex to the striatum **(A),** STN **(B)** and SN **(C)** with an enlargement of SN labeling shown in **(D)**. BDA injections were made in the motor cortex to localize regions receiving projections from the targeted area. The cut side indicates the hemisphere contralateral to the viral injection in **(A).** Circled areas in **(C)** indicate the labeled SN, most likely SNpc based on dorsal labeling. Labeled terminals are designated by arrows in **(D).** The cut in the section pictured in **(A)** indicates the hemisphere contralateral to the viral injection.

Vgat$^{flox/flox}$ strain has a similar sensitivity to MPTP (Figure 9). As there was no differential sensitivity to MPTP as assessed by IHC and to maximize a limited number of *Vgat*$^{flox/flox}$ animals, wt mice were used as controls in all subsequent experiments.

Notably, while there was a main effect of group (vehicle vs. MPTP; $F_{1,56} = 12.31$, $p < 0.001$) and treatment (AAV-GFP vs. AAV-Cre-GFP; $F_{1,56} = 20.04$, $p < 0.0001$), a Tukey HSD post hoc test revealed no significant difference between the *Vgat*$^{flox/flox}$ + AAV-Cre-GFP vehicle and *Vgat*$^{flox/flox}$ +AAV-Cre-GFP MPTP groups ($p > 0.05$),

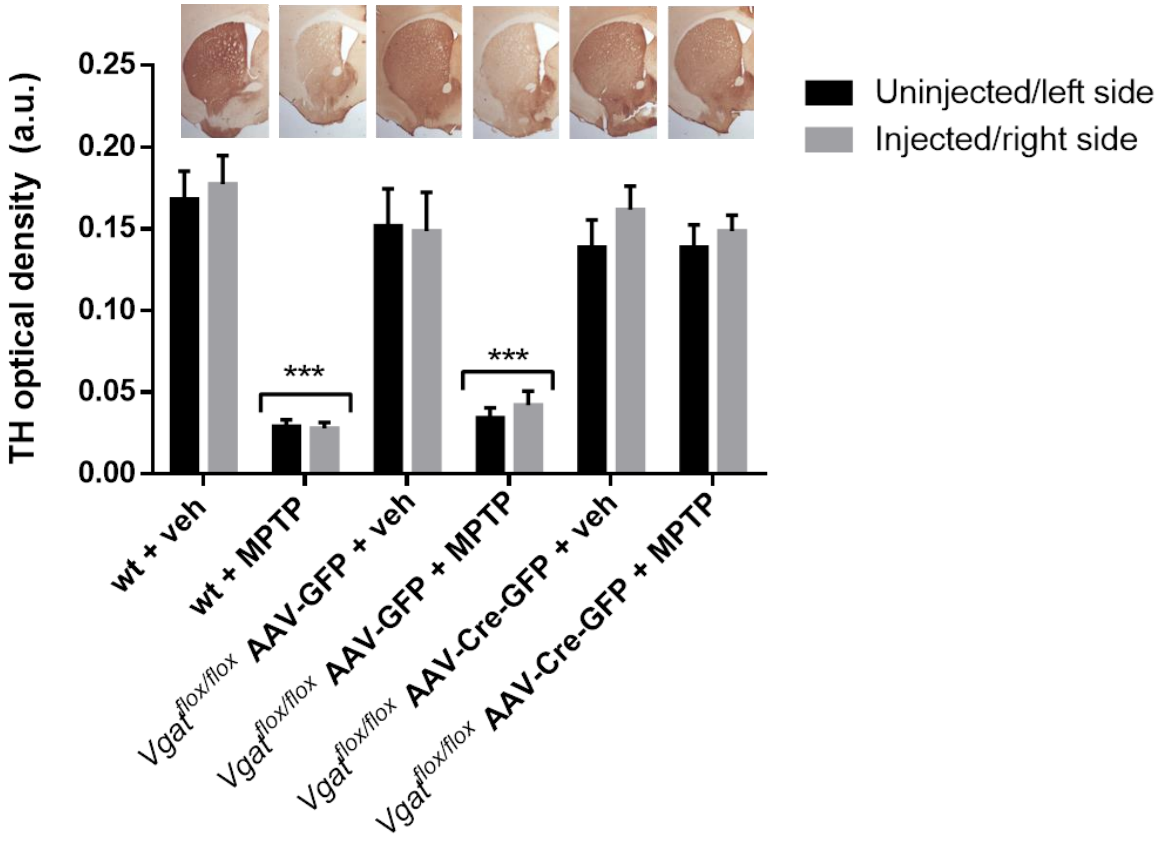

Figure 9. Striatal TH expression
Quantification of TH immunohistochemistry shows a main effect of group (veh vs. MPTP) and treatment (AAV-GFP vs. AAV-Cre-GFP) with a significant 78% decrease in dorsolateral striatal TH OD in wt mice after MPTP administration when compared to vehicle controls, but no significant difference between vehicle and MPTP groups in the *Vgat*$^{flox/flox}$ + AAV-Cre-GFP animals. TH OD in *Vgat*$^{flox/flox}$ + veh mice did not differ significantly from unlesioned wt + veh mice. Hemispheres were analyzed separately for all animals, but there was no significant difference between hemispheres in any group. *** denotes $p < 0.001$ compared to wt veh as assessed by Tukey HSD post hoc testing.

indicating that unilateral *Vgat* deletion in the motor cortex is completely and bilaterally protective against MPTP lesioning (Figure 9). The dorsolateral quadrants of the striatum ipsilateral and contralateral to the cortical AAV-Cre-GFP injection were analyzed separately to determine whether any protective effect was restricted to the hemisphere ipsilateral to the injection. Surprisingly, post hoc analysis indicated no significant difference between the TH expression between hemispheres of AAV-Cre-GFP-injected

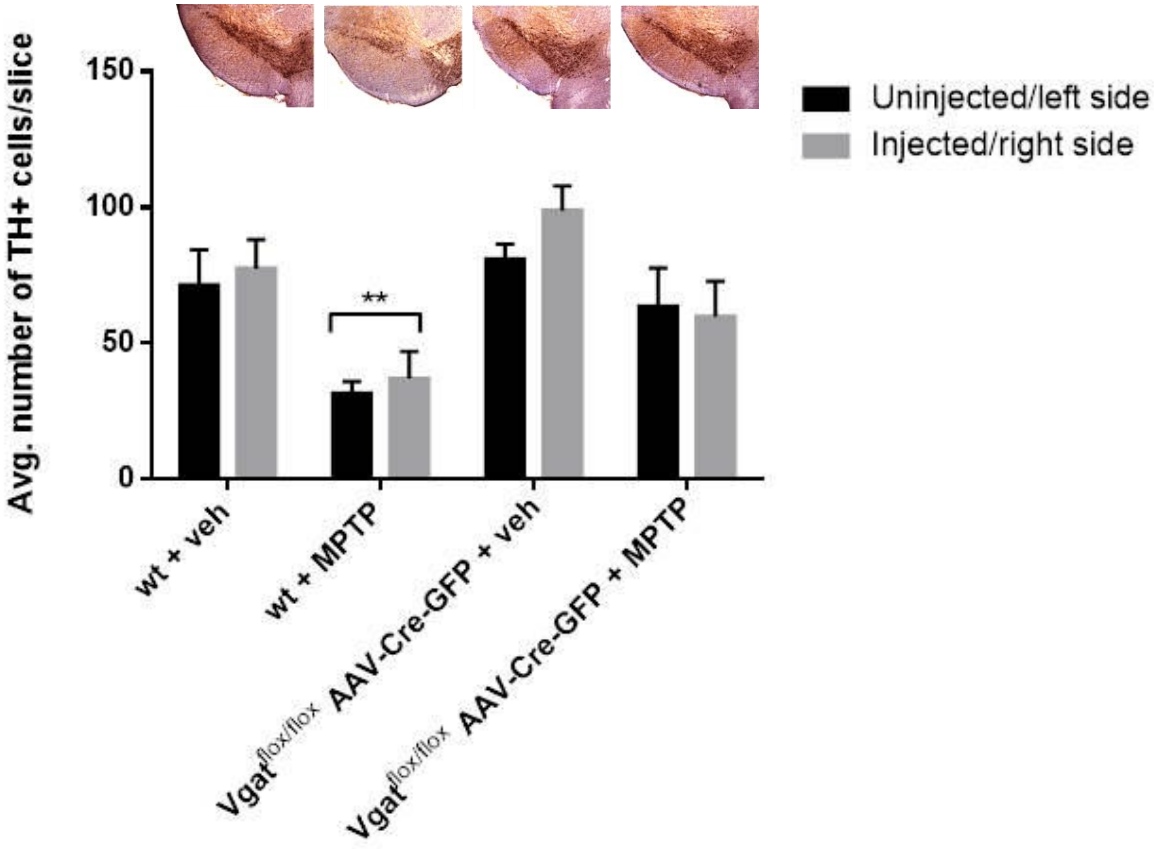

Figure 10. Cell surface counts of TH-immunoreactive SNpc cells
MPTP-lesioned wt mice showed a 54% decrease in TH-positive cells when compared to vehicle controls, but there was a trend towards a significant difference in the *Vgat*$^{flox/flox}$ + AAV-Cre-GFP mice between vehicle and MPTP groups. Hemispheres were analyzed separately for each animal and there was no significant difference between hemispheres. ** denotes $p<0.01$ compared to wt veh.

Vgat$^{flox/flox}$ mice, despite the fact that AAV-Cre-GFP was infused into only one side ($p = 0.556$).

Though preventing the loss of TH-positive nerve terminals in the striatum is crucial for normal basal ganglia function and provides evidence of protection against axonal degeneration, the prevention of loss of dopaminergic cell bodies in the SNpc is a vital target for both neuroprotection and neurorestoration. Therefore, loss of TH-immunolabeled cells in the SNpc was also used as a measure of neuroprotection. A three-way ANOVA showed a main effect of group (veh vs. MPTP; $F_{1,38} = 14.32$, $p < 0.001$), treatment (wt vs. cortical disinhibition; $F_{1,38} = 26.44$, $p < 0.001$), but not hemisphere ($F_{1,38} = 0.8841$, $p = 0.3530$). Post hoc analyses indicated that in wt animals, MPTP lesioning resulted in a significant 57% decrease in TH-positive cells compared to vehicle controls as measured by cell surface counts ($p < 0.01$). There is a strong trend towards a significant difference between the *Vgat*$^{flox/flox}$ vehicle and MPTP groups (Fig. 10, $p = 0.052$), suggesting that the protection of TH-positive SNpc cells conferred by posited cortical disinhibition may not be complete. However, there was no difference between the hemispheres ipsilateral or contralateral to the site of the viral injection, indicating that the unilateral *Vgat* knockdown has bilateral effects ($p = 0.721$).

2.3.4 Effects of posited cortical disinhibition on corticostriatal glutamate

In an effort to investigate whether the deletion of *Vgat* from the motor cortex resulted in an alteration of the activity of the corticostriatal pathway, based on the density of projections from the area of AAV-Cre-GFP infusion in the cortex to the striatum (Figure 8A), glutamate immunogold labeling was used to investigate changes in presynaptic terminal glutamate levels. It has previously been shown that following

dopamine depletion, there are changes in striatal glutamate levels, both within the terminal and extracellularly (Meshul et al., 1999). Previous studies of the striatum have shown a time-dependent change in glutamate levels after an acute unilateral 6-OHDA lesion of the nigrostriatal pathway, with a decrease in nerve terminal glutamate density 1 month after the lesion but an increase after 3 months as determined by quantitative immuno-gold labeling (Meshul et al., 1999). Microdialysis data showed inverse changes compared to the glutamate immunogold density results—an increase in extracellular glutamate levels at 1 month and a decrease at 3 months—suggesting a potential time-dependent alteration in striatal glutamate release (Meshul et al., 1999). Because of the dynamic changes in striatal glutamate after lesioning, it is conceivable that our progressive MPTP model would also result in changes in glutamate regulation that could potentially be attenuated by activation of the corticostriatal pathway.

In addition to the aforementioned rationale, I investigated the striatum of the *Vgat*$^{flox/flox}$ mice as a way of validating that *Vgat* deletion in the motor cortex could alter signaling in the striatum via the corticostriatal pathway. Nerve terminal glutamate immunogold particle density did not change significantly after MPTP ($F_{1,13} = 1.729$, $p = 0.2113$), nor was there any change in gold particle density in the *Vgat*$^{flox/flox}$ animals compared to wt controls (Fig. 11; $F_{1,13} = 0.7744$, $p = 0.3948$). *In vivo* microdialysis of the dorsolateral striatum also showed no difference in extracellular glutamate in MPTP animals when compared to vehicle controls at baseline (veh = 0.788 ± 0.173 pmol/µL, MPTP = 0.543 ± 0.115 pmol/µL). To remove glutamate transporter activity as a potential variable of glutamate levels, L-trans-pyrrolidine-2,4-dicarboxylic acid (PDC) was used after baseline levels were established, but there were no differences between extracellular

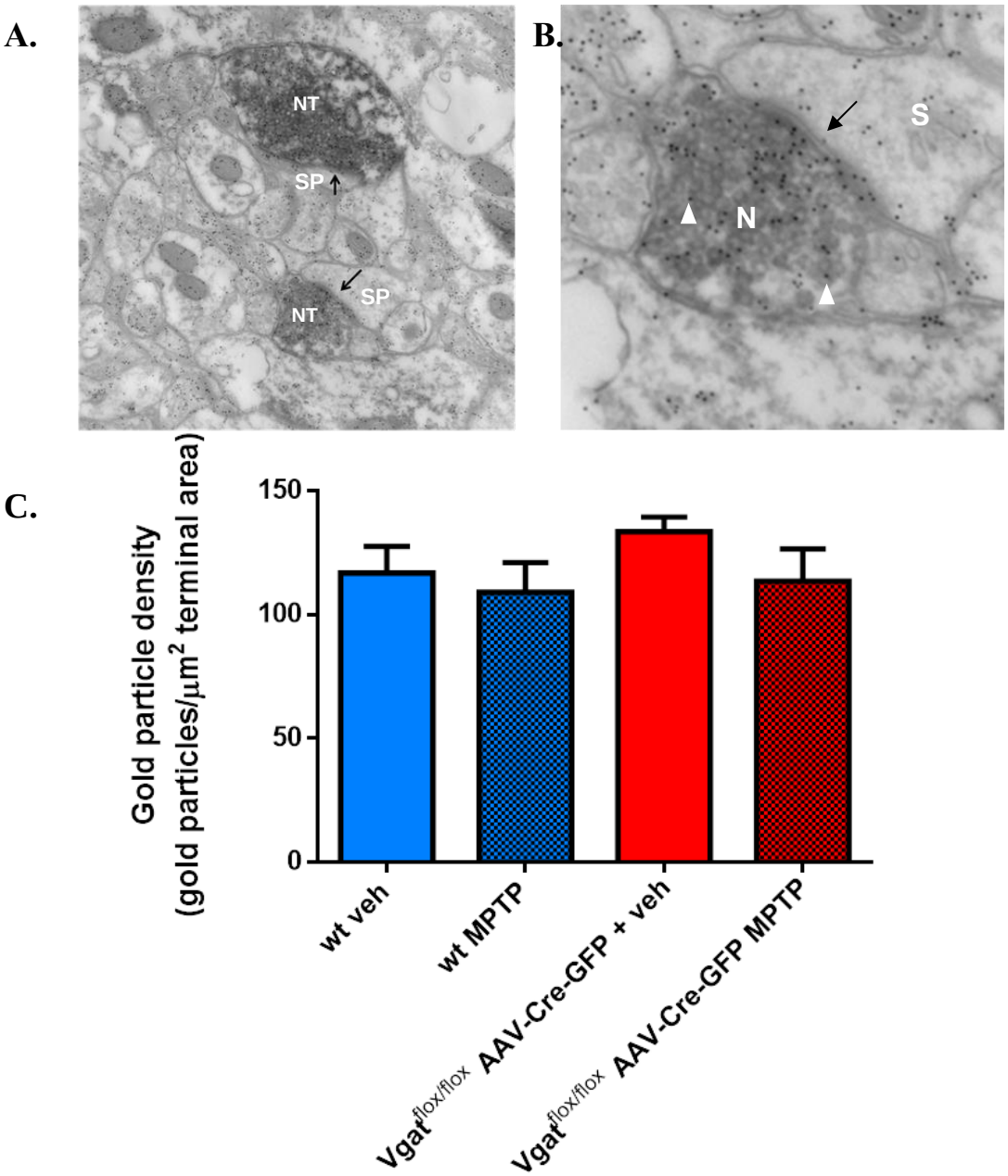

Figure 11. Striatal glutamate immunogold density
A representative electron micrograph **(A)** showing two striatal DAB-labeled VGLUT1-positive nerve terminals with arrows indicating synaptic contact onto dendritic spines. **(B)** shows an enlargement of one terminal with gold particles, indicating the localization of the glutamate antibody. Analysis was conducted by tracing the perimeter of the terminal and counting the number of gold particles contained within the terminal. A quantification of the particle density per square micron is shown in **(C)**. There were no significant differences between groups ($p>0.05$). NT denotes the nerve terminal, SP denotes the dendritic spine, black arrows indicate synaptic contacts, and white arrowheads indicate gold particles.

glutamate animals during the PDC challenge (veh = 1.87 ± 0.410 pmol/µL, MPTP = 1.25 ± 0.390 pmol/µL, p = 0.641; Fig. 12). The discrepancy between these results and those previously published could be due to differing toxin models (acute 6-OHDA vs. chronic MPTP) utilized in the studies and is discussed in the subsequent section.

I also examined changes in nerve terminal glutamate immuno-gold density in the motor cortex, where the loss of GABAergic inhibition might more directly influence glutamate transmission. Although the viral injections targeted the deeper cortical layers containing pyramidal neurons, I analyzed glutamate terminals in layer II. As reviewed by Huang (2014), specific types of layer V interneurons send projections to layer II. Layer II also contains the horizontal cortico-cortical interhemispheric connections (i.e., VGLUT1-positive terminals) and collaterals of layer V pyramidal neurons. Additionally, we have previously shown that glutamate terminals in layer II but not layer V are

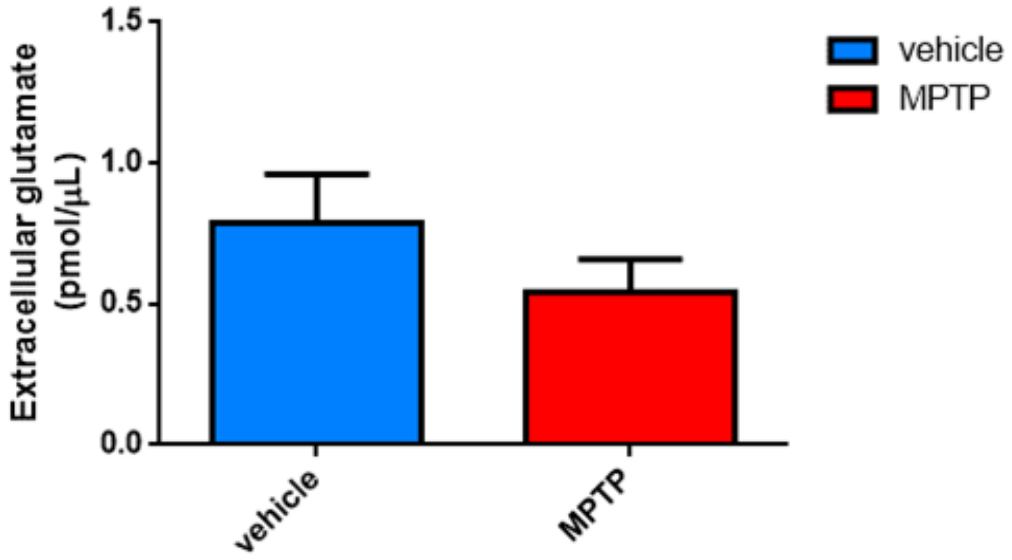

Figure 12. Changes in dorsolateral striatal glutamate extracellular levels as assessed by *in vivo* microdialysis
There was no significant difference between vehicle or MPTP-lesioned wt animals ($p > 0.05$).

sensitive to acute dopamine loss following unilateral infusion of 6-hydroxydopamine into the medial forebrain bundle (unpublished data). There were no significant main effects of either MPTP (Fig. 13; $F_{1, 14} = 2.678$, $p = 0.1035$) or posited cortical disinhibition ($F_{1,14} = 0.2033$, $p = 0.6590$), suggesting that *Vgat* deletion in GABA interneurons in the motor cortex is protective by some other mechanism than changing the levels of glutamate within the corticostriatal pathway or even within the motor cortex itself.

2.3.5 Assessment of SN activity after posited cortical disinhibition

As it was hypothesized that posited cortical disinhibition would primarily innervate the corticostriatal pathway, only striatal tissue was processed for EM. After no change in striatal glutamate was detected, other regions were assessed to determine if local activity was altered by posited cortical disinhibition. Due to the non-transient nature of the gene deletion and small temporal resolution of immediate-early gene (IEF) expression, typical indicators of neuronal activity such as c-fos and zif were not appropriate for use in our model. Therefore, CO, an enzyme necessary for electron transport and ATP synthesis, was used as a longer-term marker of neuronal activity in the same manner as Mendez-Lopez et al. (2013) and described in more detail by Wong-Riley (1989). A two-way ANOVA demonstrated a main effect of MPTP (Fig. 14; $F_{1,17} = 7.877$, $p = 0.0121$). Post hoc analyses indicated that the CO OD of the SN of lesioned wt mice had a significant 60% decrease in CO OD ($p = 0.0002$). This decrease was partially attenuated in the lesioned $Vgat^{flox/flox}$ animals, with the posited cortical disinhibition group showing a significant increase in CO OD compared to lesioned wt animals ($p = 0.0231$). The implications of these results are explored in more depth in the subsequent section.

Based on the pattern of labeling, it was impossible to accurately discriminate between the SNpr and SNpc in the analysis.

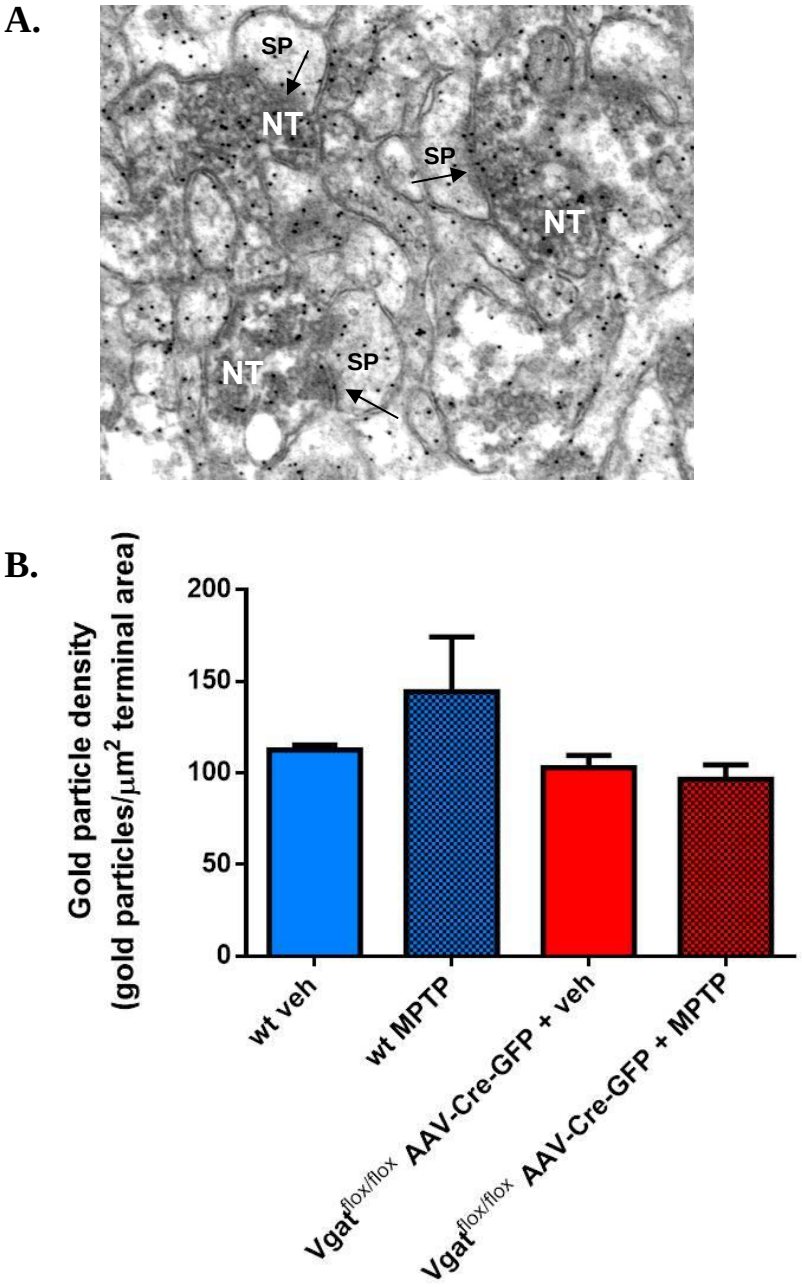

Figure 13. Cortical glutamate immunogold density
A representative electron micrograph of VGLUT-1 positive terminals in layer II of the motor cortex **(A),** with arrows indicating synaptic contacts of DAB-labeled terminals with dendritic spines (SP). Analysis of gold particle density **(B)** in layer II of the motor cortex showed no significant effect of MPTP or cortical disinhibition. Layer II was selected as it has previously been shown to be sensitive to DA denervation. NT denotes the nerve terminal, black arrows indicate synapses, and white arrowheads indicate gold particles, indicating the localization of the glutamate antibody.

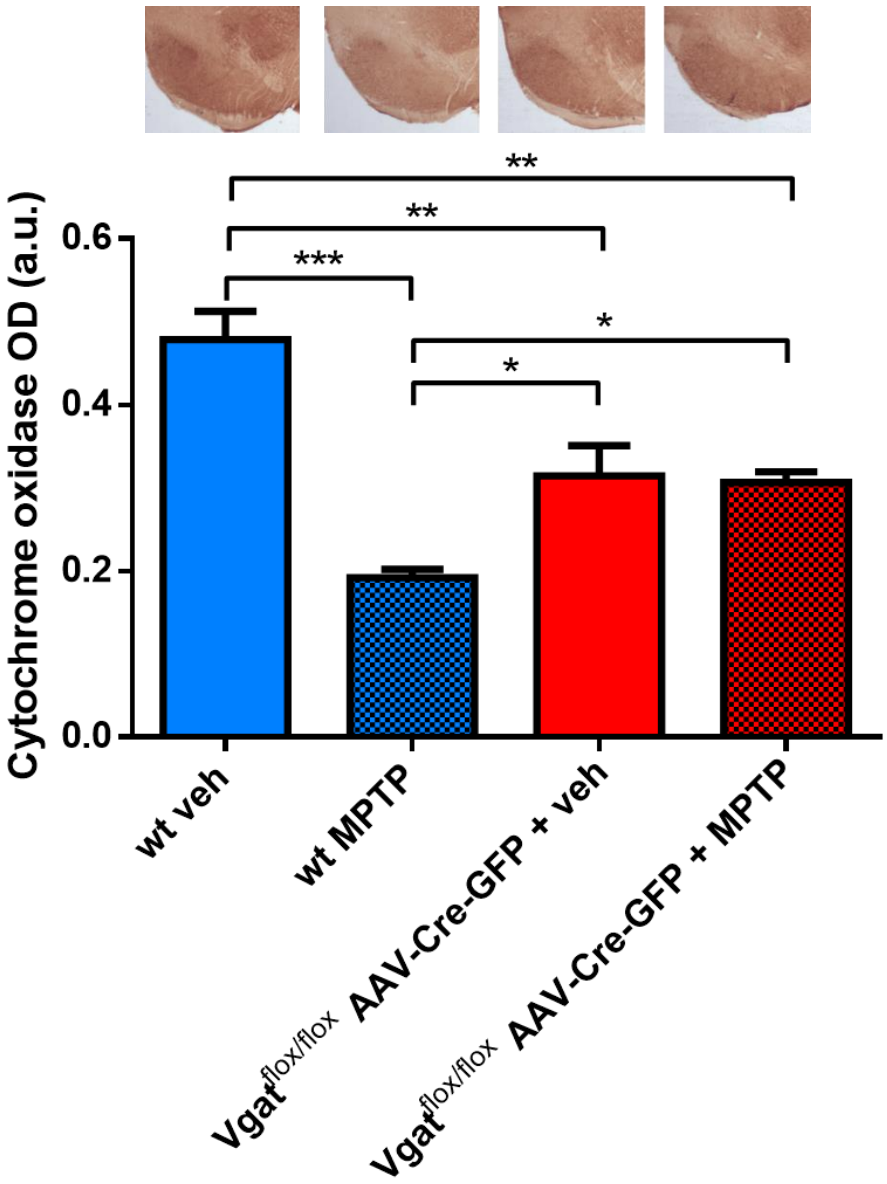

Figure 14. SN cytochrome oxidase
CO OD of the SN shows a 60% decrease in wt animals after MPTP lesioning compared to vehicle controls, indicating a decrease in metabolic activity. *Vgat*$^{flox/flox}$ animals that were lesioned showed a significant 36% decrease in CO OD compared to wt vehicle animals, but CO OD was still significantly higher in lesioned *Vgat*$^{flox/flox}$ animals than lesioned wt animals. * denotes $p < 0.05$, ** denotes $p<0.01$, *** denotes $p<0.001$.

2.4 Discussion

I have shown that unilateral deletion of *Vgat* in the motor cortex is bilaterally protective against progressive MPTP lesioning. Admittedly, concrete evidence of the extent of the VGAT protein decrease has not yet been shown in this study, although it has been verified by others (Tong et al., 2007) and we have shown that AAV-Cre-GFP injections result in an accumulation of GABA in nerve terminals (Fig. 5). The mechanism of protection remains to be elucidated, although the initial experiments described in this study provide potential pathways of neuroprotection. The bilateral effect of *Vgat* deletion was unexpected based on previous studies (Berretta et al., 1997), although these results are consistent with bilateral projections observed by BDA transport.

Less clear, however, is the mechanism by which the deletion of *Vgat* is neuroprotective. The initial hypothesis that *Vgat* deletion would increase the activation of the corticostriatal pathway by disinhibiting the motor cortex was not supported by the assessment of either presynaptic or extracellular striatal glutamate levels. Based on previous research that showed pharmacological inhibition of $GABA_A$ receptors in the motor cortex results in activation of both the motor cortex and striatum as assessed by cFos expression (Berretta et al., 1997), it was expected that activation of the corticostriatal pathway resulting from a loss of GABAergic interneuron activity would result in an alteration of glutamate signaling in either the motor cortex or striatum, but this was not detected by our analyses. Because of temporal differences between *Vgat* deletion and pharmacological $GABA_A$ blockade (i.e., 3 months versus immediate, respectively), it is not feasible to use cFos as a marker of activity in our studies as Berretta et al did (1997). It is possible that there was a change not in glutamate levels but

in the expression of glutamate transporters; this mechanism will be explored by western blot analysis of the striatum of *Vgat*$^{flox/flox}$ mice in future experiments. Additionally, electrophysiological experiments could elucidate changes in glutamate signaling in the motor cortex and are currently being considered.

Though there was no evidence of corticostriatal activation following infusion of AAV-Cre-GFP into the deeper layers of the motor cortex, the CO results potentially implicate the corticonigral pathway as underlying the observed neuroprotection. There was a decrease in CO OD within the SN in lesioned wt mice, and this decrease was attenuated in the *Vgat*$^{flox/flox}$ MPTP mice, indicating a possible activation of the corticonigral pathway. The decrease in SN CO contradicts the expected change in activity; the canonical model of basal ganglia circuitry alterations suggests an overactivation of the SN due to increased activity of the subthalamic nucleus (Maurice, Thierry, Glowinski, & Deniau, 2003). However, unpublished data from our lab corroborates the decrease in activity of the STN following loss of nigrostriatal dopamine. Microdialysis data indicate that there is a decrease in extracellular glutamate in mice progressively lesioned with MPTP compared to controls (Neubert, unpublished data from our lab), and western blot analysis of the SN shows a decrease in the vesicular glutamate transporter 1 (VGLUT1) protein but not the vesicular glutamate transporter 2 (VGLUT2) expression in our progressive model (Churchill & Sconce, unpublished data from our lab). Because VGLUT1 is solely expressed in terminals projecting from the cortex, while nerve terminals originating from primarily the STN express VGLUT2, our data suggest that a decrease in SN activity is potentially attributable to either a degradation of corticonigral projections or a decrease in activity of the pathway, leading to decreased

glutamate release and a subsequent downregulation of VGLUT1. Therefore, the increase in CO OD in lesioned *Vgat*$^{flox/flox}$ animals compared to lesioned wt animals provides a potential mechanism of neuroprotection by activation of the corticonigral pathway (Fig. 15). Because activation has been shown to be necessary for the continued viability of midbrain dopaminergic neurons (Salthun-Lassalle et al., 2004), it is possible that potential increased excitatory input to the SN results in protection against neurotoxic insult. Alternatively, activation of the hyperdirect pathway (cortex to STN) could also provide a potential explanation for the observed results whereby activation of the STN leads to a subsequent activation of the SN through direct excitatory STN-SN projections

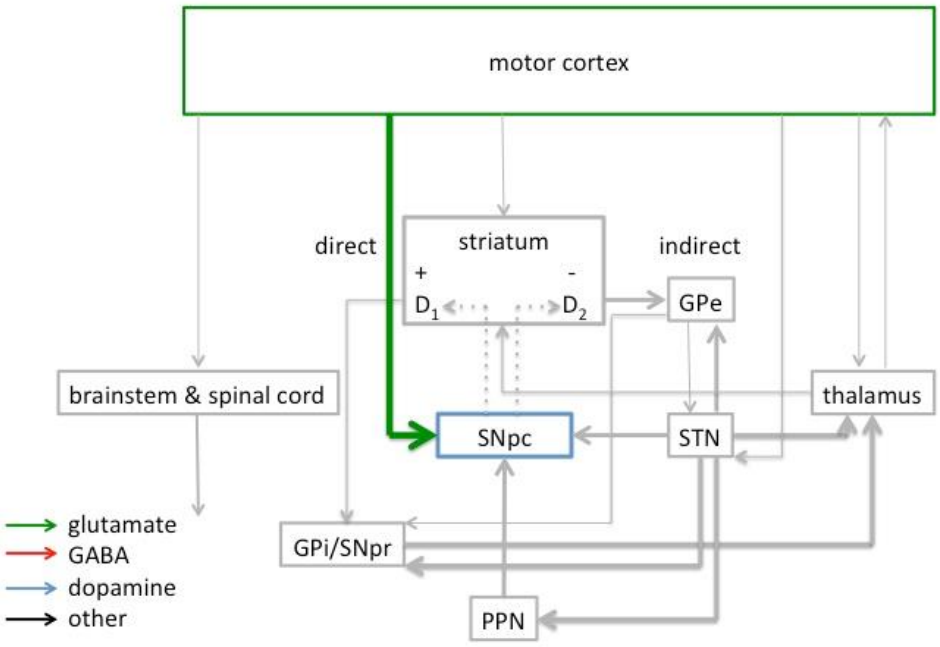

Figure 15. Basal ganglia circuit diagram with proposed mechanism of corticonigral activation. As there is a direct corticonigral projection, it is possible that disinhibition of the motor cortex results in an activation of the corticonigral pathway and an increase in activity of the SNpc (as assessed by cytochrome oxidase).

(Fig. 16). Future studies using EM analysis to investigate changes in glutamate in VGLUT1-positive terminals of the SN can elucidate whether potential alterations in either the corticonigral or hyperdirect pathways are affected by *Vgat* deletion.

This hypothesis assumes some deviations from the canonical basal ganglia circuitry alterations in PD, namely, the decrease in SN CO (and presumable activity) after MPTP lesioning. This contradicts the predicted change in SNpr activity in PD models, but CO is only one technique of understanding regional activity. The use of other methods, such as

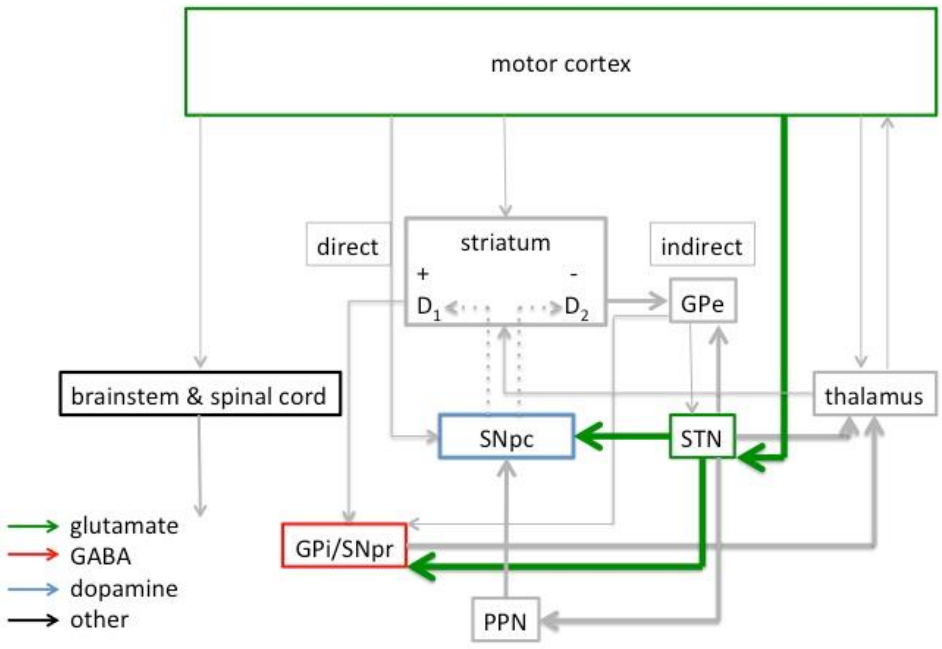

Figure 16. Basal ganglia circuit diagram with proposed mechanism of SN activation via the hyperdirect pathway. An alternative explanation of the data could be that disinhibition of the motor cortex activates the hyperdirect pathway, resulting in an increase in glutamatergic signaling from the STN to the SNpc that is consistent with the cytochrome oxidase results.

EM or electrophysiology, could enable a better understanding of the changes undergone

in the SNpr after MPTP administration. Additionally, emerging evidence suggests that alterations in the basal ganglia circuitry are not always consistent with the predicted changes. Classically, the GPe is considered to be less active in PD, although Chesselet (1996) suggests that there is no change in GPe activity after nigrostriatal lesions in rats and Nambu et al. saw no change in GPe activity in MPTP-lesioned macaques (unpublished data presented at IBAGS meeting, 2018). The widely held belief that PD results in hyperactivity of the STN has also recently been disputed; recent data suggest that changes in firing rate and pattern, rather than activity, underlie motor dysfunction in PD (Wilson & Bevan, 2011). Different models of PD have been shown to result in varying alterations to the basal ganglia, adding another complication to understanding specific changes that occur in PD.

The discrepancy between the microdialysis results in this experiment and the previously cited study (Meshul et al., 1999) can be explained by the fundamental differences between the PD models. The model used in the current study is a progressive model that results in a gradual but stable bilateral dopamine cell and terminal loss (Goldberg et al., 2011), whereas the Meshul et al. (1999) study used an acute unilateral toxin model that results in time-dependent synaptic changes, along with severe dopamine terminal and cell loss (>90%). I believe that the gradual lesion of the progressive model allows time for neuroadaptations that do not occur in acute models, resulting in varying changes within the brain as a response to the different types of models. Therefore, it is not surprising that the current study did not show the same changes in glutamate as assessed by microdialysis that has previously been shown.

In terms of behavior, many models of PD result in motor deficits, often measured by impaired Rotarod performance, gait disturbances, anosmia (loss of smell), and decreased locomotion, among others (Sedelis et al., 2001). However, PD models that generate detectable motor deficits are typically acute toxin models, resulting in severe dopamine loss and are equivalent to that seen in the end stage of the disease in PD patients. Because of the progressive nature of the model used in this study, it is possible that neuroadaptations throughout the time of lesioning result in mice that appear motorically intact. The amount of cell loss generated in the progressive model correlates with cell loss in preclinical PD patients (Leenders et al., 1986), suggesting that MPTP-lesioned mice have a very subtle phenotype. It is therefore not unexpected that I did not see any differences in gait between the groups.

While complete bilateral protection is an exciting finding, neuroprotection is not a viable therapeutic option for PD patients. To be truly translationally relevant as a treatment, we must show evidence of neurorestoration after cell loss has already occurred. The neurorestorative potential of *Vgat* deletion will be assessed in future experiments by first lesioning mice and then deleting the *Vgat* gene. Additionally, the potential mechanism of protection by activation of the corticonigral pathway will be further explored, providing a potentially novel therapeutic target for PD.

Chapter 3: Neurorestorative potential of posited cortical disinhibition in a progressive MPTP model of PD

3.1 Introduction

Parkinson's disease (PD) is a progressive neurodegenerative disorder characterized by symptoms including bradykinesia, impaired gait, rigidity, resting tremor, and cognitive impairments. The hallmark pathology underlying these symptoms is a progressive loss of dopaminergic cells in the substantia nigra pars compacta (SNpc) and their projections that terminate in the striatum. The striatum, specifically its medium spiny neurons (MSNs) that express D1 or D2 receptors, is the point at which the motor system differentiates into two pathways, the direct and indirect pathways. The loss of dopaminergic tone in the striatum differentially affects these two pathways, but results in an ultimate dysregulation of the basal ganglia and consequent motor dysfunction (Obeso et al., 2008).

As the signaling between nuclei of the basal ganglia is altered in PD, the output signal to the brain stem and spinal cord via the motor cortex is also disrupted. Reciprocal projections from the motor cortex back to areas of the basal ganglia, most notably the striatum and subthalamic nucleus (STN), become dysfunctional as a consequence of dopamine denervation.

Calabresi et al. (1999) have demonstrated that a unilateral lesion of the rat substantia nigra (SN) results in a disruption of corticostriatal signaling in the ipsilateral hemisphere. Striatal MSNs exhibit a loss of spines after lesioning of the nigrostriatal pathway, resulting in a decrease in the overall number of glutamatergic corticostriatal

synaptic contacts (Day et al., 2006). Interestingly, animal models of PD have yielded data suggesting that spine loss occurs differentially in direct- and indirect-pathway neurons, potentially compounding the dysregulating effects of dopamine denervation (Day et al., 2006; Mallet, 2006).

The pathway between the motor cortex and subthalamic nucleus, referred to as the hyperdirect pathway, also undergoes significant changes in PD. Recordings from the STN in MPTP-treated African green monkeys revealed a significant increase in the firing rate of the STN compared to baseline (Bergman, Wichmann, Karmon, & DeLong, 2017), and Hassani et al. (1996) demonstrated similar findings in 6-OHDA-lesioned rats. Resting state fMRI studies in early-stage PD patients have revealed an increase in functional connectivity between the motor cortex and STN in accordance with the animal models, suggesting that this pathway is relevant in the pathology and potentially in the treatment of PD (Baudrexel et al., 2011).

Because activation, excitability, and functional connectivity of the motor cortex have all been found to be altered in PD (Chen, Kumar, Garg, & Lang, 2001; Ridding et al., 1995; Wu et al., 2011, 2009), it is a promising target in PD to not only directly address the cortical dysfunction observed in both PD patients and models (Goldberg et al., 2002; Lefaucheur, 2005), but to also target downstream regions of the basal ganglia that receive projections arising from the motor cortex.

Targeting the motor cortex to alleviate PD symptoms has been previously studied and found to be effective (Canavero et al., 2002; Lefaucheur et al., 2004). Lefaucher et al. (2004) reported that repetitive transcranial magnetic stimulation (rTMS) unilaterally targeting the motor cortex was able to reduce motor dysfunction, with low-frequency

stimulation eliciting bilateral effects. Unfortunately, the improvement was transient and limited to a short time after stimulation had ended (Lefaucheur et al., 2004). Khedr et al. (2003) have reported that 10 daily rTMS sessions targeting the motor cortex result in an improvement in motor dysfunction that is still significant a month after stimulation has stopped, but this is still not a long-term solution for a disease that progresses over the course of decades. Direct stimulation of the motor cortex by electrodes has been found to be beneficial in both a primate model of PD as well as PD patients (Canavero & Paolotti, 2000; Canavero et al., 2002; Drouot et al., 2004), but these studies have performed limited interrogation, if any, into potential neurobiological changes that underlie behavioral improvement.

Therefore, I propose using a progressive mouse model of PD to see if alteration of cortical activity can elicit both behavioral and neurobiological recovery. The previous study (Chapter 2) demonstrated that posited cortical disinhibition is protective, but this study design cannot assess the potential of posited cortical disinhibition to elicit recovery after lesioning has already occurred. While the mechanisms of protection and restoration are not assumed to be the same, this study provided an opportunity to more completely investigate downstream changes in glutamatergic signaling to projection targets of the motor cortex beyond the striatum (which exhibited no changes in nerve terminal glutamate immunogold density after posited cortical disinhibition in chapter 2).

I hypothesized that posited cortical disinhibition would also be effective in a restorative study design. By using a lox-Cre system to prevent inhibitory GABAergic signaling in the motor cortex, I disinhibited the motor cortex and was able to further investigate the downstream effects. I hypothesized, based on previous findings, that

posited cortical disinhibition would reduce motor dysfunction by altering tyrosine hydroxylase (TH) expression and glutamatergic signaling in the basal ganglia. Based on the known alterations within the basal ganglia that affect both the striatum and the STN and the dense innervation of both of these regions by the motor cortex, I predict that glutamatergic signaling as assessed by glutamate immunogold labeling in terminals arising from the motor cortex will be altered, providing a potential mechanism to explain the observed benefit of cortical stimulation observed in other models.

3.2 Methods

3.2.1 Animals

Male *Vgat*$^{flox/flox}$ mice (on a combination 129, FVB, and C57BL6/J background), kindly provided by Dr. Patrick Fuller, were used for all experiments. All animals were group housed with littermates and maintained on a 12-hr light/dark cycle (lights on at 07:00, lights off at 19:00) with *ad libitum* access to water and chow. All experiments were carried out in accordance with federal guidelines of the Public Health Service Policy on the Humane Care and Use of Laboratory Animals and with approval by the Portland VA IACUC. Aged animals used for the restoration study were aged to 13 months before experiments began, while animals used in subsequent electron microscopy experiments were 8 weeks old.

3.2.2 Experimental design

To replicate the clinical experience in which patients do not receive treatment until after significant cell loss is present (Kordower et al., 2013), mice were first treated with MPTP before the posited cortical disinhibition took place. MPTP administration occurred over 4 weeks. Mice were given 72 hr after the last MPTP injection to recover and expel potential

toxic MPTP metabolites and then underwent intracranial injections. Two cohorts of mice, one having received vehicle injections and the other having received MPTP injections, were removed 72 hr after the last MPTP injection and euthanized to determine baseline differences between groups before the intracranial injections and 8-wk waiting period (i.e., post viral infusion). These animals, referred to as the "4 week" group, were tested behaviorally 72 hr after the last MPTP injection. All other animals were behaviorally tested 8 wks after intracranial surgeries. Each group was divided in half at each endpoint with half being perfused with fixative and used for immunohistochemistry and electron microscopy analysis and the other half of the animals being used for western blots.

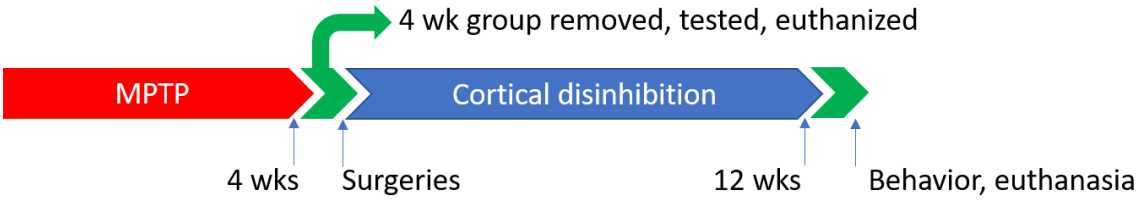

Figure 17. Schematic of neurorestoration study timeline
Mice underwent MPTP lesioning for 4 weeks followed immediately by surgeries to disinhibit the cortex. 8 weeks after surgeries, mice were behaviorally tested and euthanized. An additional cohort was removed immediately after MPTP administration to assess TH loss and ensure no spontaneous recovery occurred over the subsequent 8 weeks.

3.2.3 MPTP Administration

Mice were injected intraperitoneally 5 days/week with progressively higher doses of MPTP (Santa Cruz Biotechnology, Dallas, TX) for 4 weeks. Mice were given 10 mg/kg during week 1, 16 mg/kg during week 2, 24 mg/kg during week 3, and 32 mg/kg during week 4. Normal saline was used as a vehicle.

3.2.4 Viruses

AAV9.hSyn.eGFP.WPRE.bGH (1 x 10^{14} GC/ml) and AAV9.hSyn.HI.eGFP-Cre.WPRE.SV40 (5.5 x 10^{13} GC/ml) were obtained from the Penn Vector Core (University of Pennsylvania, Philadelphia, PA) and are referred to as AAV-GFP and AAV-Cre-GFP, respectively, for brevity. Both viruses were diluted in PBS to 1 x 10^{12} GC/ml immediately before being used.

3.2.5 Intracranial surgeries

When the animals were appropriately aged, they were anesthetized with isoflurane and placed in a mouse stereotaxic frame (Kopf Instruments, Tukunga, CA). A midline incision was made and a unilateral burr hole was drilled over the motor cortex (AP=+2.0mm, ML=-1.5mm, DV=-1.0mm from bregma; Paxinos and Franklin, 2004). A glass pipette containing AAV- GFP or AAV-Cre-GFP was lowered to the desired coordinates and the contents were infused slowly at a rate of 0.1 µL/min until 150 nL were injected. After the injection, the pipette was left in place for 5 min to allow for diffusion of the solution. Coinjections of virus (diluted to 1 x 10^{12} GC/ml) and biotinylated dextran amine (BDA; 10,000 MW diluted to 10%; Life Technologies, Grand Island, NY) were performed as described above for EM studies. Mice were allowed to recover for 2 weeks after coinjections before being euthanized.

3.2.6 Grip strength analysis

Forepaw grip strength was assessed using a grip strength meter (Columbus Instruments, Columbus, OH). Mice were held by their tails and lifted to the level of a grid attached to the meter. Once they had grasped the bar, they were gently pulled back until they released the bar and the maximum force generated was recorded. The mice were tested

three times each and the forces were averaged to generate a value for each mouse. 11 veh + AAV-GFP mice, 10 veh + AAV-Cre-GFP mice, 11 MPTP + AAV-GFP mice, and 10 MPTP + AAV-Cre-GFP mice were tested.

3.2.7 Gait analysis

Analysis of gait was performed using a DigiGait treadmill (Mouse Specifics, Inc., Quincy, MA). The treadmill consists of a transparent, motor-driven belt with a high-speed digital camera positioned underneath for ventral plane videography. One end of the DigiGait apparatus was elevated approximately 8 inches above the ground to introduce a declined running platform and exacerbate subtle phenotypic effects (Spinelli, Osterberg, Meshul, Soumyanath, & Unni, 2015). Before running, each mouse's paw was painted with red food coloring to increase contrast between the paw and fur and facilitate digital paw painting. Mice were placed into the chamber and the treadmill was turned on to run at 24 cm/s. The treadmill was turned off when mice had either run for approximately 10 seconds or ceased running and were pushed to the back of the chamber. Videos featuring 2-6 sec of running were analyzed using DigiGait Analysis software (Mouse Specifics, Inc., Quincy, MA). The results were divided into forepaw and hindpaw measurements for statistical analyses. Forepaw angle (degree as measured from midline), forepaw brake (duration and percentage of total stride that the forepaw was engaged in braking phase), and forepaw stance (duration that the forepaw was in contact with treadmill belt) are reported. 11 veh + AAV-GFP mice, 10 veh + AAV-Cre-GFP mice, 11 MPTP + AAV-GFP mice, and 10 MPTP + AAV-Cre-GFP mice were tested.

3.2.8 Tissue fixation and sectioning

At the appropriate endpoint (i.e., 4 wks or 12 wks), mice were deeply anesthetized with a ketamine/xylazine (1%/0.1% v/v) cocktail and perfused transcardially with electron microscopy fixative containing 1% glutaraldehyde, 0.5% paraformaldehyde, and 0.1% picric acid in 0.1M phosphate buffer, pH 7.3. Brains were removed from the skull, cut coronally at the level of the hypothalamus, and both halves were placed into wells containing EM fixative in a microwave tissue processor (Pelco Biowave, Ted Pella, Inc., Redding, CA) attached to a temperature-controlled fixation bath (Thermoelectric Recirculating Chiller: Pelco Steady Temp Pro, Ted Pella, Inc., Redding, CA) for 45 minutes [15 min at 150 watts (W) at 28°C followed by 15 min at 150W at 25°C and finally 15 min at 650W at 25°C)].

A separate group of 8-week-old mice were injected with either AAV-Cre-GFP or AAV-GFP and allowed to recover for 4 weeks before being anesthetized with the ketamine/xylazine cocktail described above and perfused transcardially with 4% paraformaldehyde in 0.1M phosphate buffer, pH 7.3. The brains were subsequently fixed using the microwave tissue processor as described above. These mice were used for immunofluorescent and electron microscopy experiments described in detail later. Tissue from fixed brains was cut into 40-60 µm-thick sections using a vibratome (Ted Pella Inc., Redding, CA). Slices throughout the rostro-caudal extent of the striatum, SNpc, and STN were collected for subsequent processing.

3.2.9 Immunohistochemistry (IHC)

Slices extending throughout the region of interest were selected for immunohistochemical processing, with separate sections used for each antibody. All incubations were carried

out in the PELCO BioWave® Pro microwave (Ted Pella Inc., Redding, CA) with the temperature limit set to not exceed 35^{o}C. Rinsing steps occurred under normal atmospheric pressure unless otherwise stated. Antibody incubations occurred under continuous vacuum. Tissue was rinsed twice in phosphate buffered saline (PBS) for 1 min/rinse at 150 W after each incubation step unless otherwise stated. Antigen retrieval was performed in 10 mM sodium citrate, pH 6.0, for TH and GFP proteins or in 10 mM sodium citrate, pH 9.0, for VGLUT1 protein for 5 min at 550 W with the vacuum off. The tissue was then incubated in 3% hydrogen peroxide at 150 W for 1 min with the vacuum on. The tissue was next incubated in 0.5% Triton X-100 for 5 min, 550 W under vacuum. Tissue was exposed to the primary antibodies [TH diluted to 1:500 (Immunostar, Hudson, WI), GFP diluted to 1:1000 (Fitzgerald, Acton, MA), or VGLUT1, diluted to 1:1000 (Synaptic Systems, Goettingen, Germany)] for 12 min at 200 W 4 times with the following cycle: 2 min on, 2 min off, 2 min on, 5 min off. The tissue was incubated with biotinylated goat anti-rabbit secondary antibody (1:50; Vector Laboratories, Burlingame, CA) for 15 min at 200 W for 2 cycles consisting of 4 min on, 3 min off, 4 min on, 5 min off. After secondary incubation, tissue was washed once in PBS and a second time in working imidazole buffer (5% 0.2M imidazole buffer, pH 9.0, and 16% 0.1M sodium acetate, pH 7.2). Tissue was exposed to ABC (avidin-biotin complex; Vector Laboratories, Burlingame, CA) for 11 min at 150 W under vacuum for 1 cycle consisting of 4 min on, 3 min off, 4 min on. The tissue was then incubated in diaminobenzadine (DAB; 0.5 ug/ml in 1.5% hydrogen peroxide) for 10 min under continuous vacuum at 200 W. Finally, tissue was rinsed once again in working imidazole buffer and once in PBS before being mounted, cover-slipped, and imaged on a Zeiss

Axioplan light microscope (Carl Zeiss AG, Oberkochen, Germany) and a MBF Bioscience Digital Microscope Camera (Williston, VT). Brains from 5 mice/group were used for immunohistochemical analysis.

3.2.10 Immunofluorescence

Tissue from mice perfused with paraformaldehyde underwent antigen retrieval and primary antibody incubation as described in the IHC section. The primary antibodies used were GABA (1:100; Sigma Aldrich, St. Louis, MO), NeuN (1:100; Sigma Aldrich, St. Louis, MO), Cre (1:100; Sigma Aldrich, St. Louis, MO) and CX3CR1/IBA-1 (1:100; Sigma Aldrich, St. Louis, MO). Fluorescently labeled goat anti-rabbit antibodies (Alexa Fluor 350 and Cy3; 1:50, Jackson Immunoresearch, Inc., West Grove, PA) were used for secondary antibody incubation and tissue was rinsed twice with PBS. Tissue was mounted with Vectashield anti-fade mounting medium (Vector Laboratories, Inc., Burlingame, CA) before being cover-slipped and imaged using a Zeiss Axioscope A1 fluorescent microscope (Carl Zeiss AG, Oberkochen, Germany) and ZEN imaging software (Version 2.3, Carl Zeiss AG, Oberkochen, Germany).

3.2.11 Cresyl violet (CV) counterstaining

SNpc slices previously immunohistochemically labeled for TH were counterstained in cresyl violet (CV; 0.2% in H_2O) to visualize non-TH-labeled cells.

3.2.12 Optical density (OD) analysis

Images of tissue processed for TH were analyzed using Image-Pro Plus software (version 6.3, Media Cybernetics, Silver Springs, MD). 6 slices per animal extending throughout the rostro-caudal extent of the striatum, to the level of the anterior commissure, were analyzed. The dorsolateral quadrant of the striatum (the region that is the major input

from the motor cortex) was manually traced and a computer generated mean OD was recorded. The lateral motor cortex (chosen to avoid any overlap of cortical area affected by viral infusion) was used as background measurement and was subtracted from the striatal OD to account for differences in luminance or mounting medium thickness between slices. Values were averaged to obtain a single OD value for each animal.

3.2.13 Cell surface counts

Counts of TH-immunoreactive cells in the SNpc were performed non-stereologically as we have previously shown a high correlation between cell counts obtained stereologically and by cell surface counts (Churchill et al., 2017). TH-negative but CV-positive cells within the SNpc were also counted. 6 slices evenly spaced throughout the rostrocaudal extent of the SNpc were used, and the number of cells from each slice was averaged to get a value for each animal. Counting was performed with ImageJ.

3.2.14 Fresh tissue collection

Mice used for western blot analysis were euthanized by cervical dislocation. Brains were rapidly removed and incubated in ice-cold 0.1M phosphate buffer. Brain regions of interest (motor cortex, dorsolateral striatum, and midbrain/SN) were dissected out using a dissecting microscope and a microknife. Motor cortex dissections were done under a dissecting microscope equipped with a fluorescent lamp and filter to identify and isolate GFP-expressing tissue. Midbrain/SN tissue was pooled from both hemispheres. The tissue was flash frozen on dry ice and stored at -80^{o}C until protein extraction. Brain regions from 5 mice/group were collected for western blot analysis.

3.2.15 Western blot analysis

Ice cold lysis buffer [5% 1M Tris, 2% 0.5M EDTA, 1% Triton-X 100, 0.5% Protease Inhibitor Cocktail III (Calbiochem, Billerica, MA) in 0.1M phosphate buffer] was added to frozen tissue on ice. Samples were sonicated and centrifuged at 25,000 rpm for 20 min at 4^{o}C. The supernatant was collected and analyzed by BCA assay (Thermo, Waltham, MA) to assess protein levels. 10 µg of protein were mixed with XT Sample Buffer and XT Reducing Agent (1:10; Bio-rad, Hercules, CA), boiled, and loaded onto a 4-12% Bis-Tris XT Precast Gel (Bio-Rad, Hercules, CA). Samples that were to be probed for VGLUT2 and VMAT2 were not boiled but were instead left at room temperature (RT) for 1 hr, based on suggestion from primary antibody manufacturers. Gels were electrophoresed at 200 V for 1 hr before proteins were transferred to PVDF membrane for 1 hr at 100 V. Membranes were blocked with 5% nonfat dry milk in Tris-buffered saline with 1% Tween (TBST). After washing in TBST, membranes were incubated with one of the following primary antibody dilutions in TBST: TH (1:4000, ImmunoStar, Hudson, WI), dopamine transporter (DAT; 1:1000, Proteintech, Rosemont, IL), dopamine receptor D1 (DRD1; 1:500, Santa Cruz Biotechnology, Dallas, TX), dopamine receptor D2 (DRD2; 1:1000, Millipore, Burlington, MA), brain-derived neurotrophic factor (BDNF; 1:1000, Santa Cruz Biotechnology, Dallas, TX), vesicular monoamine transporter 2 (VMAT2; 1:1000, Synaptic Systems, Goettingen, Germany), vesicular glutamate transporter 2 (VGLUT2; 1:2000, Synaptic Systems, Goettingen, Germany), and β-actin (1:6500, Sigma Aldrich, St. Louis, MO). Membranes were washed and incubated with the appropriate horseradish peroxidase-conjugated secondary antibody (1:1000, Bio-Rad, Hercules, CA). Membranes were washed, dried, and incubated with

enhanced chemifluorescence (ECF) substrate (GE Healthcare, Piscataway, NJ) to visualize protein bands. Membranes were scanned and protein densities were analyzed relative to β-actin densities using ImageJ. Each sample was run in triplicate, normalized for each membrane and averaged for each animal. Animals were averaged per group and expression was normalized to vehicle control levels to account for differences in background intensity across membranes.

3.2.16 Electron microscopy (EM)

Tissue was pre-embed processed for VGLUT1 or GFP as previously described for IHC. Tissue was then embedded in Epon-Spurs resin overnight at 60^{o}C. Blocks of the region of interest were thin sectioned using an Ultracut ultramicrotome (Leica, Buffalo Grove, IL) to 60 nm thickness using a diamond knife (Diatome, Hatfield, PA) and then post-embed labeled with glutamate immunogold labeling. This was achieved by incubating glutamate antibody (1:250 dilution in TBST, pH 7.6, with 1 mM aspartate; raised in rabbit, Sigma Aldrich, St. Louis, MO) with thin-sectioned tissue overnight. Tissue was next incubated with goat anti-rabbit IgG conjugated to 12 nm gold (diluted 1:25 in TBST, pH 8.2; Amersham, Arlington Heights, IL). Photographs of VGLUT-1- or GFP-labeled terminals (10/animal) were taken randomly throughout the neuropil section at a final magnification of 40,000X within the area or layer of interest on a JEOL 1400 transmission electron microscope equipped with an AMT digital camera (Danvers, MA). We previously reported that incubation of the antibody with 3 mM glutamate resulted in no immunogold labeling, demonstrating the specificity of the glutamate labeling (Meshul, Stallbaumer, Taylor, & Janowsky, 1994).

To quantify glutamate labeling, the number of immunogold particles located within a DAB-labeled terminal were counted using Image-Pro Plus software. Additionally, the area of the terminal was measured automatically by the software and the density of gold particles per square micron of nerve terminal area were calculated for each animal. 5 animals/group were EM processed and analyzed.

3.2.17 Statistical analysis

All data are reported as the mean ± SEM unless otherwise noted. A three-way analysis of variance (ANOVA) was used to detect significant differences based on group, treatment, and hemisphere, when appropriate. A two-way ANOVA was used when hemisphere was not a variable to detect significant differences based on group and/or treatment. If a significant effect was found, a Tukey-Kramer HSD post hoc test was used to compare groups. A Student's t-test was used when there only 2 groups were compared.

3.3 Results

3.3.1 Characterization of AAV distribution

To confirm the correct placement and expression of viral vectors, slices at the level of the viral injection were examined for GFP expression (Figure 18a). There was a differential pattern of GFP expression between AAV-GFP and AAV-Cre-GFP animals despite using equivalent viral titers and volumes. However, immunofluorescence confirmed that Cre, GFP, and NeuN all colocalized in AAV-Cre-GFP-injected animals, indicating that the expressed Cre-GFP fusion protein was trafficked to the nucleus and providing an explanation for the observed differential GFP expression. Immunoblotting of motor cortex tissue expressing GFP showed no significant increase in GFAP expression, a common marker of inflammation, in AAV-Cre-GFP-injected animals

compared to the AAV-GFP group, indicating that the localization of Cre-GFP in the nucleus did not cause an additional inflammatory response (Figure 18b, $p > 0.05$). GFAP expression was compared between the two groups to rule out inflammatory processes as being attributable to any differences between the groups. Cresyl violet (CV) counterstaining of the injected area revealed no significant lesion at the injection site

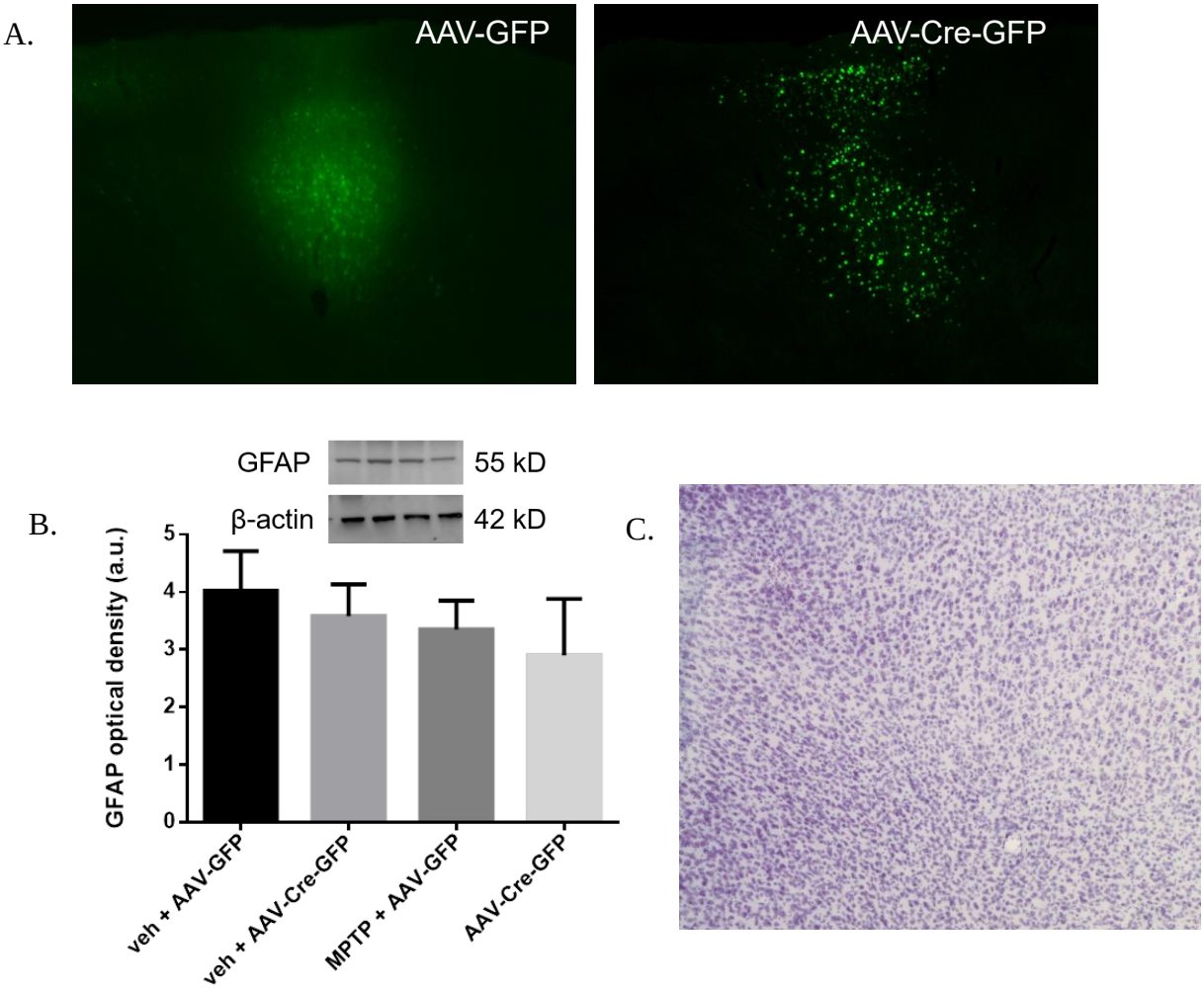

Figure 18. Characterization of adenoviral expression
Viral GFP expression in the motor cortex of *Vgatflox/flox* animals **(A)**. GFAP expression in the injection area did not vary significantly between AAV-GFP and AAV-Cre-GFP groups **(B)**. CV staining of the injection area **(C)** revealed no obvious cell loss or damage after injection and Cre-GFP expression.

(Figure 18c), confirming that the surgical procedure and viral expression caused minimal damage to the area of interest.

3.3.2 Behavioral recovery after posited cortical disinhibition

We have previously shown that progressive MPTP lesioning elicits changes in the gait of both young and aged wt mice (Hood et al., 2016; Smith, Goldberg, & Meshul, 2011). Forepaw angle has been used in other disease models to measure the extent of motor dysfunction (Amende et al., 2005). When forepaw angle was measured in running aged *Vgat*$^{flox/flox}$ mice (Figure 19), there were main effects of both group (veh vs. MPTP; $F_{1,80} = 6.727$, $p = 0.0113$) and treatment (AAV-GFP vs. AAV-Cre-GFP; $F_{1,80} = 13.39$, $p = 0.0005$), but not side (ipsilateral to injection vs. contralateral, $F_{1,80} = 0.9020$, $p = 0.3451$). Tukey HSD post doc analyses were conducted and significant differences are indicated in

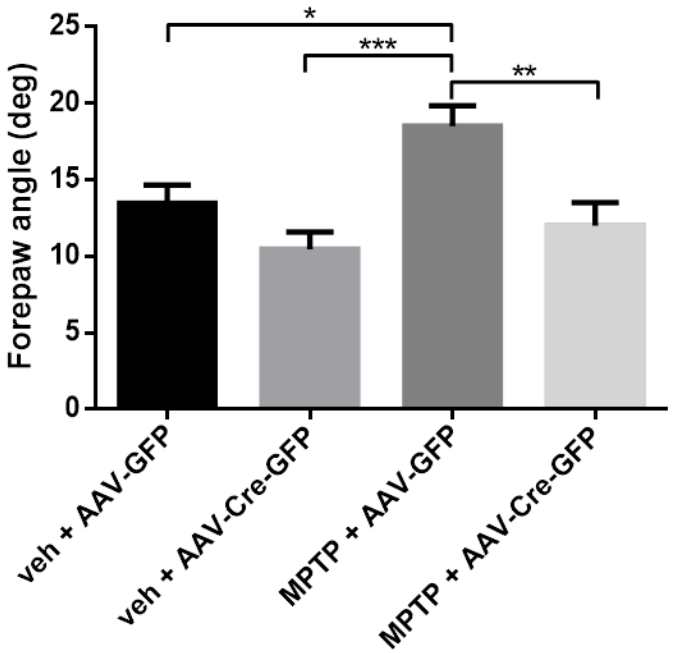

Figure 19. MPTP-induced gait deficit in forepaw angle improved after cortical disinhibition
Forepaw angle increased after MPTP lesioning but was significantly decreased after cortical disinhibition. * denotes $p<0.05$, ** denotes $p<0.01$, and *** denotes $p<0.001$ as assessed by Tukey HSD post hoc test.

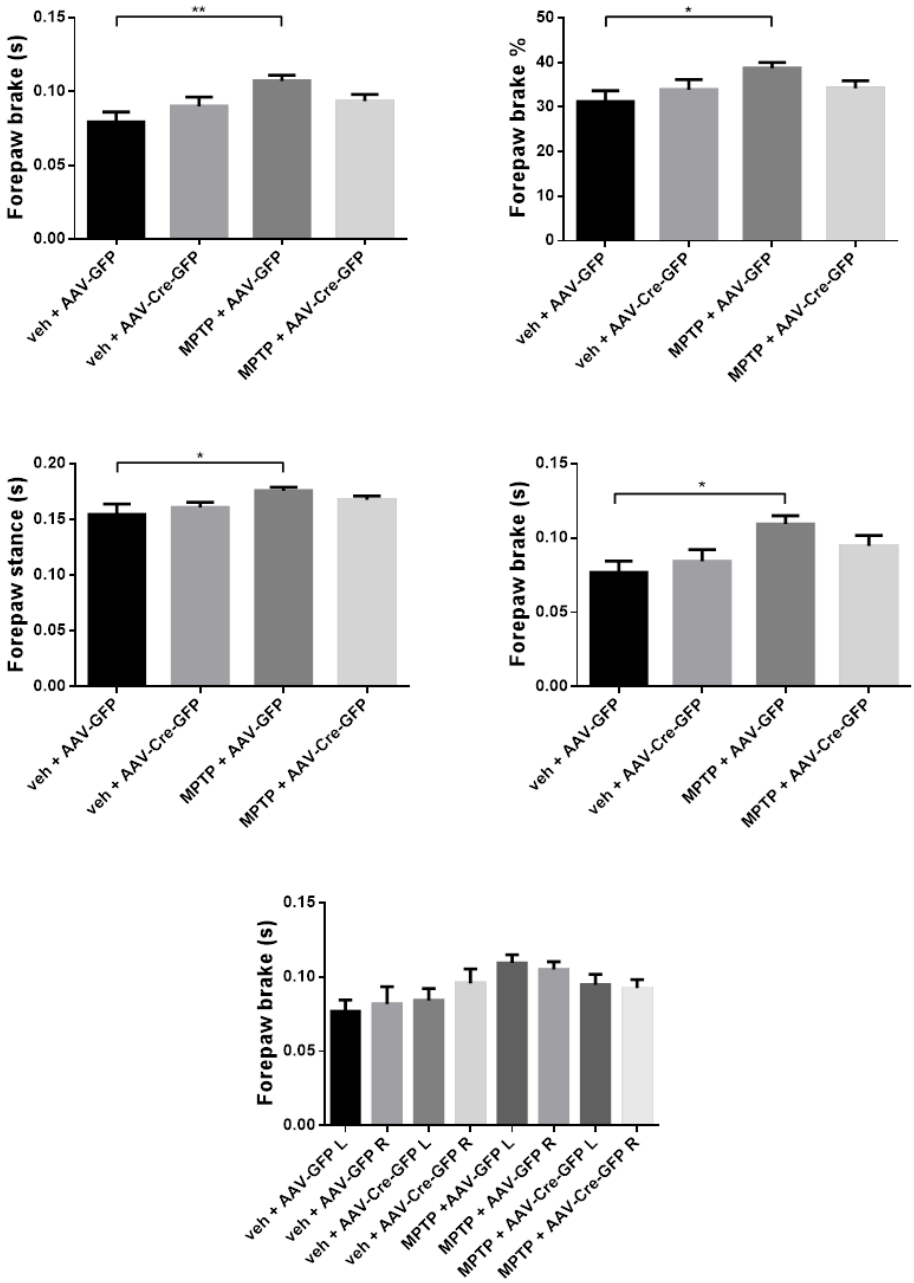

Figure 20. Other measures of gait altered by MPTP lesioning
Multiple other gait characteristics were significantly altered by MPTP. There were no significant differences between ipsilateral and contralateral sides. * denotes $p<0.05$, ** denotes $p<0.01$ as assessed by Tukey HSD post hoc tests.

figure 19. Posited cortical disinhibition resulted in a recovery of forepaw angle back to

control values, with no significant difference between the average forepaw angle of the MPTP+AAV-Cre-GFP group and the vehicle animals. Other changes in gait dynamics that were significantly affected by MPTP (no treatment effects were found) are provided in figure 20, with any group differences indicated by Tukey HSD post hoc analyses indicated on the figure. There was no significant effect of side (contralateral or ipsilateral to viral injection) in any of the observed gait measures.

Grip strength has also been identified as a sensitive and translationally relevant measure of motor dysfunction (Roberts et al., 2015). However, no changes in grip strength were observed after either MPTP lesioning or cortical dysfunction (Figure 21). As the *Vgat*$^{flox/flox}$ mice were aged, it is possible that grip strength was decreased in all

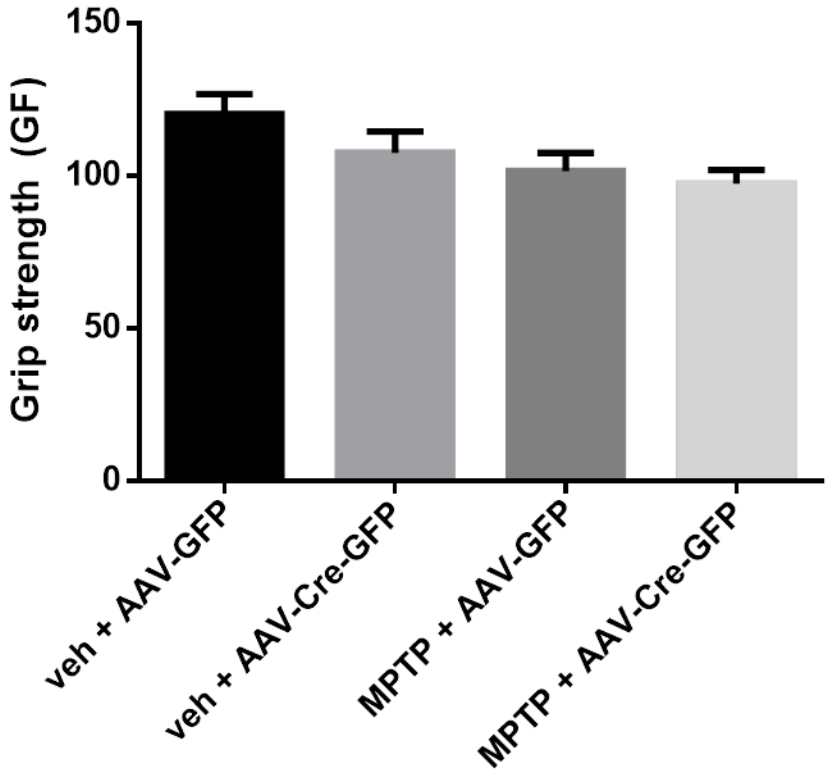

Figure 21. Grip strength did not change in response to MPTP or cortical disinhibition
Neither MPTP lesioning nor cortical disinhibition had any effect on maximal grip strength.

groups due to overall aging effects (we have not fully characterized the progressive MPTP model in aged *Vgat*$^{flox/flox}$ mice but have observed a decrease in grip strength in aged C57BL/6J mice compared to young mice).

3.3.3 Alterations in TH expression

Tyrosine hydroxylase (TH) loss is a commonly used hallmark to evaluate the extent of lesioning in PD and animal models of PD. As such, I evaluated TH loss in both the dorsolateral striatum and SNpc. Because there were no significant differences between TH expression measured at 4 weeks (directly after MPTP lesioning) and 12 weeks (after surgeries and 8 weeks of cortical disinhibition), only the endpoint TH values are reported. We have previously reported a lack of spontaneous TH recovery 8 weeks after MPTP administration ceased (Churchill et al., 2019). While there was a significant main effect of MPTP lesioning on striatal TH expression as assessed by immunoblotting (Fig 22a; $F_{1,17} = 51.27$, $p < 0.001$), there was no main effect of posited cortical disinhibition ($F_{1,17} = 0.0001$, $p = 0.9905$). This was surprising, as sprouting of TH-expressing cell terminals is thought to be a mechanism underlying behavioral recovery in PD models (Arkadir, Bergman, & Fahn, 2014; Stanic et al., 2004) and is a phenomenon we have previously observed in our own model, albeit with a different therapy (Churchill et al., 2019). However, Finkelstein et al. (2000) have shown that axonal sprouting occurs as compensation until a threshold 70% cell loss in the SNpc, at which point the cell loss is too extensive. In the current study, counts of TH-expressing cells in SNpc tissue processed by IHC revealed a significant 67% decrease in the number of TH-positive cells in AAV-GFP-injected animals after MPTP lesioning compared to control animals, with a main effect of MPTP (Fig. 22b, $F_{1,16=}$ 184.6, $p < 0.0001$) and no main effect of posited

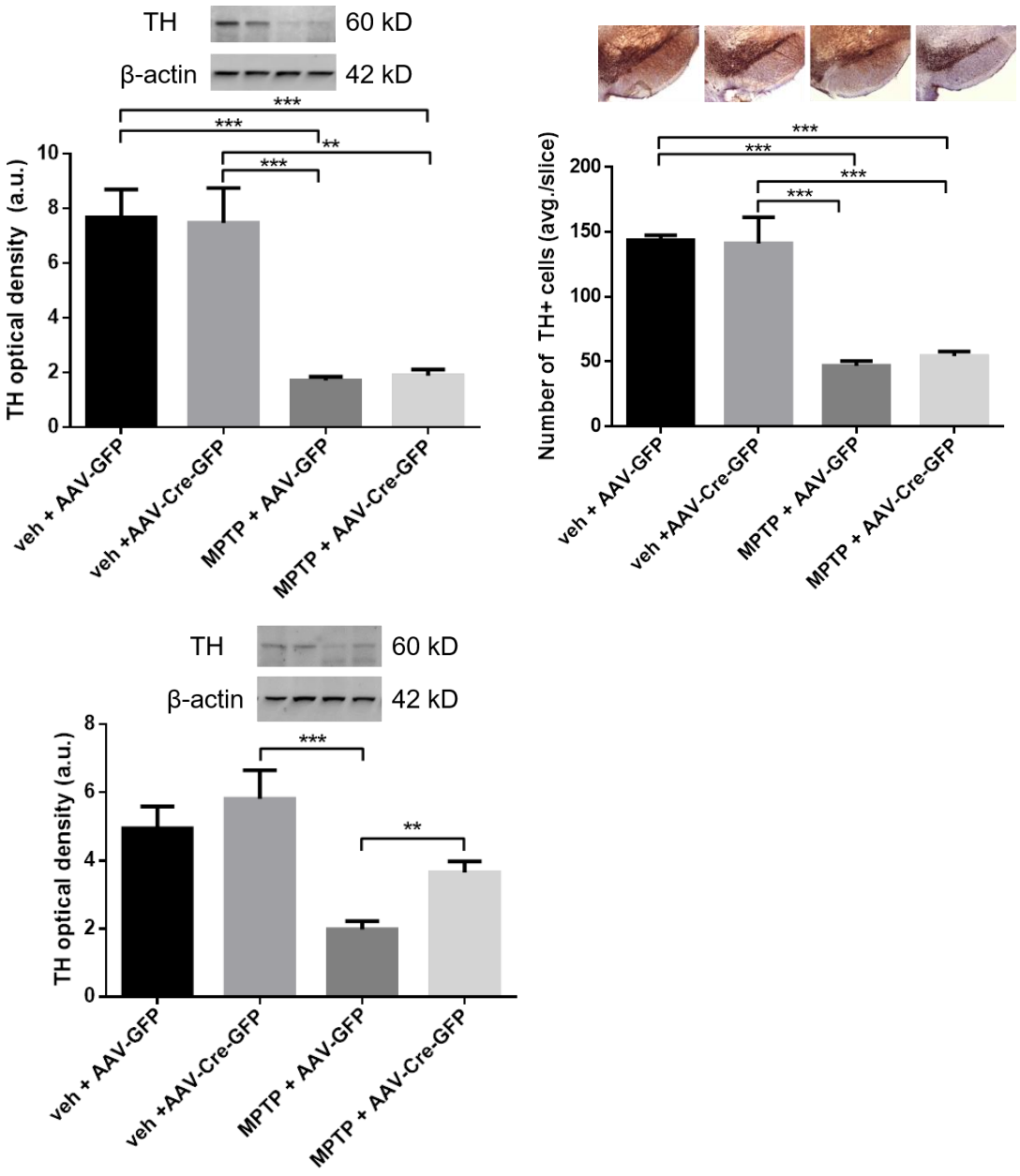

Figure 22. TH changes in the striatum and SN
Striatal TH as assessed by immunoblotting showed a 78% reduction after MPTP lesioning that was not affected by cortical disinhibition **(A)**. Similarly, cell surface counts of TH-expressing SNpc cells revealed a 70% decrease in cell number after lesioning with no recovery **(B)**. However, immunoblotting of the midbrain indicated that there was a significant recovery in TH expression after cortical disinhibition compared to AAV-GFP control group in lesioned animals **(C)**. ** denotes $p<0.01$, *** denotes $p<0.001$ as assessed by Tukey HSD post hoc analysis.

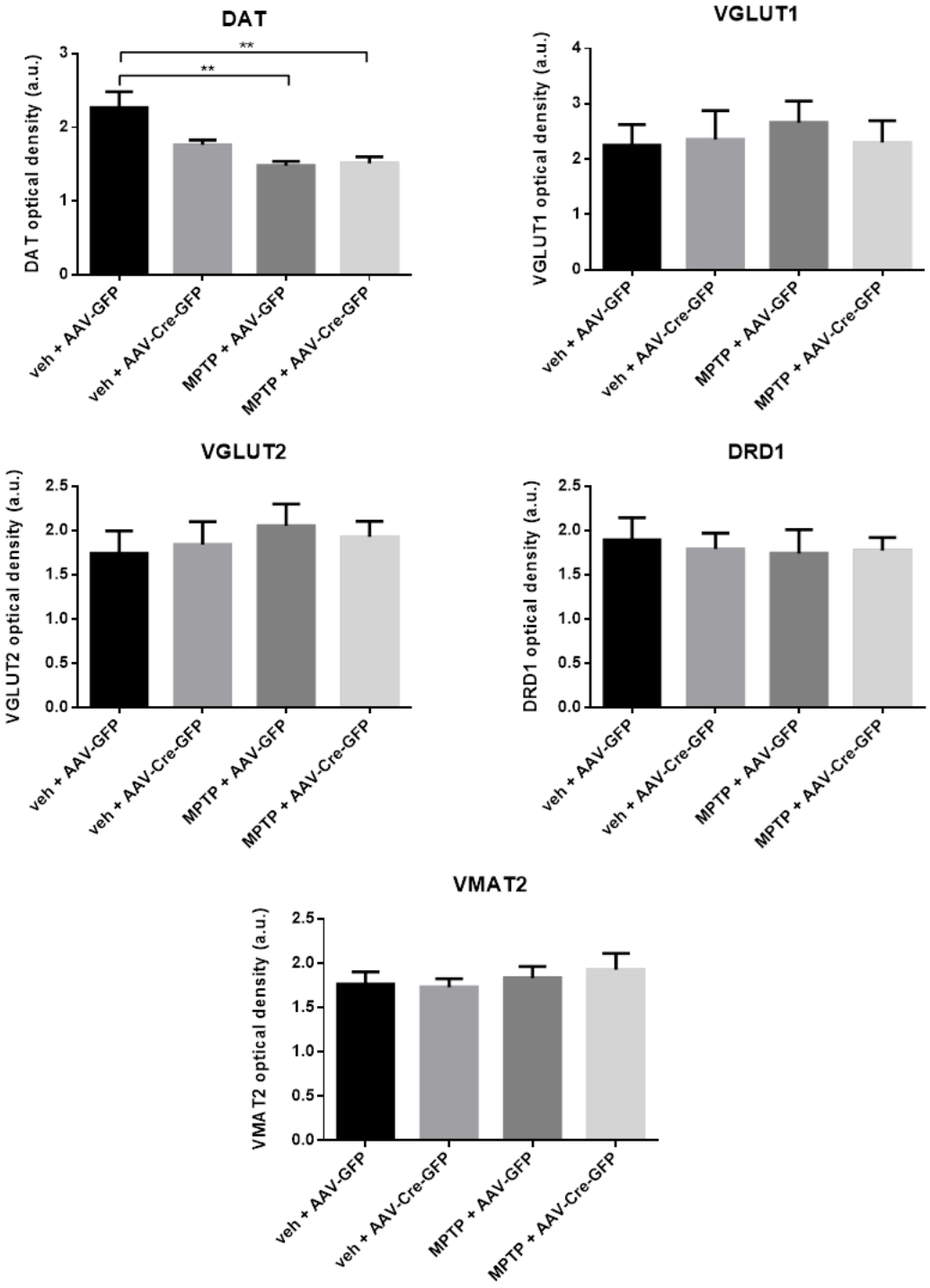

Figure 23. Striatal protein expression
Expression of other dopaminergic and glutamatergic markers were measured in striatal tissue. DAT: dopamine transporter. VGLUT: vesicular glutamate transporter. DRD1: D_1 dopamine receptor. VMAT2: vesicular monoamine transporter 2. ** denotes $p < 0.01$ as assessed by Tukey HSD post hoc analysis.

cortical disinhibition ($F_{1,16} = 0.1794$, $p = 0.6775$), so it is possible that the lesion was significant enough to prevent any compensatory axonal sprouting. However, TH expression of midbrain tissue as assessed by immunoblotting showed a significant main effect of posited cortical disinhibition ($F_{1,17} = 8.338$, $p = 0.0102$). Tukey post hoc analyses showed a significant 60% decrease in TH expression in lesioned AAV-GFP-injected compared to vehicle AAV-GFP-injected animals ($p < 0.001$) but a subsequent significant recovery after posited cortical disinhibition (Fig 22c). The increase in TH expression without an increase in cell number suggests that the cells remaining after MPTP lesioning increased TH expression in response to posited cortical disinhibition.

3.3.4 Neurobiological effects of posited cortical disinhibition

While it has been previously demonstrated that activity to SNpc cells can cause an alteration in TH expression (Aumann & Horne, 2012b), this increase in midbrain TH expression after lesioning followed by posited cortical disinhibition was unexpected as only a small proportion of projections from the motor cortex synapse on SNpc cells (Watabe-Uchida, Zhu, Ogawa, Vamanrao, & Uchida, 2012). Given the sparseness of the corticonigral pathway, increased innervation of the SNpc due to direct corticonigral projections seems unlikely, but there are polysynaptic pathways that could result in an increase in SNpc innervation after posited cortical disinhibition. Therefore, I investigated a potential mechanism to explain why posited cortical disinhibition might cause an increase in midbrain TH expression after lesioning and subsequent behavioral recovery.

The majority of the projections arising from the targeted area of the motor cortex terminate in the dorsolateral striatum (McGeorge & Faull, 1989), therefore I assayed dorsolateral striatal tissue via immunoblotting to determine if there were any changes in

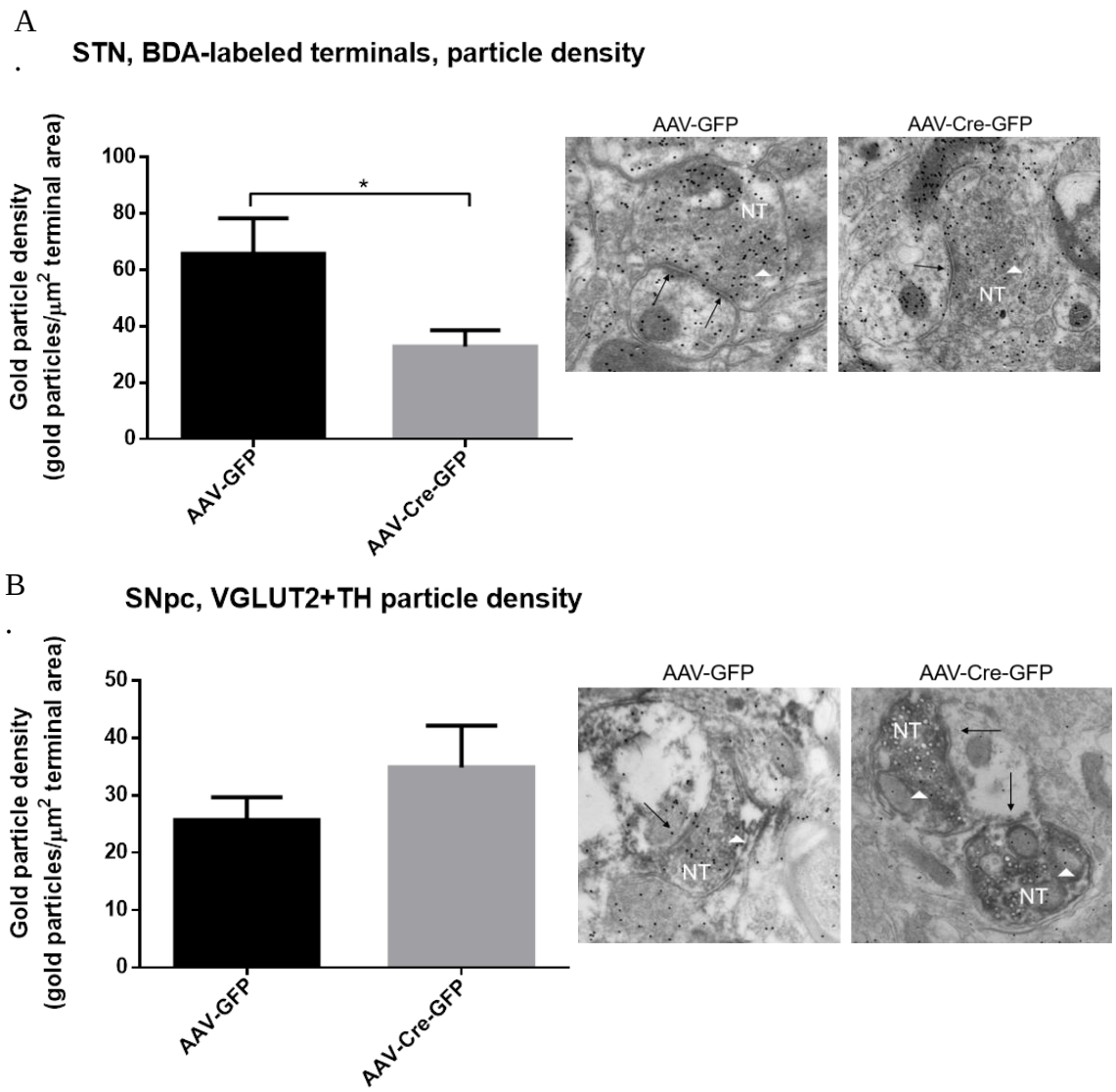

Figure 24. EM analysis of glutamate immunogold particle density
Glutamate immunogold particle density in BDA-labeled terminals (i.e., those arising from the injection area) was significantly decreased in the STN after cortical disinhibition **(A)**, suggesting an increase in glutamate release from labeled terminals. Subsequent evaluation of glutamate immunogold particles in VGLUT2-labeled terminals synapsing on dopaminergic cells did not detect any change in particle density. NT denotes nerve terminal, white arrowheads indicate immunogold particles, black arrows indicate synapses. * denotes $p<0.05$ as assessed by Student's t-test.

proteins associated with neurotransmitter signaling. I hypothesized that activation of the striatum could indirectly increase innervation of the SNpc, thereby explaining the observed increase in TH expression. Although there was no change in striatal TH

expression after posited cortical disinhibition, possibly because the SNpc lesion surpassed the threshold at which dopaminergic cells cannot continue to sprout as first reported by Finkelstein et al. (2000), it is feasible that expression of other striatal proteins may have changed in response to posited cortical disinhibition. However, with the exception of the dopamine transporter (DAT), where there was a main effect of MPTP ($F_{1,17} = 14.30$, $p = 0.0015$) there was no significant main effect of MPTP or posited cortical disinhibition in any of the other proteins studied (VGLUT1, VGLUT2, D_1 dopamine receptor, and VMAT2), suggesting that behavioral recovery cannot be attributed to changes in either dopaminergic or glutamatergic signaling systems within the striatum (Fig. 23). The decrease in striatal DAT after MPTP lesioning is expected and has been previously reported in our progressive MPTP model where we typically observe correlative changes in TH and DAT (Smith et al., 2011). Additionally, glutamate immunogold particle density in VGLUT1-labeled terminals (arising from the cortex) was not changed after *Vgat* deletion in a previous study (as described in Chapter 2, Figure 11), suggesting that the corticostriatal pathway may not be affected by posited cortical disinhibition.

Based on previous tracing studies, I demonstrated that the targeted area of the motor cortex projects strongly (and bilaterally) to the STN via the hyperdirect pathway (see Chapter 2, Figure 8B). The Cre-GFP fusion protein is transported to the nucleus, so GFP cannot be used to label terminals arising from the injection area. By co-injecting BDA and the virus, I was able to modify GABA signaling in the cortex with the virus alone, while concurrently labeling terminals arising from the injection area with BDA. EM analysis of BDA-labeled terminals revealed a significant 50% decrease in glutamate

immunogold particle density after posited cortical disinhibition compared to the AAV-GFP control group as assessed by a Student's t-test (Fig. 24a; 65.78 ± 12.56 vs. 32.82 ± 5.77, $p < 0.05$). As demonstrated by Meshul, et al (1999), immunogold particle density has an inverse correlation with extracellular glutamate levels as assessed by *in vivo* microdialysis, suggesting that the observed decrease in STN glutamate immunogold particle density after posited cortical disinhibition indicates an activation of the hyperdirect pathway and a subsequent increase in glutamate release in the STN.

Finally, I investigated whether there was any change in projections arising in the STN and terminating in the SN. The STN sends projections to both the SNpc and SNpr (Deniau, Hammond, Chevalier, & Feger, 1978), but for the purposes of examining how SNpc cells were possibly stimulated to increase their TH expression, only the direct STN-SNpc projection was studied. The glutamate immunogold particle density was assessed in VGLUT2-positive terminals synapsing on TH-expressing cells in the SNpc to identify those terminals that potentially arose in the STN, but no significant difference was found between AAV-GFP- and AAV-Cre-GFP-injected animals using a Student's t-test (Fig. 24b; 25.71 ± 3.94 vs. 34.86 ± 7.29, $p < 0.05$). This result is not altogether unexpected as other glutamatergic projections to the SNpc also express VGLUT2, such as the ventral pallidum and parafascicular nucleus of the thalamus (Canteras, Shammah-Lagnado, Silva, & Ricardo, 1990), and a lack of changes in those terminals could have diluted any effect in VGLUT2-labeled terminals arising from the STN. This is discussed in more detail in the subsequent section.

3.4 Discussion

These experiments have demonstrated that posited cortical disinhibition after MPTP lesioning can induce recovery of gait impairments and an increase in midbrain TH expression. Furthermore, immunoblotting and EM analysis suggest that activation of the hyperdirect pathway and not the corticostriatal pathway may underlie the observed recovery.

Many studies assessing the efficacy of a treatment in animal models of Parkinson's disease employ a neuroprotective design, that is, administering the treatment before or at the start of the lesioning. While this provides information about a therapy's potential to stop further progression of PD at the time of treatment, it cannot allow for the assessment of a therapy to induce any sort of recovery in the PD model. Therefore, I employed a neurorestorative model to study the potential of posited cortical disinhibition in which the disinhibition occurred after the lesioning, modeling a clinical scenario in which a PD patient has already undergone loss of SNpc cells before receiving treatment. As MPTP is excreted within 24 hours in rodents (Johannessen, Chiueh, Burns, & Markey, 1985) and the viral injections took place 72 hours after the last injection, I believe that the observed recovery is not caused by any interference in MPTP metabolism. Furthermore, we have never observed a continued loss of TH expression in the basal ganglia after the cessation of MPTP administration, meaning that this is truly a restorative and not interventional study. As PD patients typically do not present with motor symptoms until an approximate 50-60% loss of TH-expressing cells in the SNpc (Fearnley & Lees, 1991), it is important for therapeutic studies to replicate this loss

before the onset of treatment to serve as a translationally relevant model of the treatment of PD.

Because of the restorative nature of this study, I believe that this study demonstrates the potential of modulating cortical activity as a viable therapy for PD. The motor cortex has already been successfully targeted in PD patients, both with rTMS and extradural stimulation (Canavero et al., 2002; Lefaucheur et al., 2004). These studies, however, have not investigated the mechanism for the observed behavioral recovery, nor have they measured the neurobiological effects of such stimulation. This study allowed

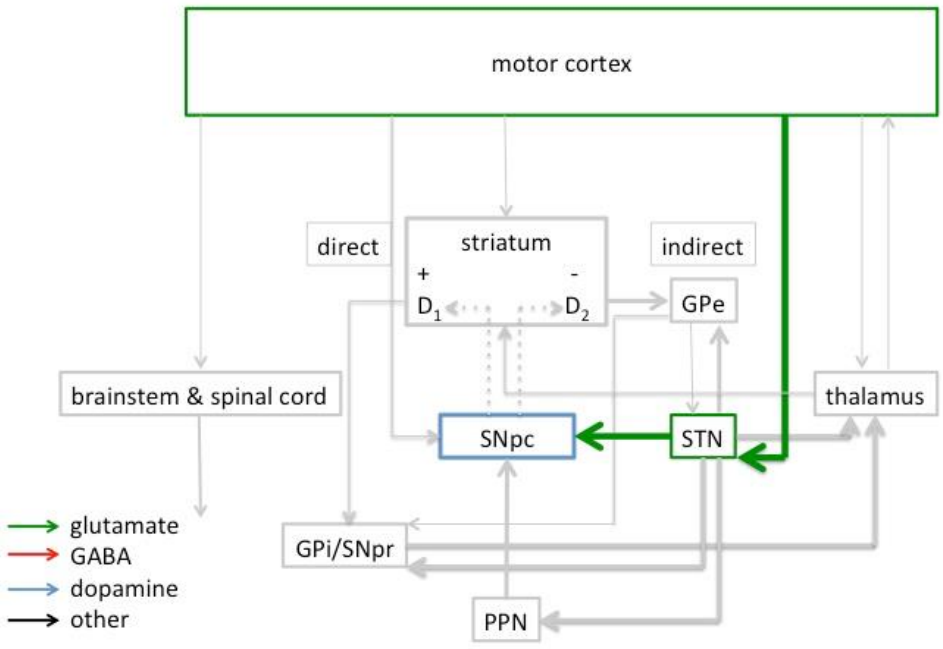

Figure 25. Potential mechanism of innervation of SNpc through activation of the hyperdirect pathway. Cortical disinhibition increased the activation of the hyperdirect pathway as assessed by electron microscopy. The STN directly projects to the SNpc, so it is conceivable that activation of the hyperdirect pathway increased the activity of the STN-SNpc projection, resulting in the observed increase in midbrain TH expression.

for a more complete investigation of underlying changes in the brain caused by posited cortical disinhibition that might allow for more targeted therapy in PD.

The increase in TH expression in the SN was unexpected but not unprecedented. He et al. (2014) previously showed that high frequency stimulation (HFS) of the STN after 6-OHDA lesioning of the nigrostriatal pathway results in an increase in TH expression of the SNpc, but not in the number of TH-labeled SNpc cells, similar to the current findings. The authors hypothesize that this occurs through activation of STN projections that synapse on SNpc cells inducing an increase in TH expression, although they did not further investigate this idea. Aumann et al. (2011) have measured TH expression in the SNpc in both *in vitro* and *in vivo* models and found that TH immunoreactivity is activity dependent, providing direct evidence that alterations in activity of SNpc afferents can affect the level of TH expression.

If the increased TH expression observed in the current study is indicative of a change in the activity of basal ganglia nuclei projecting to the SNpc, there is a question of how posited cortical disinhibition can affect SNpc afferents. There are direct projections from the motor cortex to the SNpc as described by Naito & Kita (1994), but these innervations are sparse and unlikely to elicit such a change in the protein expression of the SNpc as large as the one observed here. Given the density of the innervation from the cortex to the STN and the observed decrease in glutamate immunogold labeling in STN nerve terminals, the STN-SN pathway is a potential pathway to explain the described SN alterations. The STN sends glutamatergic projections to both the SNpc and SNpr (Iribe, Moore, Pang, & Tepper, 2017), so it is possible that an increase in activity in the STN-SNpc pathway could stimulate an increase in TH expression (Fig. 25).

To test this hypothesis, glutamate immunogold density in VGLUT2-positive terminals synapsing on TH-expressing neurons in the SNpc was assessed, but no changes were detected after posited cortical disinhibition. It is possible that no effect was observed due to a potential dilution of the effect by measuring all VGLUT2-labeled terminals, as the thalamonigral pathway would also express VGLUT2 in terminals synapsing in the SNpc, along with projections from the pedunculopontine nuclei (Pienaar et al., 2013)**.** Future studies can attempt to disambiguate the effects of different glutmatergic inputs to the SNpc by injecting AAV-Cre-GFP into the cortex and an anterograde tracer into the STN, thereby specifically labeling terminals of cells arising in the STN that may be responsible for the increase in TH expression in the SNpc.

Alternatively, it is possible that the observed effect of an increase in TH expression is not caused by the direct projection from the STN to the SNpc but instead by a projection from the STN to the SNpr. Iribe et al. (2017) demonstrated that the STN innervates the SNpc through both monosynaptic connections directly to the SNpc in addition to polysynaptic connections via the SNpr. Therefore, it is possible that the downstream effects of STN activation are mediated by the SNpr, either by direct contact onto dopaminergic dendrites from the SNpc that extend into the SNpr or by contact onto SNpr interneurons (Fig. 26). As the SNpr interneurons that signal to the dopaminergic cells in the SNpc are GABAergic (Tepper, Martin, & Anderson, 1995), it is somewhat counterintuitive that an increase in glutamatergic input to the SNpr would result in an activation and consequent increase in TH expression, but this phenomenon has been previously described. Freestone et al. (2015) used electrophysiology to replicate the findings of Grace & Bunney (1979) and then determined that the paradoxical effect of an

increase in glutamatergic input to the SNpr eliciting an activation of TH-expressing cells of the SNpc was mediated by the endocannabinoid system. An evaluation of this potential mechanism could be performed using the same previously proposed EM experiment, assessing glutamate immunogold particle density in BDA-labeled terminals of the SNpr. Follow-up experiments would be necessary to identify the circuitry affected; whether projections from the SNpr synapse onto GABAergic interneurons in the SNpc, dopaminergic neurons of the SNpc, or both. To date, this circuitry has not been elucidated.

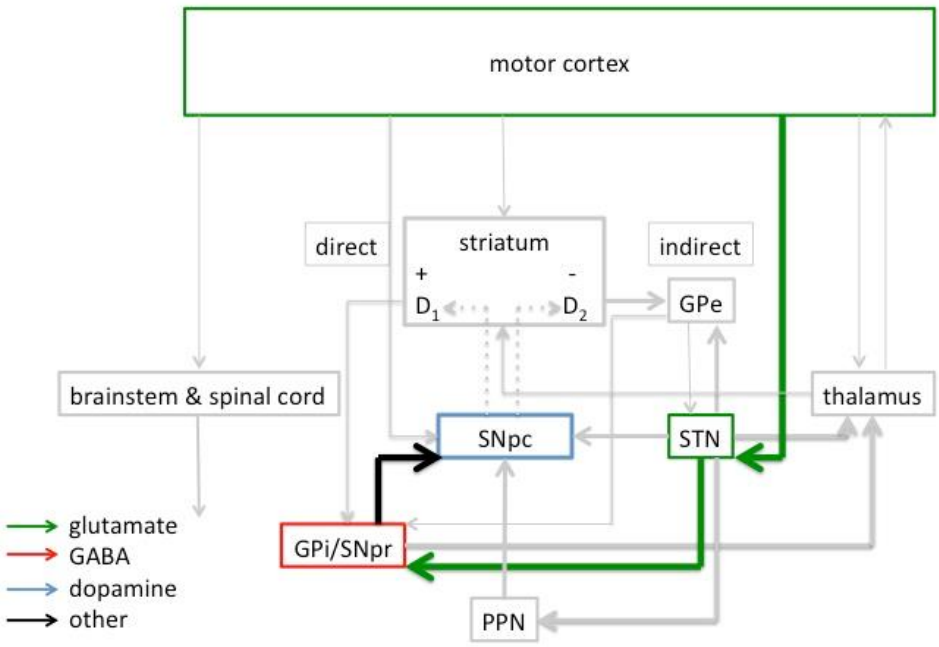

Figure 26. Proposed mechanism of SNpc innervation by activation of the SNpr via thalamonigral projections. Cortical disinhibition and subsequent activation of the hyperdirect pathway could have led to a downstream activation of the SNpr as the STN is known to send projections to the SNpr. Activation of the SNpr, although predominantly GABAergic, has been shown to increase downstream activation of the SNpc.

All of the aforementioned proposed mechanisms to explain how activation of the hyperdirect pathway could influence the SNpc elicit the same effect: activation of the SNpc. Given that the STN projects to both the SNpc and SNpr, it seems likely that the actual underlying mechanism is not exclusive to a single pathway from the STN but is instead a combination of SNpc and SNpr innervation. This could be elucidated by further EM experiments.

Stimulation of the hyperdirect pathway appears counterintuitive for treatment of a disease in which the STN is proposed to be overactive. Lesions of the STN are effective for treating motor symptoms of PD (Hagai Bergman, Wichmann, & DeLong, 1990), and, paradoxically, stimulation of the STN is also a viable treatment for PD, enough so that the STN is routinely targeted for deep brain stimulation (DBS) in PD patients (Kumar et al., 1998). However, the canonical circuit diagram of the basal ganglia is an oversimplification of the changes in neural circuitry that occur in PD; it does not capture changes in firing rate or local field potentials, both of which are known to change in basal ganglia nuclei after dopamine denervation. High frequency stimulation of the STN has repeatedly been found to stimulate the release of dopamine into the striatum in animal models of PD (Bruet et al., 2001; He et al., 2014; Pazo, Höcht, Barceló, Fillipini, & Lomastro, 2010) Therefore, it is reasonable to consider cortical disinhibition that activates the hyperdirect pathway to be a viable therapy for the treatment of PD.

The initial hypothesis for this study proposed that any recovery would be mediated through the corticostriatal pathway, but no changes in response to posited cortical disinhibition were observed in the striatum, despite the density and bilaterality of corticostriatal projections. However, a number of studies have demonstrated that acute

nigrostriatal denervation has differential effects on direct- and indirect-pathway MSNs (Day et al., 2006; Mallet, 2006; Villalba & Smith, 2013). Therefore, it is possible that there may have been specific changes in either striatonigral or striatopallidal MSNs in response to MPTP and posited cortical disinhibition, and these changes were not able to be detected by using immunoblotting. Future studies could investigate this potential by performing studies in transgenic mouse lines expressing GFP in either D_1 receptor- or D_2 receptor-expressing MSNs. Differential changes in spine density in D_1 receptor- and D_2 receptor-expressing MSNs in response to MPTP lesioning and posited cortical disinhibition could be easily assessed as previously described (Day et al., 2006). Additionally, EM studies could also be conducted using pre-embed labeling of GFP to label glutamate terminals arising from the injection region as well as direct- or indirect-pathway MSNs to identify pathway-specific changes in nerve terminal glutamate immunogold density. As there are two different types of corticostriatal projection neurons (pyramidal tract and intratelencephalic tract), it is possible that these pathways undergo differential changes in response to MPTP or cortical disinhibition (Reiner, Jiao, Del Mar, Laverghetta, & Lei, 2003). The proposed follow-up studies would allow for further investigation of pathway-specific changes and potential involvement of the striatum in the observed recovery.

Admittedly, the current study does have limitations. The EM analysis of the alterations in glutamatergic signaling after posited cortical disinhibition was performed in young animals with the assumption that these changes would not vary with age, but it is possible that this is not the case. Subsequent EM studies should utilize aged animals to compare the results with those described here to ascertain whether age might affect

downstream effects of posited cortical disinhibition. Additionally, the mechanistic studies were all performed in unlesioned animals. Midbrain TH expression was only altered by posited cortical disinhibition after lesioning occurred and not in vehicle-treated animals, suggesting that certain alterations that occur in the basal ganglia after posited cortical disinhibition may not be captured by using unlesioned animals.

EM analysis to determine glutamate immunogold density was used exclusively to assess changes in the activation of certain regions, but this may not capture all of the changes that occur. As previously stated, other animal models of PD, such as 6-OHDA models, have found alterations in firing rates of basal ganglia nuclei, and this level of detail is not possible to ascertain by EM (Ni, Bouali-Benazzouz, Gao, Benabid, & Benazzouz, 2001). Further studies using techniques such as electrophysiology or sampling of local field potentials can give a complete understanding of alterations in the mouse brain that occur after MPTP lesioning and posited cortical disinhibition. However, the current study presents compelling data to suggest that posited cortical disinhibition has neurorestorative potential and warrants further investigation.

Chapter 4: Discussion

The current studies have demonstrated that posited cortical disinhibition is both protective and restorative in a progressive MPTP model of PD. Taken together, these findings indicate that posited cortical disinhibition could both protect SNpc cells and their terminals from future lesioning as well as restore depleted midbrain TH and a specific aspect of gait (i.e., forepaw angle), although an intervention study design would be necessary to fully ascertain this potential.

The loss of TH-expressing cells in the SNpc is a cardinal pathological feature of PD. That disinhibition of the motor cortex is capable of protecting them from loss and inducing an increase in TH expression after lesioning is notable, therefore translation to clinical application could be hugely beneficial to PD patients. The improvement in gait after posited cortical disinhibition alone suggests that therapeutically targeting the motor cortex in PD could be beneficial.

Current treatment of PD involves stimulation of the STN by DBS, but DBS involves risks and can have adverse outcomes. Some patients are deemed too high risk for the surgery and are therefore limited to pharmacological treatments. However, the EM studies performed in chapter 3 suggest that the pyramidal cells that are eventually affected following posited cortical disinhibition of the deeper layers of the motor cortex innervate the STN (figure 8), providing a potential less invasive way to target the STN. Preliminary clinical trials evaluating the efficacy of extradural stimulation of the motor cortex of PD patients has provided marked motor improvement in patients while being less invasive—2 patients in the initial study were deemed unsuitable candidates but did

qualify for the cortical stimulation procedure (Canavero et al., 2002). This is not to say that the blockade of GABAergic signaling in deeper layers of the motor cortex of a mouse model of PD is equivalent to extradural stimulation of the motor cortex in PD patients, but both alter cortical activity and result in behavioral improvements after SNpc cell loss.

The method used here to disinhibit the cortex more closely matches the proposed underlying mechanism of rTMS. Lenz & Vlachos (2016) have suggested that rTMS inhibits GABAergic signaling in the stimulation region, much in the same way that AAV-Cre-GFP injection into the motor cortex of *Vgat*$^{flox/flox}$ mice decreases the release of GABA from GABAergic interneurons. Daily rTMS of the motor cortex increased walking speed and improved UPDRS scores in PD patients a month after cessation of the therapy (Khedr et al., 2003). While these results are promising, rTMS still requires a period of daily stimulation and the observed improvements are not permanent. The Cre-lox system used here results in a permanent knockout of *Vgat*, and while this system is not translatable at the moment, other clinically viable genetic manipulation techniques such as RNA interference (RNAi) could be implemented to elicit the same effect. rTMS studies show that while short-term cortical disinhibition yields an improvement in motor dysfunction, long-term cortical disinhibition in PD patients has the potential to be even more beneficial based on the results presented here.

Admittedly, the studies here are limited by the lack of direct evidence that *Vgat* has been knocked down in the motor cortex. However, our previous studies using the same mice and AAV-Cre-GFP virus injected into the EPN/GPi demonstrated a significant increase in GABA immunogold labeling within the nerve terminals of the

motor thalamus, where the EPN/GPi directly projects. This indicates that the GABA accumulated in the nerve terminal cytoplasm, since it was not taken up into the synaptic vesicles due to the knockdown of the *Vgat* gene (see chapter 1, Fig. 5). This result is consistent with the expected effect of *Vgat* knockdown in GABAergic cells. Additionally, the decrease in glutamate immunogold particle density in terminals arising from the cortical injection region and terminating in the STN, indicating an increase in glutamate release from those terminals, as we have previously shown (Meshul et al., 1999), serves as indirect evidence that there was a decrease in GABAergic tone, resulting in an increase in excitatory output from the motor cortex.

To verify that the Cre-lox system is resulting in the excision of *Vgat* in the motor cortex, *in situ* hybridization could be performed to confirm *Vgat* knockdown in conjunction with EM analysis of the injection area to assess GABA immunogold particle density in nerve terminals of GABAergic interneurons. Assuming the Cre-lox system functions as expected, GABA immunogold particle density would increase in the terminals of cortical GABAergic interneurons in the area of the AAV-Cre-GFP injection.

The studies described demonstrate that posited cortical disinhibition has the potential to be beneficial in PD, but there are factors that limit the interpretation of the results. Primarily, while we believe the progressive MPTP model to be more translationally relevant in modeling PD than existing genetic and toxin models, it is still a model that does not recapitulate the underlying cause of PD. Because the pathogenesis of PD is not yet understood, this is a limitation shared by all studies involving animal models of PD, but is nonetheless a limitation. While posited cortical disinhibition does effectively protect against MPTP lesioning, the mechanism of protection may not be

protective against the etiology of PD. Similarly, posited cortical disinhibition increases TH expression in the midbrain after TH lesioning, but may not be capable of producing the same effect in SNpc cells affected by PD pathology.

Altering activity of the cortex is a promising therapy for PD, but fails to address other known dysfunctions that occur in PD. Many genes associated with autosomal forms of PD are associated with mitochondrial structure and function, and mutation of these genes can lead to changes in mitochondrial activity and an increase in oxidative stress. Additionally, cortical disinhibition does not address the inflammation that occurs in PD. Inflammatory processes have been shown to exacerbate neuronal loss and novel therapies attenuating inflammation are successful at restoring motor function and biomarkers associated with dopamine and glutamate in PD models (Churchill et al., 2019). While there are practical limitations to the scope of any project, selectively targeting certain features of PD pathology may yield a therapy that is not efficacious in PD. Assessing the efficacy of cortical disinhibition in other PD models can rectify this problem.

Many models of PD use young animals as they are more freely available, but PD occurs primarily in aged individuals, and numerous aspects of the brain change with age. I have previously demonstrated that exercise, while effective in countering the effects of MPTP lesioning in young animals, is not beneficial in aged animals (Hood et al., 2016). The experiments in Chapter 2 were exclusively performed in young animals, repeating the study in aged animals could result in a different effect of cortical disinhibition. In addition, EM experiments in Chapter 3 were performed in young animals as the assumption was age would not affect neuronal response to posited cortical disinhibition, but this may be incorrect. Age negatively impacts neuronal plasticity (Mahncke,

Bronstone, & Merzenich, 2006), so the proposed mechanism by which posited cortical disinhibition increased midbrain TH expression in aged animals may not hold true. These experiments should be repeated in aged animals to be more reflective of PD pathology.

While the permanence of *Vgat* knockout allows for longer experimental timelines, these experiments only looked at a single time point to assess protection or restoration. The progressive MPTP model produces a lesion over the course of 4 weeks and changes within the SNpc and striatum have been shown to remain unchanged for up to two months after termination of MPTP administration (unpublished data), but dynamic changes within the basal ganglia as a response to posited cortical disinhibition have not been characterized. The changes in glutamate within terminals of the basal ganglia were measured once, but Meshul et al. (1999) have demonstrated that glutamatergic alterations in the basal ganglia in response to a lesion are dynamic. The current study generalizes changes in glutamate immunogold density in the STN to be permanent, but the observed increase in innervation after posited cortical disinhibition could change over time. A study with multiple time points to assess time sensitive modifications after posited cortical disinhibition would be necessary to assess the long-term effects of altering the activity of the motor cortex.

Interpretation of the data presented here was conducted with the assumption that the canonical basal ganglia circuit diagram and PD-induced changes to basal ganglia circuit diagram are generalizable to the progressive MPTP model, but this may not be the case. In fact, alterations in innervation of the striatum and SN as assessed by EM and CO, respectively, do not fit the described model. It is entirely possible that the methods used to assess regional activity are not adequate to detect the expected changes. Many

descriptions of alterations within the basal ganglia were performed using electrophysiological techniques, and using these techniques could expand the characterization of the progressive MPTP lesioning and subsequent changes after posited cortical disinhibition. The observed decrease in CO in the SN after MPTP lesioning is confusing and difficult to reconcile with the canonical model, but others have also described deviations from the expected changes in circuitry (Nambu, 2008). It is possible that the progressive MPTP administration produces different changes in the basal ganglia than acute toxin-based experiments used to generate portions of the model as the brain could reorganize differently in response to a slower, milder insult compared to a rapid lesion. It is also feasible that since the model represents a simplified framework for understanding a very complicated system, certain changes within the circuitry after MPTP lesioning are not captured by EM, CO, or other methods employed here. The conflict between the observations described here and the model does not necessarily invalidate either set of descriptions, but instead necessitates the need for further characterization of basal ganglia alterations in PD.

I have alluded to future experiments necessary to strengthen the conclusions made here, but there are many studies that could be performed to address remaining questions and clarify the therapeutic potential of cortical disinhibition. Notably, EM experiments designed to complete the hypothesized innervation of the SNpc via the STN could provide a more comprehensive mechanism for the increase in TH expression observed in the midbrain after posited cortical disinhibition in lesioned animals. BDA injected in the STN would label nerve terminals in both the SNpc and SNpr and would allow for the measurement of potential changes in glutamate efferents from the STN after cortical

disinhibition. Additionally, *in* vivo electrophysiological experiments measuring alterations in firing rate of basal ganglia nuclei as a response to cortical disinhibition could contribute greater understanding of the mechanism underlying cortical disinhibition in a PD model.

All analyses of the striatum treated this region as homogenous, although this is not the case. There are clear differences between both inputs and outputs of direct and indirect MSNs, so techniques such as immunohistochemistry and immunoblotting that cannot differentiate between these distinct neurons may abolish any potential differences that occur. Targeting the deeper layers of the motor cortex with the viral injections should preferentially affect the PT pathway, the output from the cortex that predominantly synapses on indirect pathway striatopallidal MSNs (Mallet, 2006). Therefore, future experiments that can isolate direct and indirect pathway neurons for subsequent analysis after cortical disinhibition would be important to fully rule out the role of the corticostriatal pathway in a proposed mechanism of protection or restoration in this model.

For possible clinical translation, the Cre-lox system is untenable. Therefore, developing a model using RNAi, a technique of genetic modification that can be used clinically, is important. Determining whether RNAi knockdown of *Vgat* is as effective as Cre-mediated *Vgat* knockout in a PD model is an important first step to determine the clinical viability of long-term cortical disinhibition via gene modification. Alternatively, long-term stimulation can also be achieved through implanted electrodes. Although adapting the current electrodes used in PD patients for extradural motor cortex stimulation to fit the mouse brain presents its own challenges, using a similar method of

stimulation could provide more directly comparable data from a mouse model that could be used in the treatment of PD patients.

While there are certainly limitations to the current studies and further experiments necessary to fully describe the observations described here, these results do indicate that posited cortical disinhibition is an effective therapy in a progressive MPTP model of PD. The protection against TH loss when posited cortical disinhibition is performed before lesioning and increase in TH expression in the midbrain induced by posited cortical disinhibition after lesioning and improvement in a measure of gait, both indicate that posited cortical disinhibition can beneficially alter the basal ganglia in a PD disease model. The studies herein represent a foundation to further explore gene modification-induced cortical disinhibition as a novel treatment for PD, one that could accomplish the as yet unachieved goal of altering disease progression.

References

Amende, I., Kale, A., McCue, S., Glazier, S., Morgan, J. P., & Hampton, T. G. (2005). Gait dynamics in mouse models of Parkinson's disease and Huntington's disease. *Journal of NeuroEngineering and Rehabilitation*, *2*(1), 20. https://doi.org/10.1186/1743-0003-2-20

Arkadir, D., Bergman, H., & Fahn, S. (2014). Redundant dopaminergic activity may enable compensatory axonal sprouting in Parkinson disease. *Neurology*, *82*(12), 1093–1098. https://doi.org/10.1212/WNL.0000000000000243

Aumann, T. D., Egan, K., Lim, J., Boon, W. C., Bye, C. R., Chua, H. K., … Horne, M. K. (2011). Neuronal activity regulates expression of tyrosine hydroxylase in adult mouse substantia nigra pars compacta neurons. *Journal of Neurochemistry*, *116*(4), 646–658. https://doi.org/10.1111/j.1471-4159.2010.07151.x

Aumann, T., & Horne, M. (2012a). Activity-dependent regulation of the dopamine phenotype in substantia nigra neurons. *Journal of Neurochemistry*, *121*(4), 497–515. https://doi.org/10.1111/j.1471-4159.2012.07703.x

Aumann, T., & Horne, M. (2012b). Activity-dependent regulation of the dopamine phenotype in substantia nigra neurons. *Journal of Neurochemistry*, *121*(4), 497–515. https://doi.org/10.1111/j.1471-4159.2012.07703.x

Auyeung, M., Tsoi, T. H., Mok, V., Cheung, C. M., Lee, C. N., Li, R., & Yeung, E. (2012). Ten year survival and outcomes in a prospective cohort of new onset Chinese Parkinson's disease patients. *Journal of Neurology, Neurosurgery and Psychiatry*, *83*(6), 607–611. https://doi.org/10.1136/jnnp-2011-301590

Baquet, Z. C., Williams, D., Brody, J., & Smeyne, R. J. (2009). A comparison of model-based (2D) and design-based (3D) stereological methods for estimating cell number in the substantia nigra pars compacta (SNpc) of the C57BL/6J mouse. *Neuroscience*, *161*(4), 1082–1090. https://doi.org/10.1016/j.neuroscience.2009.04.031

Baudrexel, S., Witte, T., Seifried, C., von Wegner, F., Beissner, F., Klein, J. C., … Hilker, R. (2011). Resting state fMRI reveals increased subthalamic nucleus-motor cortex connectivity in Parkinson's disease. *NeuroImage*, *55*(4), 1728–1738. https://doi.org/10.1016/j.neuroimage.2011.01.017

Benes, F. M., & Lange, N. (2001). Two-dimensional versus three-dimensional cell counting: a practical perspective. *Trends in Neurosciences*, *24*(1), 11–17. Retrieved from http://www.ncbi.nlm.nih.gov/pubmed/11163882

Bergman, H., Wichmann, T., Karmon, B., & DeLong, M. R. (2017). The primate subthalamic nucleus. II. Neuronal activity in the MPTP model of parkinsonism. *Journal of Neurophysiology*, *72*(2), 507–520. https://doi.org/10.1152/jn.1994.72.2.507

Bergman, H., Wichmann, T., & DeLong, M. R. (1990). Reversal of experimental parkinsonism by lesions of the subthalamic nucleus. *Science*, *249*(4975), 1436–

1438. https://doi.org/10.1126/science.2402638

Bernheimer, H., Birkmayer, W., Hornykiewicz, O., Jellinger, K., & Seitelberger, F. (1973). Brain dopamine and the syndromes of Parkinson and Huntington Clinical, morphological and neurochemical correlations. *Journal of the Neurological Sciences*, *20*(4), 415–455. https://doi.org/10.1016/0022-510X(73)90175-5

Berretta, S., Parthasarathy, H. B., & Graybiel, A. M. (1997). Local Release of GABAergic Inhibition in the Motor Cortex Induces Immediate-Early Gene Expression in Indirect Pathway Neurons of the Striatum. *J. Neurosci.*, *17*(12), 4752–4763. Retrieved from http://www.jneurosci.org/content/17/12/4752.long

Betarbet, R., Sherer, T. B., & Greenamyre, J. T. (2002). Animal Models of Parkinson's Disease. *BioEssays*, *24*, 308–318. https://doi.org/10.1016/B978-008045046-9.00522-2

Blandini, F., & Armentero, M.-T. (2012). Animal models of Parkinson's disease. *FEBS Journal*, *279*(7), 1156–1166. https://doi.org/10.1111/j.1742-4658.2012.08491.x

Blandini, F., Armentero, M.-T., & Martignoni, E. (2008). The 6-hydroxydopamine model: News from the past. *Parkinsonism & Related Disorders*, *14*, S124–S129. https://doi.org/10.1016/J.PARKRELDIS.2008.04.015

Bruet, N., Windels, F., Bertrand, A., Feuerstein, C., Poupard, A., & Savasta, M. (2001). High frequency stimulation of the subthalamic nucleus increases the extracellular contents of striatal dopamine in normal and partially dopaminergic denervated rats. *Journal of Neuropathology and Experimental Neurology*, *60*(1), 15–24. https://doi.org/10.1093/jnen/60.1.15

Calabresi, P., Bernardi, G., Giacomini, P., Centonze, D., Gubellini, P., & Picconi, B. (1999). Unilateral dopamine denervation blocks corticostriatal LTP. *Journal of Neurophysiology*, *82*(6), 3575–3579. https://doi.org/10.1152/jn.1999.82.6.3575

Canavero, S., & Paolotti, R. (2000). Extradural motor cortex stimulation for advanced Parkinson's disease: Case report. *Movement Disorders*, *15*(1), 169–171. https://doi.org/10.1002/1531-8257(200001)15:1<169::AID-MDS1030>3.0.CO;2-W

Canavero, S., Paolotti, R., Bonicalzi, V., Castellano, G., Greco-Crasto, S., Rizzo, L., … Ragazzi, P. (2002). Extradural motor cortex stimulation for advanced Parkinson disease. *Journal of Neurosurgery*, *97*(5), 1208–1211. https://doi.org/10.3171/jns.2002.97.5.1208

Canteras, N. S., Shammah-Lagnado, S. J., Silva, B. A., & Ricardo, J. A. (1990). Afferent connections of the subthalamic nucleus: a combined retrograde and anterograde horseradish peroxidase study in the rat. *Brain Research*, *513*(1), 43–59. https://doi.org/10.1016/0006-8993(90)91087-W

Chen, R., Kumar, S., Garg, R. R., & Lang, A. E. (2001). Impairment of motor cortex activation and deactivation in Parkinson's disease. *Clinical Neurophysiology*, *112*(4), 600–607. https://doi.org/10.1016/S1388-2457(01)00466-7

Chesselet, M. (1996). Basal ganglia and movement disorders: an update. *Trends in*

Neurosciences, *19*(10), 417–422. https://doi.org/10.1016/0166-2236(96)10052-7

Churchill, M. J., Pflibsen, L., Sconce, M. D., Moore, C., Kim, K., & Meshul, C. K. (2017). Exercise in an animal model of Parkinson's disease: Motor recovery but not restoration of the nigrostriatal pathway. *Neuroscience*, *359*, 224–247. https://doi.org/10.1016/J.NEUROSCIENCE.2017.07.031

Churchill, M. J., Cantu, M. A., Kasanga, E. A., Moore, C., Salvatore, M. F., & Meshul, C. K. (2019). Glatiramer Acetate Reverses Motor Dysfunction and the Decrease in Tyrosine Hydroxylase Levels in a Mouse Model of Parkinson's Disease. *Neuroscience*. https://doi.org/10.1016/j.neuroscience.2019.06.006

Day, M., Wang, Z., Ding, J., An, X., Ingham, C. A., Shering, A. F., … Surmeier, D. J. (2006). Selective elimination of glutamatergic synapses on striatopallidal neurons in Parkinson disease models. *Nature Neuroscience*, *9*(2), 251–259. https://doi.org/10.1038/nn1632

de Lau, L. M., & Breteler, M. M. (2006). Epidemiology of Parkinson's disease. *The Lancet Neurology*, *5*(6), 525–535. https://doi.org/10.1016/S1474-4422(06)70471-9

DeLong, M. R. (1990). Primate models of movement disorders of basal ganglia origin. *Trends in Neurosciences*, *13*(7), 281–285. https://doi.org/10.1016/0166-2236(90)90110-V

Deniau, J. M., Hammond, C., Chevalier, G., & Feger, J. (1978). Evidence for branched subthalamic nucleus projections to substantia nigra, entopeduncular nucleus and globus pallidus. *Neuroscience Letters*, *9*(2–3), 117–121. https://doi.org/10.1016/0304-3940(78)90058-7

Drouot, X., Oshino, S., Jarraya, B., Besret, L., Kishima, H., Remy, P., … Palfi, S. (2004). Functional Recovery in a Primate Model of Parkinson's Disease following Motor Cortex Stimulation. *Neuron*, *44*(5), 769–778. https://doi.org/10.1016/J.NEURON.2004.11.023

Ehringer, H., & Hornykiewicz, O. (1960). Verteilung Von Noradrenalin Und Dopamin (3-Hydroxytyramin) Im Gehirn Des Menschen Und Ihr Verhalten Bei Erkrankungen Des Extrapyramidalen Systems. *Klinische Wochenschrift*, *38*(24), 1236–1239. https://doi.org/10.1007/BF01485901

Fearnley, J. M., & Lees, A. J. (1991). Ageing and Parkinson's Disease: Substantia Nigra Regional Selectivity. *Brain*, *114*(5), 2283–2301. https://doi.org/10.1093/brain/114.5.2283

Finkelstein, D., Stanic, D., Parish, C. L., Tomas, D., Dickson, K., & Horne, M. K. (2000). Axonal sprouting following lesions of the rat substantia nigra. *Neuroscience*, *97*(1), 99–112. https://doi.org/10.1016/S0306-4522(00)00009-9

Freestone, P. S., Wu, X. H., de Guzman, G., & Lipski, J. (2015). Excitatory drive from the Subthalamic nucleus attenuates GABAergic transmission in the Substantia Nigra pars compacta via endocannabinoids. *European Journal of Pharmacology*, *767*, 144–151. https://doi.org/10.1016/J.EJPHAR.2015.09.050

Gibrat, C., Saint-Pierre, M., Bousquet, M., Lévesque, D., Rouillard, C., & Cicchetti, F. (2009). Differences between subacute and chronic MPTP mice models: investigation of dopaminergic neuronal degeneration and α-synuclein inclusions. *Journal of Neurochemistry*, *109*(5), 1469–1482. https://doi.org/10.1111/j.1471-4159.2009.06072.x

Goetz, C. G. (1986). Charcot on Parkinson's disease. *Movement Disorders*, *1*(1), 27–32. https://doi.org/10.1002/mds.870010104

Goetz, C. G. (2011). The history of Parkinson's disease: early clinical descriptions and neurological therapies. *Cold Spring Harbor Perspectives in Medicinee*, *1*(1), a008862. https://doi.org/10.1101/cshperspect.a008862

Goldberg, J. A., Boraud, T., Maraton, S., Haber, S. N., Vaadia, E., & Bergman, H. (2002). Enhanced Synchrony among Primary Motor Cortex Neurons in the 1-Methyl-4-Phenyl-1,2,3,6-Tetrahydropyridine Primate Model of Parkinson's Disease. *J. Neurosci.*, *22*(11), 4639–4653. Retrieved from http://www.jneurosci.org/content/22/11/4639.short

Goldberg, N. R. S., Haack, A. K., Lim, N. S., Janson, O. K., & Meshul, C. K. (2011). Dopaminergic and behavioral correlates of progressive lesioning of the nigrostriatal pathway with 1-methyl-4-phenyl-1,2,3,6-tetrahydropyridine. *Neuroscience*, *180*, 256–271. https://doi.org/10.1016/j.neuroscience.2011.02.027

Goldberg, N. R. S., Fields, V., Pflibsen, L., Salvatore, M. F., & Meshul, C. K. (2012). Social enrichment attenuates nigrostriatal lesioning and reverses motor impairment in a progressive 1-methyl-2-phenyl-1,2,3,6-tetrahydropyridine (MPTP) mouse model of Parkinson's disease. *Neurobiology of Disease*, *45*(3), 1051–1067. https://doi.org/10.1016/j.nbd.2011.12.024

Goldberg, N. R. S., Hampton, T., McCue, S., Kale, A., & Meshul, C. K. (2011). Profiling changes in gait dynamics resulting from progressive 1-methyl-4-phenyl-1,2,3,6-tetrahydropyridine-induced nigrostriatal lesioning. *Journal of Neuroscience Research*, *89*(10), 1698–1706. https://doi.org/10.1002/jnr.22699

Grace, A. A., & Bunney, B. S. (1979). Paradoxical GABA excitation of nigral dopaminergic cells: Indirect mediation through reticulata inhibitory neurons. *European Journal of Pharmacology*, *59*(3–4), 211–218. https://doi.org/10.1016/0014-2999(79)90283-8

Hassani, O.-K., Mouroux, M., & Féger, J. (1996). Increased subthalamic neuronal activity after nigral dopaminergic lesion independent of disinhibition via the globus pallidus. *Neuroscience*, *72*(1), 105–115. https://doi.org/10.1016/0306-4522(95)00535-8

He, Z., Jiang, Y., Xu, H., Jiang, H., Jia, W., Sun, P., & Xie, J. (2014). High frequency stimulation of subthalamic nucleus results in behavioral recovery by increasing striatal dopamine release in 6-hydroxydopamine lesioned rat. *Behavioural Brain Research*, *263*, 108–114. https://doi.org/10.1016/J.BBR.2014.01.014

Hilker, R., Portman, A. T., Voges, J., Staal, M. J., Burghaus, L., van Laar, T., …

Leenders, K. L. (2005). Disease progression continues in patients with advanced Parkinson's disease and effective subthalamic nucleus stimulation. *Journal of Neurology, Neurosurgery, and Psychiatry*, *76*(9), 1217–1221. https://doi.org/10.1136/jnnp.2004.057893

Hoehn, M. M., & Yahr, M. D. (1967). Parkinsonism: onset, progression, and mortality. *Neurology*, *17*(5), 427–427. https://doi.org/10.1212/WNL.17.5.427

Hood, R. L., Liguore, W. A., Moore, C., Pflibsen, L., Meshul, C. K., Moore, C., & Meshul, C. K. (2016). Exercise intervention increases spontaneous locomotion but fails to attenuate dopaminergic system loss in a striatal dopamine depletion model in aged mice. *Brain Research*, *1646*, 535–542. https://doi.org/10.1016/j.brainres.2016.06.032

Huang, Z. J. (2014). Toward a Genetic Dissection of Cortical Circuits in the Mouse. *Neuron*, *83*(6), 1284–1302. https://doi.org/10.1016/J.NEURON.2014.08.041

Huse, D. M., Schulman, K., Orsini, L., Castelli-Haley, J., Kennedy, S., & Lenhart, G. (2005). Burden of illness in Parkinson's disease. *Movement Disorders*, *20*(11), 1449–1454. https://doi.org/10.1002/mds.20609

Iribe, Y., Moore, K., Pang, K. C. H., & Tepper, J. M. (2017). Subthalamic Stimulation-Induced Synaptic Responses in Substantia Nigra Pars Compacta Dopaminergic Neurons In Vitro. *Journal of Neurophysiology*, *82*(2), 925–933. https://doi.org/10.1152/jn.1999.82.2.925

Jankovic, J. (2008). Parkinson's disease clinical features and diagnosis. *Journal of Neurology, Neurosurgery & Psychiatry*, *79*, 368–376. https://doi.org/10.1136/jnnp.2007.131045

Johannessen, J. N., Chiueh, C. C., Burns, R. S., & Markey, S. P. (1985). IV. Differences in the metabolism of MPTP in the rodent and primate parallel differences in sensitivity to its neurotoxic effects. *Life Sciences*, *36*(3), 219–224. https://doi.org/10.1016/0024-3205(85)90062-1

Johnson, M. D., Miocinovic, S., McIntyre, C. C., & Vitek, J. L. (2008). Mechanisms and Targets of Deep Brain Stimulation in Movement Disorders. *Neurotherapeutics*, *5*(2), 294–308. https://doi.org/10.1016/j.nurt.2008.01.010

Khedr, E. M., Farweez, H. M., & Islam, H. (2003). Therapeutic effect of repetitive transcranial magnetic stimulation on motor function in Parkinson's disease patients. *European Journal of Neurology*, *10*(5), 567–572. https://doi.org/10.1046/j.1468-1331.2003.00649.x

Kordower, J. H., Olanow, C. W., Dodiya, H. B., Chu, Y., Beach, T. G., Adler, C. H., … Bartus, R. T. (2013). Disease duration and the integrity of the nigrostriatal system in Parkinson's disease. *Brain*, *136*(8), 2419–2431. https://doi.org/10.1093/brain/awt192

Kordower, J. H., Olanow, C. W., Dodiya, H. B., Chu, Y., Beach, T. G., Adler, C. H., … Bartus, R. T. (2013). Disease duration and the integrity of the nigrostriatal system in

Parkinson's disease. *Brain : A Journal of Neurology*, *136*(8), 2419–2431. https://doi.org/10.1093/brain/awt192

Kowal, S. L., Dall, T. M., Chakrabarti, R., Storm, M. V, & Jain, A. (2013). The current and projected economic burden of Parkinson's disease in the United States. *Movement Disorders : Official Journal of the Movement Disorder Society*, *28*(3), 311–318. https://doi.org/10.1002/mds.25292

Kumar, R., Lozano, A. M., Kim, Y. J., Hutchison, W. D., Sime, E., Halket, E., & Lang, A. E. (1998). Double-blind evaluation of subthalamic nucleus deep brain stimulation in advanced Parkinson's disease. *Neurology*, *51*(3), 850–855. https://doi.org/10.1212/WNL.51.3.850

Kumar, R., Lozano, A. M., Kim, Y. J., Hutchison, W. D., Sime, E., Halket, E., & Lang, A. E. (2010). Double-blind evaluation of subthalamic nucleus deep brain stimulation in advanced Parkinson's disease, *27*(1), 1–20. https://doi.org/10.3171/2009.4.FOCUS0986.Getting

Leenders, K. L., Palmer, A. J., Quinn, N., Clark, J. C., Firnau, G., Garnett, E. S., … Marsden, C. D. (1986). Brain dopamine metabolism in patients with Parkinson's disease measured with positron emission tomography. *Journal of Neurology, Neurosurgery & Psychiatry*, *49*(8), 853–860. https://doi.org/10.1136/jnnp.49.8.853

Lefaucheur, J.-P. (2005). Motor cortex dysfunction revealed by cortical excitability studies in Parkinson's disease: influence of antiparkinsonian treatment and cortical stimulation. *Clinical Neurophysiology : Official Journal of the International Federation of Clinical Neurophysiology*, *116*(2), 244–253. https://doi.org/10.1016/j.clinph.2004.11.017

Lefaucheur, J.-P., Drouot, X., Von Raison, F., Ménard-Lefaucheur, I., Cesaro, P., & Nguyen, J.-P. (2004). Improvement of motor performance and modulation of cortical excitability by repetitive transcranial magnetic stimulation of the motor cortex in Parkinson's disease. *Clinical Neurophysiology : Official Journal of the International Federation of Clinical Neurophysiology*, *115*(11), 2530–2541. https://doi.org/10.1016/j.clinph.2004.05.025

Lenz, M., & Vlachos, A. (2016). Releasing the Cortical Brake by Non-Invasive Electromagnetic Stimulation? rTMS Induces LTD of GABAergic Neurotransmission. *Frontiers in Neural Circuits*, *10*, 96. https://doi.org/10.3389/fncir.2016.00096

Li, Y., Liu, W., Oo, T. F., Wang, L., Tang, Y., Jackson-Lewis, V., … Li, C. (2009). Mutant LRRK2(R1441G) BAC transgenic mice recapitulate cardinal features of Parkinson's disease. *Nature Neuroscience*, *12*(7), 826–828. https://doi.org/10.1038/nn.2349

Lotze, M., Montoya, P., Erb, M., Hülsmann, E., Flor, H., Klose, U., … Grodd, W. (1999). Activation of Cortical and Cerebellar Motor Areas during Executed and Imagined Hand Movements: An fMRI Study. *Journal of Cognitive Neuroscience*, *11*(5), 491–501. https://doi.org/10.1162/089892999563553

Mahncke, H. W., Bronstone, A., & Merzenich, M. M. (2006). Brain plasticity and functional losses in the aged: scientific bases for a novel intervention. *Progress in Brain Research*, *157*, 81–109. https://doi.org/10.1016/S0079-6123(06)57006-2

Mallet, N. (2006). Cortical Inputs and GABA Interneurons Imbalance Projection Neurons in the Striatum of Parkinsonian Rats. *Journal of Neuroscience*, *26*(14), 3875–3884. https://doi.org/10.1523/jneurosci.4439-05.2006

Manyam, B. V. (1990). Paralysis agitans and levodopa in "Ayurveda": Ancient Indian medical treatise. *Movement Disorders*, *5*(1), 47–48. https://doi.org/10.1002/mds.870050112

Maurice, N., Thierry, A.-M., Glowinski, J., & Deniau, J.-M. (2003). Spontaneous and Evoked Activity of Substantia Nigra Pars Reticulata Neurons during High-Frequency Stimulation of the Subthalamic Nucleus. *J. Neurosci.*, *23*(30), 9929–9936. Retrieved from http://www.jneurosci.org/content/23/30/9929.full

McGeorge, A. J., & Faull, R. L. M. (1989). The organization of the projection from the cerebral cortex to the striatum in the rat. *Neuroscience*, *29*(3), 503–537. https://doi.org/10.1016/0306-4522(89)90128-0

Mendez-Lopez, M., Arias, J. L., Bontempi, B., & Wolff, M. (2013). Reduced cytochrome oxidase activity in the retrosplenial cortex after lesions to the anterior thalamic nuclei. *Behavioural Brain Research*, *250*, 264–273. https://doi.org/10.1016/j.bbr.2013.04.052

Meredith, G. E., & Rademacher, D. J. (2011). MPTP mouse models of Parkinson's disease: An update. *Journal of Parkinson's Disease*. NIH Public Access. https://doi.org/10.3233/JPD-2011-11023

Meshul, C. K., Emre, N., Nakamura, C., Allen, C., Donohue, M., & Buckman, J. (1999). Time-dependent changes in striatal glutamate synapses following a 6-hydroxydopamine lesion. *Neuroscience*, *88*(1), 1–16. https://doi.org/10.1016/S0306-4522(98)00189-4

Meshul, C. K., Stallbaumer, R. K., Taylor, B., & Janowsky, A. (1994). Haloperidol-induced morphological changes in striatum are associated with glutamate synapses. *Brain Research*, *648*(2), 181–195. https://doi.org/10.1016/0006-8993(94)91117-7

Naito, A., & Kita, H. (1994). The cortico-nigral projection in the rat: an anterograde tracing study with biotinylated dextran amine. *Brain Research*, *637*(1–2), 317–322. https://doi.org/10.1016/0006-8993(94)91252-1

Nakamura, S., & Vincent, S. R. (1986). Histochemistry of MPTP oxidation in the rat brain: Sites of synthesis of the parkinsonism-inducing toxin MPP+. *Neuroscience Letters*, *65*(3), 321–325. https://doi.org/10.1016/0304-3940(86)90282-X

Nambu, A. (2008). Seven problems on the basal ganglia. *Current Opinion in Neurobiology*, *18*(6), 595–604. https://doi.org/10.1016/j.conb.2008.11.001

Nambu, A., Tokuno, H., & Takada, M. (2002). Functional significance of the cortico-subthalamo-pallidal "hyperdirect" pathway. *Neuroscience Research*, *43*(2), 111–

117. https://doi.org/10.1016/S0168-0102(02)00027-5

Nesbitt, K. M., Jaquins-Gerstl, A., Skoda, E. M., Wipf, P., & Michael, A. C. (2013). Pharmacological mitigation of tissue damage during brain microdialysis. *Analytical Chemistry*, *85*(17), 8173–8179. https://doi.org/10.1021/ac401201x

Ni, Z.-G., Bouali-Benazzouz, R., Gao, D.-M., Benabid, A.-L., & Benazzouz, A. (2001). Time-course of changes in firing rates and firing patterns of subthalamic nucleus neuronal activity after 6-OHDA-induced dopamine depletion in rats. *Brain Research*, *899*(1–2), 142–147. https://doi.org/10.1016/S0006-8993(01)02219-3

Obeso, J. A., Rodríguez-Oroz, M. C., Benitez-Temino, B., Blesa, F. J., Guridi, J., Marin, C., & Rodriguez, M. (2008). Functional organization of the basal ganglia: therapeutic implications for Parkinson's disease. *Movement Disorders : Official Journal of the Movement Disorder Society*, *23 Suppl 3*, S548-59. https://doi.org/10.1002/mds.22062

Olanow, C. W., & Tatton, W. G. (1999). Etiology and pathogenesis of Parkinson's disease. *Annual Review of Neuroscience*, *22*, 123–144. https://doi.org/10.1016/S1098-3597(99)90001-7

Parkinson, J. (2002). *NEUROPSYCHIATRY CLASSICS An Essay on the Shaking Palsy Member of the Royal College of Surgeons*. *J Neuropsychiatry Clin Neurosci* (Vol. 14). Retrieved from https://neuro.psychiatryonline.org/doi/pdfplus/10.1176/jnp.14.2.223

Pazo, J. H., Höcht, C., Barceló, A. C., Fillipini, B., & Lomastro, M. J. (2010). Effect of electrical and chemical stimulation of the subthalamic nucleus on the release of striatal dopamine. *Synapse*, *64*(12), 905–915. https://doi.org/10.1002/syn.20809

Petroske, E., Meredith, G. ., Callen, S., Totterdell, S., & Lau, Y.-S. (2001). Mouse model of Parkinsonism: a comparison between subacute MPTP and chronic MPTP/probenecid treatment. *Neuroscience*, *106*(3), 589–601. https://doi.org/10.1016/S0306-4522(01)00295-0

Pflibsen, L., Stang, K. A., Sconce, M. D., Wilson, V. B., Hood, R. L., Meshul, C. K., & Mitchell, S. H. (2015). Executive function deficits and glutamatergic protein alterations in a progressive 1-methyl-4-phenyl-1,2,3,6-tetrahydropyridine mouse model of Parkinson's disease. *Journal of Neuroscience Research*, *93*(12), 1849–1864. https://doi.org/10.1002/jnr.23638

Pienaar, I. S., Elson, J. L., Racca, C., Nelson, G., Turnbull, D. M., & Morris, C. M. (2013). Mitochondrial abnormality associates with type-specific neuronal loss and cell morphology changes in the pedunculopontine nucleus in Parkinson disease. *The American Journal of Pathology*, *183*(6), 1826–1840. https://doi.org/10.1016/j.ajpath.2013.09.002

Polymeropoulos, M. H., Lavedan, C., Leroy, E., Ide, S. E., Dehejia, A., Dutra, A., … Nussbaum, R. L. (1997). Mutation in the α-synuclein gene identified in families with Parkinson's disease. *Science*, *276*(5321), 2045–2047. https://doi.org/10.1126/science.276.5321.2045

Porras, G., Li, Q., & Bezard, E. (2012). Modeling Parkinson's disease in primates: The MPTP model. *Cold Spring Harbor Perspectives in Medicine*, *2*(3), a009308. https://doi.org/10.1101/cshperspect.a009308

Reiner, A., Jiao, Y., Del Mar, N., Laverghetta, A. V., & Lei, W. L. (2003). Differential morphology of pyramidal tract-type and intratelencephalically projecting-type corticostriatal neurons and their intrastriatal terminals in rats. *Journal of Comparative Neurology*, *457*(4), 420–440. https://doi.org/10.1002/cne.10541

Reiner, A., Veenman, C. L., Medina, L., Jiao, Y., Del Mar, N., & Honig, M. G. (2000). Pathway tracing using biotinylated dextran amines. *Journal of Neuroscience Methods*, *103*(1), 23–37. https://doi.org/10.1016/S0165-0270(00)00293-4

Ridding, M. C., Rothwell, J. C., Inzelberg, R., & Rothwell, J. C. (1995). Changes in excitability of motor cortical circuitry in patients with Parkinson's disease. *Annals of Neurology*, *37*(2), 181–188. https://doi.org/10.1002/ana.410370208

Rizzone, M. G., Fasano, A., Daniele, A., Zibetti, M., Merola, A., Rizzi, L., … Albanese, A. (2014). Long-term outcome of subthalamic nucleus DBS in Parkinson's disease: From the advanced phase towards the late stage of the disease? *Parkinsonism and Related Disorders*, *20*(4), 376–381. https://doi.org/10.1016/j.parkreldis.2014.01.012

Roberts, H. C., Syddall, H. E., Butchart, J. W., Stack, E. L., Cooper, C., & Sayer, A. A. (2015). The Association of Grip Strength With Severity and Duration of Parkinson's: A Cross-Sectional Study. *Neurorehabilitation and Neural Repair*, *29*(9), 889–896. https://doi.org/10.1177/1545968315570324

Sabatini, U., Boulanouar, K., Fabre, N., Martin, F., Carel, C., Colonnese, C., … Rascol, O. (2000). Cortical motor reorganization in akinetic patients with Parkinson's disease: A functional MRI study. *Brain*, *123*(2), 394–403. https://doi.org/10.1093/brain/123.2.394

Salthun-Lassalle, B., Hirsch, E. C., Wolfart, J., Ruberg, M., & Michel, P. P. (2004). Rescue of mesencephalic dopaminergic neurons in culture by low-level stimulation of voltage-gated sodium channels. *The Journal of Neuroscience : The Official Journal of the Society for Neuroscience*, *24*(26), 5922–5930. https://doi.org/10.1523/JNEUROSCI.5668-03.2004

Sanders, T. H., & Jaeger, D. (2016). Optogenetic stimulation of cortico-subthalamic projections is sufficient to ameliorate bradykinesia in 6-ohda lesioned mice. *Neurobiology of Disease*, *95*, 225–237. https://doi.org/10.1016/j.nbd.2016.07.021

Sauer, B. (1998). *Inducible Gene Targeting in Mice Using the Cre/lox System*. *METHODS: A Companion to Methods in Enzymology* (Vol. 14). Retrieved from http://web.as.uky.edu/biology/faculty/mirabito/BIO 510 2009/pdf files/inducible gene targeting using Cre lox.pdf

Schober, A. (2004). Classic toxin-induced animal models of Parkinson?s disease: 6-OHDA and MPTP. *Cell and Tissue Research*, *318*(1), 215–224. https://doi.org/10.1007/s00441-004-0938-y

Schuster, R. (1988). Determination of amino acids in biological, pharmaceutical, plant and food samples by automated precolumn derivatization and high-performance liquid chromatography. *Journal of Chromatography B: Biomedical Sciences and Applications*, *431*(C), 271–284. https://doi.org/10.1016/S0378-4347(00)83096-0

Sconce, M. D., Churchill, M. J., Moore, C., & Meshul, C. K. (2015). Intervention with 7,8-dihydroxyflavone blocks further striatal terminal loss and restores motor deficits in a progressive mouse model of Parkinson's disease. *Neuroscience*, *290*, 454–471. https://doi.org/10.1016/j.neuroscience.2014.12.080

Sedelis, M., Schwarting, R. K., & Huston, J. P. (2001). Behavioral phenotyping of the MPTP mouse model of Parkinson's disease. *Behavioural Brain Research*, *125*(1–2), 109–125. https://doi.org/10.1016/S0166-4328(01)00309-6

Sen, S., Kawaguchi, A., Truong, Y., Lewis, M. M., & Huang, X. (2010). Dynamic changes in cerebello-thalamo-cortical motor circuitry during progression of Parkinson's disease. *Neuroscience*, *166*(2), 712–719. https://doi.org/10.1016/j.neuroscience.2009.12.036

Smith, B. A., Goldberg, N. R. S., & Meshul, C. K. (2011). Effects of treadmill exercise on behavioral recovery and neural changes in the substantia nigra and striatum of the 1-methyl-4-phenyl-1,2,3,6-tetrahydropyridine-lesioned mouse. *Brain Research*, *1386*, 70–80. https://doi.org/10.1016/j.brainres.2011.02.003

Spinelli, K. J., Osterberg, V. R., Meshul, C. K., Soumyanath, A., & Unni, V. K. (2015). Curcumin Treatment Improves Motor Behavior in α-Synuclein Transgenic Mice. *PLOS ONE*, *10*(6), e0128510. https://doi.org/10.1371/journal.pone.0128510

Stanic, D., Parish, C. L., Zhu, W. M., Krstew, E. V., Lawrence, A. J., Drago, J., … Horne, M. K. (2004). Changes in function and ultrastructure of striatal dopaminergic terminals that regenerate following partial lesions of the SNpc. *Journal of Neurochemistry*, *86*(2), 329–343. https://doi.org/10.1046/j.1471-4159.2003.01843.x

Stephens, B., Mueller, A. J., Shering, A. F., Hood, S. H., Taggart, P., Arbuthnott, G. W., … Ingham, C. A. (2005). Evidence of a breakdown of corticostriatal connections in Parkinson's disease. *Neuroscience*, *132*(3), 741–754. https://doi.org/10.1016/j.neuroscience.2005.01.007

Strafella, A. P., Ko, J. H., Grant, J., Fraraccio, M., & Monchi, O. (2005). Corticostriatal functional interactions in Parkinson's disease: a rTMS/[^{11} C]raclopride PET study. *European Journal of Neuroscience*, *22*(11), 2946–2952. https://doi.org/10.1111/j.1460-9568.2005.04476.x

Tepper, J. M., Martin, L. P., & Anderson, D. R. (1995). GABAA receptor-mediated inhibition of rat substantia nigra dopaminergic neurons by pars reticulata projection neurons. *Journal of Neuroscience*, *15*(4), 3092–3103. Retrieved from https://www.jneurosci.org/content/jneuro/15/4/3092.full.pdf

Tong, Q., Ye, C.-P., Jones, J. E., Elmquist, J. K., & Lowell, B. B. (2008). Synaptic release of GABA by AgRP neurons is required for normal regulation of energy balance. *Nature Neuroscience*, *11*(9), 998–1000. https://doi.org/10.1038/nn.2167

Tong, Q., Ye, C., McCrimmon, R. J., Dhillon, H., Choi, B., Kramer, M. D., … Lowell, B. B. (2007). Synaptic Glutamate Release by Ventromedial Hypothalamic Neurons Is Part of the Neurocircuitry that Prevents Hypoglycemia. *Cell Metabolism*, *5*(5), 383–393. https://doi.org/10.1016/j.cmet.2007.04.001

Verschuur, C. V. M., Suwijn, S. R., Boel, J. A., Post, B., Bloem, B. R., van Hilten, J. J., … de Bie, R. M. A. (2019). Randomized Delayed-Start Trial of Levodopa in Parkinson's Disease. *New England Journal of Medicine*, *380*(4), 315–324. https://doi.org/10.1056/NEJMoa1809983

Villalba, R. M., & Smith, Y. (2013). Differential striatal spine pathology in Parkinson's disease and cocaine addiction: A key role of dopamine? *Neuroscience*, *251*, 2–20. https://doi.org/10.1016/J.NEUROSCIENCE.2013.07.011

Watabe-Uchida, M., Zhu, L., Ogawa, S. K., Vamanrao, A., & Uchida, N. (2012). Whole-Brain Mapping of Direct Inputs to Midbrain Dopamine Neurons. *Neuron*, *74*(5), 858–873. https://doi.org/10.1016/J.NEURON.2012.03.017

Wilson, C. J., & Bevan, M. D. (2011). Intrinsic dynamics and synaptic inputs control the activity patterns of subthalamic nucleus neurons in health and in Parkinson's disease. *Neuroscience*, *198*, 54–68. https://doi.org/10.1016/j.neuroscience.2011.06.049

Wong-Riley, M. T. T. (1989). Cytochrome oxidase: an endogenous metabolic marker for neuronal activity. *Trends in Neurosciences*, *12*(3), 94–101. https://doi.org/10.1016/0166-2236(89)90165-3

Wu, T., Long, X., Wang, L., Hallett, M., Zang, Y., Li, K., & Chan, P. (2011). Functional connectivity of cortical motor areas in the resting state in Parkinson's disease. *Human Brain Mapping*, *32*(9), 1443–1457. https://doi.org/10.1002/hbm.21118

Wu, T., Wang, L., Chen, Y., Zhao, C., Li, K., & Chan, P. (2009). Changes of functional connectivity of the motor network in the resting state in Parkinson's disease. *Neuroscience Letters*, *460*(1), 6–10. https://doi.org/10.1016/J.NEULET.2009.05.046

Xu, Q., Shenoy, S., & Li, C. (2011). Mouse models for LRRK2 Parkinson's disease. *Parkinsonism & Related Disorders*, *18*, S186–S189. https://doi.org/10.1016/s1353-8020(11)70058-x